

**Application of OSL dating on coastal sediments –
Case studies from shallow marine sediments of Southern
North Sea, Germany, and coastal sub-surface and surface
sediments from south India**

Inaugural Dissertation
zur
Erlangung des Doktorgrades
im Fachbereich Geowissenschaften
der Freien Universität Berlin

vorgelegt von

LINTO ALAPPAT
aus Kerala, Indien

BERLIN, 2011

Erstgutachter: Prof. Dr. Manfred Frechen

Zweitgutachterin: Prof. Dr. Margot Böse

Eingereicht am: 15- 10- 2010

Tag der Disputation: 07- 12- 2010

The main aim of this research work is the application of contemporary techniques in optically stimulated luminescence (OSL) dating to reveal the chronology of coastal deposits from various geographical and geological settings and to investigate the relationship between periods of sediment accumulation and climate change. To address this concern, samples were collected from three different areas, namely, 1) shallow continental shelf sediments from Southern North Sea, 2) inland and coastal dunes as well as deltaic sediments from the south east coast of India and 3) palaeo-beach ridges from the south west coast of India. The reliability of the OSL ages obtained is assured using independent age controls such as radiocarbon (^{14}C) dating whenever possible. Additionally, sedimentological techniques such as grain size analysis, quartz grain surface texture analysis using scanning electron microscopy (SEM) and heavy mineral studies are applied to characterise the grain transportation and sedimentary provenance.

The study on continental shelf sediments of Southern North Sea provided an insight into the fate of Late Weichselian and Early Holocene sediments accumulated in the German sector of the Southern North Sea. The study revealed that sedimentation continued to take place during the late deglaciation period over an extended period of time (between 19 ka and 8 ka) until the early Holocene transgressing sea occupied the area. A possible interface of the Pleistocene-Holocene sediments along the core transect is provided based on lithology and measured OSL and radiocarbon ages.

Older samples collected from the sub-surface sediments of Cauvery delta, southeast India helped to understand another aspect of OSL dating, namely the use of feldspar as a dosimeter for age determination. Due to early saturation of quartz OSL signal, the samples from this area showed the necessity to apply infrared stimulated luminescence (IRSL) dating to potassium feldspar. Making use of the lately introduced technique called elevated temperature post-IR IRSL the chronology of the area could be elucidated. The measured OSL ages revealed that except an upper layer of Holocene sediments (< 5m), the majority of the upper ~50m of Cauvery delta sediments were deposited between marine isotope stage (MIS) -5 and MIS-10 or older.

The OSL ages obtained from the dune sediments in the east coast of South India revealed the chronology of dune formation/ sand mobility. It outlines the possible

evolution of coastal dunes of the Cauvery delta region with widespread periodic dune formation/ reactivation having taken place during the Late Holocene to very recent times due to a variety of reasons such as climatic variation and land use changes. The sand mobility index calculated based on threshold wind speed, precipitation and evapo-transpiration showed that dunes in the area have been largely active during the past century.

The OSL dating of sand collected from the beach ridges along the west coast of South India proved to be divided into two main stages of ridge formation close to 3 and 4 ka. These results indicate a possible stage of wide spread beach ridge formation during middle to late Holocene period, providing evidence for a regressing sea on the west coast of India particularly in the coasts of Kerala during that time.

The findings of these individual studies not only contribute to the understanding of the regional palaeo-climate but also help to assess climate change of a particular time involved in a global palaeo-environmental context. The studies unravel interesting changes in the investigated coastlines during late Pleistocene to Holocene time which provides a chronological frame for events of deposition resulting from periodic transgression and regression, palaeo-aridity and enhanced windiness. The results correlate well with the early Holocene transgression and middle Holocene sea level high stand in both Southern North Sea and east and west coasts of South India.

Das Ziel der vorliegenden Arbeit ist es, basierend auf modernen Techniken der optisch stimulierten Lumineszenz (OSL) Chronologien für Küstensedimente unterschiedlichen Ursprung zu erstellen. Diese Chronologien sollen dann genutzt werden, um die Beziehung von Sedimentakkumulation und Klimawandel zu untersuchen. Um dieser Fragestellung gerecht zu werden, wurden die Sedimente von drei Gebieten bearbeitet: 1) flach-kontinentalen Schelfsedimente der südlichen Nordsee, 2) Inlands- und Küstendünen sowie deltaische Sedimente der südöstlichen Küste Indiens, und 3) Paläo-Strandwälle der Südwest-Küste Indiens. Die Zuverlässigkeit der Lumineszenzalter wurde, wenn möglich, durch unabhängige Alterkontrollen wie beispielsweise Radiokarbondatierung (^{14}C) überprüft. Zusätzlich wurden sedimentologische Daten (Korngrößenverteilung, Oberflächenstruktur von Quarzkörnern mittels Rasterelektronenmikroskopie, Schwermineralanalyse) durchgeführt, um den Transportmechanismus sowie das Herkunftsgebiet der Sedimente zu bestimmen.

Die Arbeit an den Sedimenten des Kontinentalschelfs der südlichen Nordsee (Deutschland) hat es ermöglicht, eine Übersicht über die Sedimentakkumulation von Spät-Weichsel bis ins Frühholozän zu erhalten. Während der späten Abschmelzphase erfolgte über einen langen Zeitraum (zwischen 19 ka und 8 ka) Sedimentation, die im Frühholozän durch die Meerestransgression beendet wurde. Die Pleistozän-Holozän-Grenze entlang des untersuchten Transekts konnte durch lithologische Untersuchungen sowie mittels der OSL- und ^{14}C -Alter bestimmt werden.

Ältere Sedimentproben aus dem Untergrund des Cauvery Deltas, Südost-Indien, haben neben angewandten Fragestellungen zu einem besseren Verständnis von der Verwendung von Feldspat als Dosimeter beigetragen. Wegen der Sättigung des OSL-Signals in den Proben wurde das infra-rot stimulierter Lumineszenz (IRSL)-Signal von Kaliumfeldspat zur Altersbestimmung verwendet. Mittels eines post-IR IRSL-Signals konnte die Chronologie des Untersuchungsgebietes geklärt werden: Die Alter weisen darauf hin, dass, abgesehen von einer geringmächtigen holozänen Lage (< 5m), der Großteil der ~50 m mächtigen Deltasedimente zwischen MIS 5 und MIS 10 abgelagert wurde.

Durch die OSL-Alter der Dünensedimente an der Ostküste Südindiens konnten die Dünenformation sowie die Sandmobilitätsphasen in einem zeitlichen Kontext erfasst werden. Die Ergebnisse lassen darauf schließen, dass die Küstendünen in der Region des Cauvery Delta periodischen Abläufen von Dünenformation und Reaktivierung seit dem Spätholozän bis heute ausgesetzt ist. Gründe hierfür mögen zum einen in Klimavariationen, aber zum anderen auch im Landnutzungswandel liegen. Der Sandmobilitätsindex, welcher auf Grundlage der maximalen Windgeschwindigkeit, der Niederschläge sowie der Evapotranspiration berechnet wurde, zeigt, dass die Dünen in der Region während des letzten Jahrhunderts größtenteils aktiv waren.

Die OSL-Datierungen von Strandwällen entlang der Westküste Südindiens konnten zeigen, dass es zwei Hauptphasen, eine ~ 3 ka und eine ~ 4 ka, der Formation gab. Zusammengenommen könnten diese Ergebnisse auf eine insgesamt aktive Phase der Strandwallformation vom Mittel- bis Spätholozän hindeuten, was ein Hinweis für den Rückgang des Meeresspiegels an der Westküste Indiens, vor allem an den Küsten Kerelas, zu dieser Zeit sein kann.

Die Erkenntnisse aus den einzelnen Studien tragen nicht nur zum Verständnis der regionalen Paläoklimas bei, sondern leisten auch einen Beitrag, den Klimawandel zu einer bestimmten Zeit in einem globalen Kontext zu beurteilen. Die Arbeiten zeigen interessante Veränderungen entlang von unterschiedlichen Küstenlinien seit dem Spätpleistozän auf, wodurch ein chronologischer Rahmen für das Ablagerungsgeschehen durch Transgression und Regression, Paläo-Trockenheit und verstärkte Windtätigkeit gegeben ist. Die Ergebnisse korrelieren gut mit der Transgression im Frühholozän und mit dem Meeresspiegelhochstand im mittleren Holozän sowohl in der südlichen Nordsee als auch an der Ost- und Westküste Südindiens.

ACKNOWLEDGEMENT

Here I attempt to acknowledge everyone who has lent their help and support during the past three years of my study. As the list is too long I hope you would forgive me for my briefness.

First I would like to thank the Leibniz Institute for Applied Geophysics and Deutsche Akademischer Austausch Dienst (DAAD) for their financial support and laboratory facilities during the entire course of my study.

I am extremely grateful to Prof. Dr. Manfred Frechen for introducing me to luminescence dating, for his continued support and confidence in me and for pushing me to work when I tended to get sloppy.

I am grateful to Prof Srinivasalu who has always supported me from the time I was his student during my post graduation and has been a part of many sampling visits we had in India during my doctorate studies. I would like to thank Dr. Ramesh Ramachandran for his help and for introducing me to Prof. Manfred.

I am grateful to Dr. Sumiko Tsukamoto for helping me understand the basics of luminescence, her valuable suggestions and timely help. I would like to acknowledge the support of my colleagues at the LIAG who from my first day in Germany have helped me through this “strange and new” environment to make it my home for the past three years. To mention a few of them, Ágnes Novothny, Alexander Kunz, Lara Wacha, Tobias Lauer, Christine Thiel, Tony Reimann and Esther Schmidt. Life is not just work but also a bit of fun and games and I enjoyed such evening gatherings also with Paul Königer, Susanne Stadler. Though I was a bit reluctant in the beginning, it all turned out to be fun and all of you helped me, especially during the last days of my stay in Germany. I would also like to thank Melanie Sierralta for her help in dealing with administrative formalities. My special thanks to my colleagues Gudrun Drewes, Petra Posimowski, Sonja Riemenschneider, Vollmer Karsten, Frank Oppermann and Sabine Mogwitz, at LIAG who always used to welcome me with a „wie gehts’ and helping me to speak German in a better way.

I thank my friend of many years Abhishekh for his help in preparing the maps in this thesis and Paneerselvam especially for sending samples to Germany. Special thanks to Christine for helping me with the formalities of submission. Father Matthew for his prayerful support and letting me enjoy a bit of South Germany. I enjoyed the company of

Mrs. Doreen Wissman and Dr. Eike Christian, and thank them for all their help throughout my stay in Germany. I thank all those who have directly or indirectly helped me during sampling especially colleagues from IOM and Department of Geology, Anna University, Chennai.

Without my parents, brother and sister I wouldn't be where I am today. From the humble settings of a village in the neighborhoods of Chalakudy to becoming a PhD student in Hannover my family has been with me through thick and thin. I will always cherish their undaunted confidence in me and my decisions. Anish chettan has shown good sense of understanding to help me out specially I was away from home. When I submit this thesis I keep few words of gratitude unsaid, fearing that it would be too shallow to ink it, for my brother and my wife Neetha. Neetha helped me to move on during many difficult occasions and her timely help has contributed significantly to shape this thesis. I also thankfully acknowledge the help of her parents and sister, particularly during the final stages of my PhD.

I see another tiny part of me in my son and I hope he would grow up to acknowledge this work. He never fails to bring a smile on my face whenever I hold him and I could enjoy a few moments of peace when all things were chaos around me especially during these last days before submission.

LINTO ALAPPAT

TABLE OF CONTENTS

Abstract	i
Kurzfassung	iii
Acknowledgments	v
List of Figures	viii
List of Tables	xii
Chapter 1 Introduction	
1.1 Coastal sediments as an archive of palaeoclimate information	1
1.2. Luminescence dating of coastal sediments	2
1.2.1. Notion of luminescence in minerals	3
1.2.2. Essentials of luminescence dating	4
1.2.3. Single Aliquot Regenerative Dose (SAR) protocol	12
1.2.4. Partial bleaching	13
1.2.5. Anomalous fading in feldspar	14
1.3. Sample collection	18
1.4. Origin and aim of the thesis	19
1.5. Outline of thesis	23
Chapter 2 Establishing the Late Pleistocene-Holocene sedimentation boundary in the Southern North Sea using OSL dating of shallow continental shelf sediments	
Abstract	34
2.1 Introduction	35
2.2 Geological setting	37
2.3 Materials and Methods	40
2.3.1 Samples	40
2.3.2 Optically stimulated Luminescence (OSL) dating	41
2.3.3 Experimental details	42
2.4 Age model decision-making process	50

2.5	Sedimentological and chronological results	54
2.6	Discussion	58
2.7	Conclusion	62
2.8	Acknowledgements	63
2.9	References	64

Chapter 3 Chronology of Cauvery delta sediments from shallow subsurface cores using high-temperature post- IR IRSL dating of feldspar

	Abstract	72
3.1	Introduction	73
3.2	Geology and Geomorphology of the area	74
3.3	Core descriptions	77
3.4	Analytical Procedures	79
	3.4.1 OSL of Quartz	82
	3.4.2 IRSL of K-feldspar	84
	3.4.3 Differential bleaching	85
3.5	Results	89
3.6	Discussion	90
3.7	Conclusions	92
3.8	Acknowledgements	93
3.9	References	93

Chapter 4 Evolution and chronology of late Holocene coastal dunes in the Cauvery delta region of Tamil Nadu, India

	Abstract	100
4.1	Introduction	101
4.2	Study area and samples	103
	4.2.1 Geology and geomorphology of the area	104
	4.2.2 Samples	106
4.3	Methods	111
	4.3.1 Luminescence dating	111
	4.3.2 Sedimentological studies	114
	4.3.3 Dune mobility index	115

4.4	Luminescence dating results	117
4.4.1	Tettagudi dunes	121
4.4.2	Sembodai dunes	122
4.4.3	Eastern coastal dunes	122
4.5	Results of sedimentological studies	124
4.5.1	Grain size analysis	124
4.5.2	Quartz grain surface morphology	124
4.5.3	Heavy mineral assemblages	126
4.6	Discussion	129
4.6.1	Luminescence chronology	129
4.6.2	Sediment provenance and transportation	130
4.6.3	Climate variability and dune reactivation	133
4.7	Conclusions	138
4.8	Acknowledgements	139
4.9	References	140

Chapter 5 Evidences of Late Holocene shoreline progradation in the coasts of Kerala, South India obtained from OSL dating of palaeobeach ridges

	Abstract	148
5.1	Introduction	149
5.2	Regional geology and Geomorphology	150
5.2.1	Study area and Sampling	153
5.3	Experimental details	157
5.4	Results	161
5.5	Chronology of beach ridges of Kerala	166
5.5.1	Late Pleistocene to Holocene scenario on Indian west coast	169
5.6	Conclusions	172
5.7	Acknowledgements	172
5.8	References	173

Chapter 6	Conclusions and future directions	177
	Curriculum Vitae	180
	Selbständigkeitserklärung	183

LIST OF FIGURES

- 1.1 Energy- level diagram depicts the luminescence process (adapted from Aitken, 1998). 4
- 1.2 Schematic representation of natural and laboratory processes involved in the luminescence dating study. Meter level shows luminescence signal strength at various stages of processes involved. 7
- 1.3 a) SAR growth curve showing signal saturation for a selected quartz sample(UG Lum: 1719) from Cauvery delta sediments (Alappat et al., 2010b) with inset showing the natural decay curve. b) Dose response curve using SAR protocol for a sample from Southern North Sea (Alappat et al., 2010a). Inset shows the decay curve for natural and regeneration dose. 8
- 1.4 Decay chains of Uranium (^{238}U), Thorium (^{232}Th) and Potassium (^{40}K) 11
- 1.5 IRSL signal as a function of time showing 3 components A1, A2, A3 separated using the curve fitting to three exponential functions. The remaining slower components are considered as a constant shown as Y0 in the figure. 16
- 1.6 Normalised Lx/ Tx as a function of time delay in the fading test of one sample. The rates of fading of three different components are shown. 17
- 1.7 Rate of fading (λ , %/ decade) for three components of 6 measured aliquots. Average fading rate for individual components of 6 aliquots are given. 17
- 1.8 Shows the variation in rate of fading (λ , %/ decade) for post IR-IRSL (225°C) and IRSL (50°C) for a sample collected from core sediments of Cauvery delta. 18
- 1.9 Diagram illustrates the sampling apparatus used in luminescence sampling of dunes. The portion of the sample marked (b) inside the tube is used for measurements after discarding disturbed outer part (a). 19
- 1.10 Digital elevation map of Southern North Sea area prepared using the DEM images of ASTER-GDEM, a product of METI and NASA. 20
- 1.11 Digital elevation map of South India prepared using the DEM images of ASTER-GDEM, a product of METI and NASA, showing both east and west coasts. 21

- 2.1 Map showing the core positions and bathymetry of the German sector of the North Sea (source: MARGIS/Digital atlas of the North Sea, DANS-Vo.9), http://www.awi.de/en/research/researchdivisions/geosciences/marine_geochemistry/marinegis/digital_atkas_of_the_north_sea/. The inset map shows the geographical location of the study area. 38
- 2.2 Quality-checking criteria tested for sample 26VC: a) Dose response curve using SAR protocol. Inset shows the decay curve for natural and regeneration dose. A preheat of 200°C and cut heat of 160°C were used and early background subtraction was applied to extract the fast component of the quartz decay curve. b) Dependence of dose recovery, recycling and recuperation ratios on various preheat temperatures. c) OSL signal as a function of preheat shows the rate of thermal transfer at different preheat temperatures. 43
- 2.3 Types of single aliquot D_e distribution observed in the study as shown by the scatter of measured D_e values for three samples (a (06VC), b (26VC) and c (35VC)). The Gaussian curve shows the relative probability of D_e values of individual aliquots to the weighted mean of the distribution. Dispersion values (RSD %) to that of the mean and weighted mean D_e distribution are also shown. The radial plot shows the weighted D_e distribution (filled circle in the shaded region) and D_e using the selected age model (blue shading) within two standard deviations of the distribution. 53
- 2.4 Schematic representation of core lithology and depth along the analysed transect (see inset). OSL and radiocarbon ages are shown. The estimated Pleistocene-Holocene 11.7 ka interface (yellow line) is based on lithology and the chronology derived from the current study. 56
- 3.1 Map showing the basic geomorphology of the Cauvery delta region. 75
- 3.2 Diagram showing the lithology and post- IR IRSL feldspar chronology of core Valangaiman and Uttarangudi. The ages presented are „fading-corrected-MAM’ age estimates (Table 3.2). 78

- 3.3 (a) Normalised OSL components observed during pulse annealing with medium and slow components showing thermal instability at increasing temperature. (b) SAR growth curve showing saturation for a selected quartz sample (UG Lum: 1719) with inset shows the natural decay curve. A preheat of 280°C and a cut heat of 260°C was used for all measurements. 83
- 3.4 The D_e distributions of selected samples are shown as frequency histograms with individual D_e values are plotted in ranked order. 88
- 4.1 Map showing the sampling locations and basic geomorphology of the study area. Inset, map of India shows the location of Tamil Nadu where the Cauvery delta is located (Fig. 1a). The drainage basin of Cauvery River is spread across parts of Karnataka and Tamil Nadu, from where it brings sediments to the coast (Fig. 1b). A detailed geomorphology map of the southern tip of Cauvery delta in Kodiyakkarai region showing successive development of beach ridges parallel and sub- parallel to the coast (Fig. 1c). 103
- 4.2 General geology map of the Cauvery river basin (Modified from Geological Society of India map appended to the textbook on the Geology of India by Vaidyanadhan and Ramakrishnan, 2008) 105
- 4.3 a) Picture showing the vertical profile of Tettagudi area (TKN-1) with different sand units and depth marked. Three OSL samples were collected from the profile (TKN-1A, TKN-1B and TKN-1C). **3b.** Diagrammatic representation of profiles in Tettagudi area (TKN-1 and TKN-2). Visible unconformities, stages of sand accumulation, grain size and measured OSL ages are shown. 107
- 4.4 Diagrammatic representation of profiles in Sembodai area (SBD-1, SBD-2 and SBD-3). Visible unconformities, stages of sand accumulation, grain size and measured OSL ages are shown. The inset map shows the lateral distribution of sample profiles with locations marked. 108
- 4.5 a) Picture showing the sampling profile in Puduppalli area (PP-1) in the eastern most coastal dune belt with different sand units marked. Three OSL

- samples were collected from the profile (PP-1A, PP-1B and PP-1C) and the measured OSL ages are given. **5b.** Picture showing the sampling profile of Vedaranniyam foredune (VDC-1) with different sand layers marked. Five OSL samples were collected from the profile (VDC-1A, VDC-1B, VDC-1C, VDC-1D and VDC-1E) and the measured OSL ages are given. The coarse grained shell bearing high energy event layer (most likely from the 2004 December Indian Ocean Tsunami) is marked with white hatched line. 110
- 4.6 Diagram showing the details of quality checking criteria tested for all the samples in the study. Test results of selected younger samples in the profile (VDB-1A, TKN-2A, SBD-2A, SBD-3A and VDC-1A) and older (TKN-1C, TKN-2E, KD-1A and PP-1C) samples are shown. A final preheat temperature of 160/180° C was selected for measurements and early background subtraction was applied to extract the fast component of the quartz decay curve. The plot shows the dependence of dose recovery, recycling and recuperation ratios on various preheat temperatures for the young (a, b) and old (c, d) samples. A fixed cut heat of 160° C was used for all the tests. For each temperature the mean of three aliquots and the standard deviation are shown. 113
- 4.7 OSL signal (D_e in Gy) measured after completely bleaching the sample plotted against different preheat temperature showing the rate of thermal transfer of charge at different preheat temperatures for selected samples. It is observed that there is a slight increase in OSL signal at higher temperatures ($>240^\circ\text{C}$) due to thermal transfer. 114
- 4.8 SAR growth curve from a young sample (TKN- 1A ; 73 ± 8 a) in the Tettagudi profile with an equivalent dose of 0.19 ± 0.01 Gy, showing OSL signals from regenerated laboratory doses as filled circles and that from a recycled dose as an open diamond. The sensitivity corrected natural OSL signal shown as filled square is interpolated onto the growth curve to give the equivalent dose (D_e : 0.19 ± 0.01 Gy). Inset is the natural OSL decay curve together with the OSL signal from a regenerated laboratory dose 0.23 Gy. b) The D_e distribution of 23 accepted aliquots showing a tight Gaussian curve indicating that the 117

samples were well bleached prior to deposition and exposed to a uniform radiation dose.

- 4.9 Plot showing the Lancaster's sand mobility index (M- index) for the last century. The measured OSL ages are plotted along with the calculated M-index values. Darker line shows the running average of mobility values and the lighter line in the background depicts the annual variation in the mobility index. The observed correlation with enhanced mobility values and OSL ages are highlighted with grey background. a) Sand mobility plot for the southern dunes (Nagapattinam) and b) for Northern dunes (Cuddalore region). The OSL ages for Cuddalore region was obtained from recent studies made by Kunz et al., (2010a, b). 123
- 4.10 Scanning electron microscope image shows the quartz grain surface textures for selected grains. a) Grain showing the crescentic shaped impact marks on the grains due to wind action. b) A moderately well rounded grain with the signatures of previous transportation event is largely masked due to the last event of aeolian transport of grain. c) An angular grain with freshly broken appearance indicating very little transport and source proximal deposition of the sands. d) A polished grain shows drag marks on the surface observed in the easternmost coastal dunes, likely to have been formed due to contact with bed during sub-aqueous transport by coastal currents. 125
- 4.11 Plot showing the correlation between the OSL ages and regional precipitation. The summer rainfall (SW) and annual rainfall (mainly SW and NE) for the Nagapattinam district is plotted (1901-2008) along with measured OSL ages as probability density function in which each peak represent maximum probability of certain event of sand movement. The dark line shows the running average of rainfall and observed correlation with OSL ages are highlighted with grey background. 135
- 4.12 Histogram showing the periods of sand mobility in Cauvery delta region during the last 3.5 ka. The OSL ages along with observed errors are shown for Nagapattinam (this study) and Cuddalore region (Kunz et al., 2010a, b). 137

- 5.1 Map showing the digital elevation model of Kerala prepared using the DEM images of ASTER-GDEM, a product of METI and NASA. The sampling locations are also marked in the map. 151
- 5.2 General geology map of the study area (Modified from Geological Society of India map) showing major rock formations exposed in the area along with drainage net work which contribute to the sediment input to the coastal plain. 152
- 5.3 Picture showing the vertical profile of Kooniparambu, Chaliyangad (KNP-1) with different sand units and depth marked. Four OSL samples were collected from the profile (KNP-1B, D, E and F. Visible unconformities and measured OSL ages are shown. 154
- 5.4 Picture showing the sampling profile in Cherakalpalli area (CKP (N)-1). OSL sample points, visible unconformities in the ridge and measured OSL ages are shown. 156
- 5.5 Diagram showing the details of quality checking criteria tested for all the samples in the study. Test results of two selected samples from the study (CKP (N)-1C and KNP-1D) are shown. Tests were carried out at two different cut-heat temperatures (160 and 180° C). A final preheat temperature of 160/180° C was selected for measurements and early background subtraction was applied to extract the fast component of the quartz decay curve. The plot shows the dependence of recycling and recuperation ratios on various preheat, cut-heat temperatures for the samples. For each temperature the mean D_e of three aliquots are shown. 158
- 5.6 Examples of distribution of selected samples having large scatter in the measured D_e values. Finite mixture model was applied for the samples and relative proportion of different distributions and D_e values are marked with hatched line in the background. Bold hatched line in the diagram indicates the selected D_e distribution for the age calculation. 165
- 5.7 OSL ages plotted against total number of samples measured in this study showing the periods of deposition of beach ridges centred at 3 and 4 ka. 170

LIST OF TABLES

2.1	Modified SAR procedure used for OSL quartz measurements.	44
2.2	Summary of data showing the radionuclide concentration, beta, gamma and cosmic-ray dose rate in the sample. Total dose rate is also given in mGy/a. A measured water content of $40 \pm 10\%$ was applied in the calculation.	46
2.3	Summary of data showing the sample details, single aliquot D_e distribution characteristics and statistics of the measured OSL quartz samples in the study. The number of accepted aliquots „n’ using the acceptance criteria are given with the total measured aliquots in the brackets. Sample ages obtained using different age models are shown. The favoured age model using the single aliquot decision-making process is highlighted in bold.	49
2.4	Summary of data showing the results of ^{14}C dating in the study. Non-calibrated and calibrated ages are shown. Calibrated ages are given in age BP.	50
3.1	Details of feldspar dose rate measurements. Internal potassium content (%) was measured from K-feldspar grains using solution ICP-OES and concentrations of U, Th and Rb in the K-feldspar grains were measured using solution ICP-MS analysis. The ^{40}K , Uranium and Thorium concentrations in the sediment was measured using high-resolution gamma spectrometer. An average water content of $15 \pm 5\%$ was applied in the calculation. * 150-250 μm , † 100-200 μm , ‡ 100-150 μm .	81
3.2	Summary of quartz measurement details (number of aliquots accepted/measured (n), D_e , and OSL age). Errors here and in Table 3.3 are $\pm 1\sigma$. §- minimum depositional age due to saturation of quartz OSL signal.	82
3.3	Summary of data showing the sample details, D_e distribution characteristics and statistics of the measured IRSL and post- IR IRSL. The over dispersion, σ_d represents the relative standard deviation of the measured single aliquot D_e distribution obtained using the „central age model’. The number of accepted aliquots „n’ using the acceptance criteria are given with the total	

measured aliquots in the brackets. Sample ages for IRSL and post- IR IRSL signals obtained using weighted mean D_e and minimum age model, fading rate (g) and fading corrected ages are shown. Inferred final ages are highlighted in bold. * 150-250 μm , † 100-200 μm , ‡ 100-150 μm .

87

4.1 Details of quartz OSL measurements of Vedaranniyam foredunes along with the zero dose sample (VDB-1A) collected from intertidal zone. The ^{40}K , Uranium and Thorium concentrations in the sediment was measured using high-resolution gamma spectrometer. An average water content of $6 \pm 3\%$ (Kunz et al., in press a, b) ($20 \pm 5\%$ for intertidal sample; VDB-1A) was applied in the dose rate calculation. The calendar years are calculated based on the sampling date in 2008 January. Over dispersion, σD represents the relative standard deviation of the measured single aliquot D_e distribution obtained using the „central age model’. The number of accepted aliquots ‚n’ using the acceptance criteria are given with the total measured aliquots in the brackets.

118

4.2 Summary of quartz measurement details (depth, radionuclide concentration, number of aliquots accepted/measured (n), D_e , dose rate, and OSL age) of inland and coastal dunes in Nagapattinam district. The ^{40}K , Uranium and Thorium concentrations in the sediment was measured using high-resolution gamma spectrometer. An average water content of $6 \pm 3\%$ (Kunz et al., in press a, b) was applied in the dose rate calculation. The calendar years are calculated based on the sampling date in 2008 January. The over dispersion, σD represents the relative standard deviation of the measured single aliquot D_e distribution obtained using the „central age model’. The number of accepted aliquots ‚n’ using the acceptance criteria are given with the total measured aliquots in the brackets. MAM was applied for few samples which showed significant scatter in their D_e values. The inferred final ages are given in bold. Errors here and in Table 1 are $\pm 1\sigma$.

119-
120

4.3 Data showing the details of heavy mineral analyses in the selected samples using optical microscopy. 300 grains from each sample was mounted on a glass slide and grains were counted for various heavy mineral assemblages. Percentage of heavies present in each sample is given.

128

- 5.1 Summary of quartz measurement details including depth, radionuclide concentration, dose rate, cosmic dose, D_e , number of aliquots accepted/measured (n), and OSL age of beach ridges of Kerala. The ^{40}K , Uranium and Thorium concentrations in the sediment was measured using high-resolution gamma spectrometer. An average water content of $6 \pm 3\%$ (Kunz et al, in press) was applied in the dose rate calculation. The over dispersion, $\square D$ represents the relative standard deviation of the measured single aliquot D_e distribution obtained using the 'central age model'. The number of accepted aliquots 'n' using the acceptance criteria are given with the total measured aliquots in the brackets. The inferred final ages are given in bold. Errors are given as $\pm 1 \sigma$. 162-163
- 5.2 Data showing the details of heavy mineral analyses in the selected samples using optical microscopy. 300 grains from each sample was mounted on a glass slide and grains were counted for various heavy mineral assemblages. Percentage of heavies present in each sample is given. 167

INTRODUCTION

1.1 Coastal sediments as an archive of palaeoclimate information

“Warming of the climate system is unequivocal, as is now evident from observations of increases in global average air and ocean temperatures, widespread melting of snow and ice and rising global average sea level...” (IPCC, 2007).

Climate change may happen due to natural variability or as a result of human intervention and usually lasts for an extended period of time. Studies on various aspects of the past climate suggest that climatic variability has occurred periodically in the past especially during the Quaternary period in response to various forcings, e.g. orbital variations and solar activity changes (insolation) (Wolff et al., 2010; Harrison and Goñi, 2010). The former occurs gradually, producing shifts in climate over thousands of years resulting in glacial and interglacial periods (Harrison and Goñi, 2010).

Palaeoclimate investigations are generally focused either on biological proxy records such as pollen (Scott, 1982; Farooqui et al., 2010), macro and micro fossils (Cann et al., 1988) and tree rings (Tegel et al., 2010; Shao et al., 2010; Büntgen et al., 2010; Luoto and Helama, 2010), or on geochemical/ geophysical records of ice cores, banded corals, foraminifera, speleothems, (Walker and Surge, 2006; Pellegrini and Longinelli, 2008; Wolff et al., 2010) and palaeomagnetic studies (Barletta et al., 2010) etc.

A change in climate immediately affects the coastal areas around the globe by causing changes in sea level. Accordingly, in the context of Quaternary climate change it is ideal to study sediment archives along the coast which may hold rich evidences of coastline advance and retreat as well as past variations in climate and its landscape response (Islam and Tooley, 1999). Reconstruction of palaeo sea level is a long and complicated chain, which involves recollecting the fragments of evidences left in nature, recording of those fragments, dating of the event in question and final interpretation of available data (Mörner et al., 2010). Quaternary landscape evolution is closely related to palaeoclimatological as well as palaeoenvironmental research, hence making it an integrative, interdisciplinary and multi-methodological field of science (Damm et al.,

2010). Coastal environments represent various landforms with both erosional and depositional features (e.g., shallow continental shelf regions, deltaic plains and beach ridges) that preserve thick sequences of Quaternary sediments. This offers an opportunity to investigate emergence and submergence of land based on the intricate relation between sea-level changes and tectonics (Chen et al., 2003; Cheong et al., 2003), sediment dynamics, instantaneous processes and events such as storms, hurricanes and tsunamis (Banerjee et al., 2001) as well as local environmental changes.

As far as chronology is concerned the most widely applied method in these coastal environments is the radiocarbon dating. In this method of dating organic material like peat and biogenic carbonate like molluscs and shells incorporated in to the deposits are used to reconstruct late Pleistocene to Holocene climatic variations. However hindrances such as absence of well preserved organic material in sediments and also when the age of the material is beyond the dating range of the method alternative methods in age determination of the strata are required. Another disadvantage of using organic material is the possibility that these might be included in the system by constant reworking that is seen in coastal areas. This leads to significantly erroneous results or the derivation of relative ages with respect to the organic material dated and may lead to misinterpretations. Moreover, the age range of radiocarbon dating is limited up to ~ 50,000 years (~9 to 10 half-lives of ^{14}C), as it depends on the half life of ^{14}C which is 5,568 years (Libby half life) (Hua, 2009). ^{14}C variations caused by a variety of natural and anthropogenic activities in the recent past (particularly since AD 1650- 1950) have resulted in large fluctuations (wiggles) in the calibration curve, which again decreases the precision of single radiocarbon dates (Hua, 2009). Radiocarbon dating becomes less reliable when the age range is >30,000 years BP as the results can be strongly affected by minor contamination and large standard deviations can result from limited sample size (Cann et al., 1988). A more widely applicable dating method will therefore be necessary to establish chronologies of coastal sediments.

1.2. Luminescence dating of coastal sediments

Luminescence dating has several advantages as a chronological tool in coastal environments over other methods. This includes the use of most abundant minerals like

quartz and feldspar as dosimeters for age determination, wide dating range, direct dating of events and provides ages in calendar years (Jacobs, 2008). Direct dating of materials is particularly important in dynamic settings such as coastal environments. In such environments Optically Stimulated Luminescence (OSL) is an ideal method as it has a wide dating range and is the only available method to date clastic sediments (quartz or feldspar) which are abundant in coastal areas. A few seconds (few minutes in the case of feldspar) of exposure to sun light make sand (quartz and feldspar) a suitable material for dating studies. However, care must be taken with respect to sands deposited immediately (like tsunamis, storm and hurricane deposits) (Murari et al., 2007) and in situations where solar radiations are inundated due to transporting medium that hinders the proper resetting of accumulated signal to zero from previous event.

1.2.1. Notion of luminescence in minerals

The luminescence (meaning „weak glow’ in Latin) occurs when an electron, which had received energy from ionizing radiation and was trapped in the crystal lattice, absorbs enough energy from light or heat then releases the energy as light. The mechanism of luminescence can be explained based on the energy band model. The concept of traps and centres which are responsible for luminescence in minerals are explained in Aitken, (1985; 1998). Briefly, when electrons are detached from parent nuclei in the valence band, they are diffused in to higher energy levels in the crystal lattice by ionizing radiation (Fig. 1.1a). Majority of the evicted electrons drop back down to the valence band soon after when it loses its energy and a few of them are trapped in the defect centres (Fig.1b). The defects in quartz are related to impurity atoms (e.g., Al or Ti) or O and Si vacancies, which are prone to modification when exposed to ionizing or particle radiation (Bahadur, 2006). Because of its nearly similar atomic size Al^{3+} can easily substitute for Si^{4+} in lattice and the charge compensation is provided in some cases by holes trapped at oxygen sites (Bahadur, 2006).

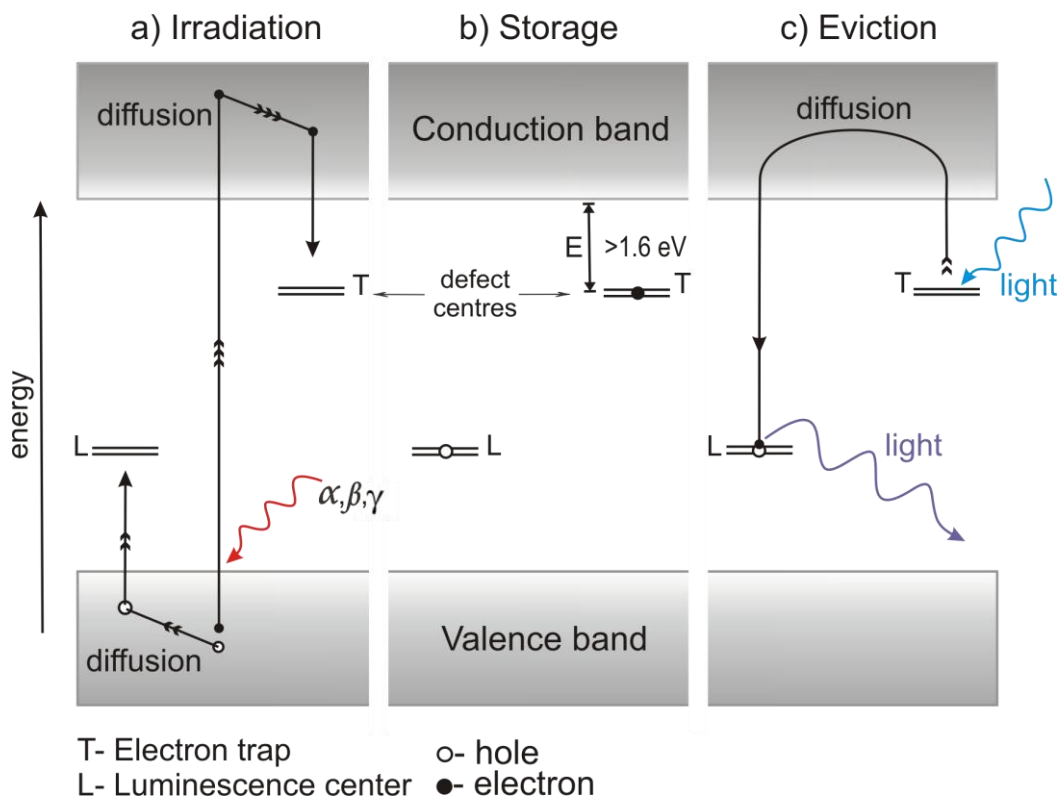


Figure 1.1. Energy- level diagram depicts the luminescence process (adapted from Aitken, 1998).

The electrons can remain for a prolonged period of time in thermally stable traps until the mineral is exposed to sufficient energy which releases the electrons from these traps. The removal of electron in the crystal lattice by radiation produces a deficiency of negative charge in the valence band termed as hole (Fig. 1.1a). A recombination centre (luminescence centre) forms when the hole is trapped at a defect with a negative charge and attracts free electrons (Fig. 1.1b). The excitation of traps with light or heat, releases the electrons from these traps and recombines it with the hole at luminescence centres (radiative recombination centres) which release photons (Fig. 1.1c). Longer exposure to nuclear radiation increases the number of trapped electrons in the crystal.

1.2.2. Essentials of luminescence dating

In the early 1960s Thermoluminescence (TL) dating was used in archaeology to date ceramic materials, pottery and fired clay (Aitken et al., 1964; Zimmerman, 1967;

Zimmerman and Huxtable, 1971). Later, in 1985 (Huntley et al., 1985) with greater understanding of the phenomena of stimulation and bleaching of sediments and the responsive signal led to development of OSL dating technique. Since then it has been applied to a wide range of sedimentary archives, mainly glacial (Gemmel, 1999; Klasen et al., 2006; Duller, 2006), fluvial (Thomas et al., 2007; Jain and Tandon, 2003; Lauer et al., 2010), aeolian (Roberts, 2008; Singhvi and Porat, 2008; Frechen et al., 2003, Frechen et al., 2004, Singhvi et al., 2001) and lacustrine (Juyal et al., 2009) deposits and archaeological materials for dating where conventional dating techniques are inadequate due to the lack of proper dating materials or time specific dating limits. Wintle, (2008a) narrates a comprehensive description of the history of luminescence dating method and developments over the last five decades. The method is useful for a broad range of time from few tens of years (Ollerhead et al., 1994; Ballarini et al., 2003; Madsen et al., 2005; Clemmensen and Murray, 2006) to more than a hundred thousand years (Stokes et al., 2003). The upper limit of quartz OSL signal is considered as being close to Eemian (MIS 5e, 116-132 kyr) unless the dose rate is low (Huntley et al., 1993; Wintle, 2008b). Bailey (2000a) suggested that the thermal stability and high dose saturation characteristics of the slow component in quartz show a great deal of potential for long range dating (e.g., Singarayer et al., 2000; Rhodes et al., 2006), though in this case signal resetting may be of concern. On the other hand, IRSL dating of feldspar can yield much older ages of up to ~350ka (Alappat et al., 2010b).

A comprehensive description on the basic principles of luminescence dating technique and its physical background is provided in the books of Aitken (1985; on thermoluminescence) and Aitken (1998; optically stimulated luminescence dating of sediments). The contemporary developments in OSL dating methodology and instrumentation are provided in the book of Bøtter-Jensen et al. (2003). Periodical reviews on OSL dating (Wintle, 2008b) and protocols are presented in number of publications among which the recent ones concerning the SAR protocol are given in Murray and Wintle, 2000 and Wintle and Murray, 2006. Preusser et al. (2010) provides detailed description of quartz as natural dosimeters, dealing with its origin, structure, defects as well as its applications and problems encountered. The following short summary of background to optical dating can be seen elaborated in these key sources.

Luminescence dating makes use of the quality of certain minerals to absorb energy from the natural radioactivity of surrounding sediments and accumulate it over time in defect centres in its crystal structure. Optically stimulated luminescence is the ray of light

emitted from a crystal when it is stimulated using a light source and the emitted light is proportional to the energy absorbed in the crystal from previous exposure to radiations. The release of luminescence can also take place upon the stimulation of traps by heat and in such cases it is termed as thermoluminescence. The prerequisites for the application of OSL dating in an insulator or semi-conductor (metals have no luminescence) is that the material must have absorbed energy for a certain period of time while being exposed to ionizing radiation and emit photons after being stimulated by a light source (as explained by Mckeever (1985) for thermoluminescence). The presence of activators (such as impurity atoms and lattice defects) and its ability to absorb and store radiation energy in the crystal is essential in luminescence dosimetry.

Among other conditions for the application of this method, the most important is that the trapped electrons which contribute to luminescence in the minerals are reduced to zero level at deposition. The rock forming minerals are weathered, disintegrated from the parent rock and transported by natural agents like wind, river, glaciers etc, deposited and buried (Fig. 1.2). These cycles may repeat a number of times in the life time of a mineral grain and luminescence dating provides age for the latest event of burial. During transportation the mineral grains are exposed to sunlight and results in depletion of previously absorbed signals (bleaching) each time before deposition. In case of aeolian deposits, the sand grains are transported by a mechanism called „saltation’ in which the grains are raised in to the air by blowing wind when a certain threshold velocity is reached. This process makes the grains well exposed to sunlight and the mineral grains are generally well bleached. The problem of partial/ heterogeneous bleaching is described in a separate section (1.2.4).

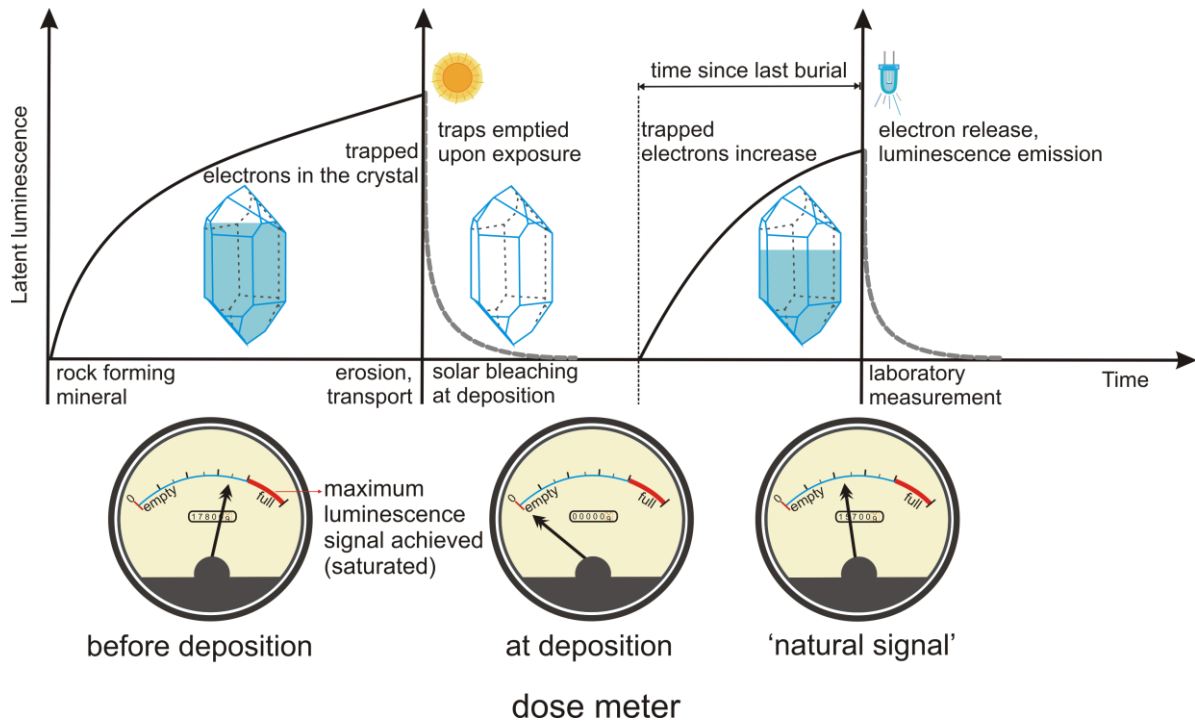


Figure 1.2. Schematic representation of natural and laboratory processes involved in the luminescence dating study. Meter level shows luminescence signal strength at various stages of processes involved.

In a fluvial regime the sand grains are either transported as suspended material or as bed load. In case of bed load transport or due to turbidity in water the light intensity to which the mineral grains are exposed may be attenuated to various degrees and the degree of bleaching becomes different for individual grains. This would result in the minerals retaining some of the residual signal from a former event of deposition and the grains are partially/ differentially bleached (Olley et al., 1999). During glacial transport also a similar problem arises as sand may be transported as grains entrapped inside the ice sheet or as mass movement which will hinder the proper draining of signal. However, in many natural depositional settings the grains are well exposed to sunlight for a sufficient time and the luminescence signal is set to zero before deposition. The natural signal absorbed by the mineral grain increases over time and measured luminescence signal is directly proportional to ionizing radiation absorbed by the mineral after deposition. The grains are then buried and sealed off from light after deposition. During laboratory measurements this signal level is measured by stimulating the mineral to a focussed beam of light and the

trapped electrons are released in a process called radiative recombination which emits luminescence and counted using a highly sensitive photomultiplier tube. An analogy of a fuel meter is used in the illustration (dose meter in the figure 1.2) to exemplify the luminescence signal strength in a mineral grain at various stages in the process. The latent luminescence signal is grown up to a high level during burial until the last stage of erosion and is then emptied to zero level during transport and deposition (Fig. 1.2). When the mineral grains are buried for an extended period of time, the traps are completely full or occupied and in such a case no more electrons can be trapped. This is termed as „saturation’ (Aitken, 1998; Wintle and Murray, 2006) in terms of luminescence signal (Fig. 1.2).

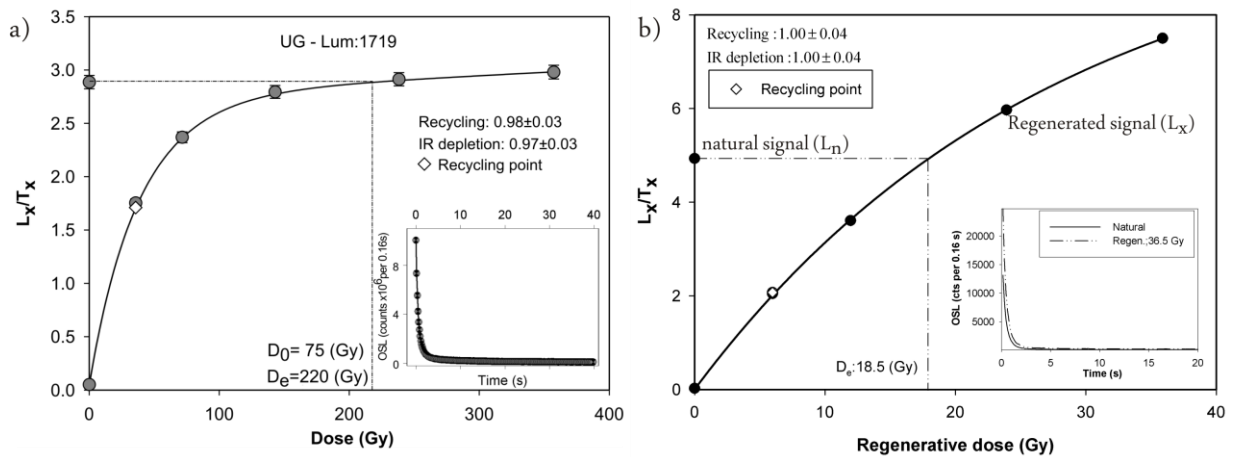


Figure 1.3. a) SAR growth curve showing signal saturation for a selected quartz sample (UG Lum: 1719) from Cauvery delta sediments (Alappat et al., 2010b) with inset showing the natural decay curve. b) Dose response curve using SAR protocol for a sample from Southern North Sea (Alappat et al., 2010a). Inset shows the decay curve for natural and regeneration dose.

Dose is the measure of absorbed energy released from the sample in the form of photons during radiative recombination when stimulated with light of a particular wavelength. The photon counts are proportional to the trapped electrons in the mineral grain and are considered to be completely related to the last burial event. Total absorbed energy in the sample is obtained by projecting the natural dose (natural OSL signal) to the

dose response curve of artificially induced known dose (regenerative dose) points (Fig. 1.3a and b). The corresponding dose equivalent (equivalent dose, D_e) of the natural OSL signal to the regenerated OSL signal is calculated. D_e is therefore the level of artificial dose which is required to produce identical amount of natural OSL signal in the sample. It would be possible to obtain a meaningful value of D_e when the natural signal (L_n/T_n) is no more than 85% of maximum achievable value (Wintle, 2008b). D_0 is the dose saturation level which controls the maximum age limit that one sample can reach for luminescence dating (Singarayer and Bailey, 2003). It is considered that a D_e value should not exceed $2D_0$ in order to produce a good age estimate (Wintle and Murray, 2006). Such a case was encountered in the present study, for example in sample Lum. 1719 recovered from Cauvery delta sediments (Fig. 1.3a) it was not possible to determine true D_e value using quartz OSL. This was because the corrected natural luminescence intensity (L_n/T_n) was greater than the signal at saturation shown by the saturation exponential in combination with linear curve fitted to the regenerated points.

The rate of accumulation of trapped electrons, referred to as Dose rate (D) is normally considered as constant throughout the burial. The natural dose rate in sediments is expressed as gray per thousand years (Gy/ka^{-1}). Total dose rate of a sample includes the beta dose rate, gamma dose rate and cosmic ray component. A sand size grain receives less alpha dose rate than a silt size since the maximum range of an alpha particle in a silicate grain is $\sim 20 \mu m$ (Aitken, 1985). The maximum range of beta particle in sand is $\sim 2 mm$. Since the range of alpha and beta particles are related to the diameter of the grain, grain size plays a significant role in the calculation of alpha and beta radiation contribution in a mineral grain. The HF etching of quartz extract carried out prior to measurement usually removes the alpha irradiated outer layer of the mineral grain to nullify the effect of alpha dose rate. Radiation dose for the buried sample is mainly derived from the decay of naturally occurring radionuclides such as ^{235}U , ^{238}U and ^{232}Th and their daughter nuclides as well as ^{40}K (Fig. 1.4) and ^{87}Rb ($\sim 1\%$ of annual dose rate) present in the sample and its immediate surroundings. The beta and gamma dose rates were obtained by determining the concentrations of these isotopes using a high purity germanium detector (HPGe detector, Canberra Ltd. N-type and Marinelli). The radiation dose received by a sample can be calculated from bulk of the sample (700g/ 50 g) using Gamma spectrometry. The cosmic ray flux reaching the earth's surface also contributes a small extent in the annual dose received by the sample. The cosmic dose varies over sample burial depth, altitude and

geographical location (Prescott and Stephan, 1982; Prescott and Hutton, 1994). Uranium and thorium are responsible for the majority of naturally occurring radioactivity. The radioactive decay of these elements produces several daughter products such as Ra, Rn and several isotopes of Po, Pb and Bi. In radioactive decay chains (Fig 1.4) the radioactive parent decays in to daughter nuclei until it reaches a stable isotope (^{206}Pb and ^{208}Pb for ^{238}U and ^{232}Th respectively). Some of these daughter products are significant emitters of a variety of radiation (α -, β - and γ -radiation). The α - and β -particle contribution in to the total annual dose rate originates mainly from the radionuclides present within the mineral grain due to limited penetration distance for these particles. The γ -component of dose rate arises from radionuclides present in the surrounding sediments. The radioactive decay chains of ^{238}U , ^{232}Th and ^{40}K are shown in figure 1.4.

The age of the sample is then calculated by dividing the amount of radiation absorbed since burial (D_e) by the dose rate of the surrounding sediments (Aitken, 1998).

$$\text{Age} = \text{Equivalent dose } (D_e) \text{ (Gy)} / \text{Dose rate } (D) \text{ (Gy/a)}$$

The movement of water through sediments can affect the concentration of soluble isotopes and cause disequilibrium of the isotopes in the uranium and thorium decay chains. Water content in soil causes attenuation of radiation dose and also leads to the dissolution and re-precipitation of carbonate in sediments, which affects dose rate in sediments (Aitken, 1985). In situ water content in the sediment was determined to the measured dry weight (at 110°C) of the sample and was incorporated in the beta and gamma dose rate calculation for correcting of dose rate attenuation in the sample due to moisture content.

Application of OSL dating on coastal sediments...

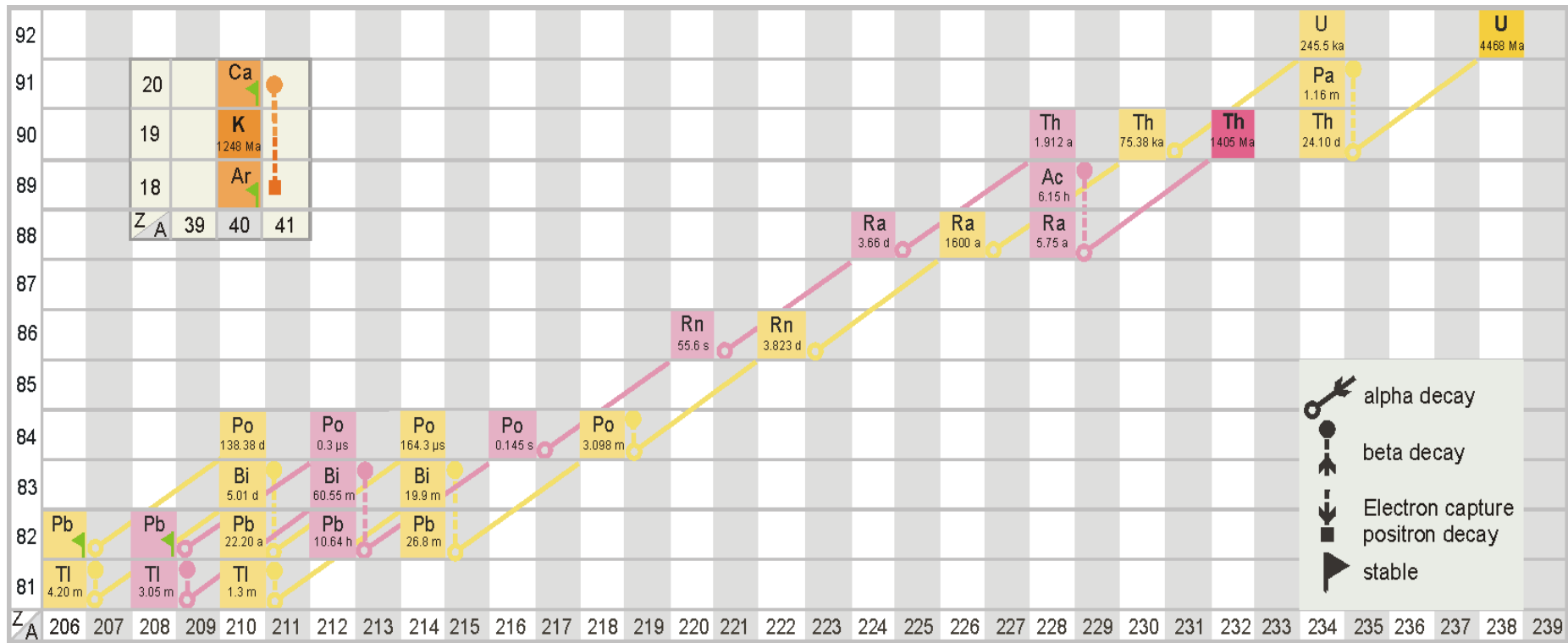


Figure 1.4. Decay chains of Uranium (^{238}U), Thorium (^{232}Th) and Potassium (^{40}K)

1.2.3. Single Aliquot Regenerative Dose (SAR) protocol

The development of single aliquot regenerative-dose (SAR) procedure (Murray and Wintle, 2000) marks a great advancement in the field of luminescence dating because of its improved accuracy and precision due to extensive tests incorporated in every step of the measurement. In the present study this widely accepted protocol (Murray and Wintle, 2000) was used for the measurement of quartz and feldspar minerals. SAR procedure makes repeated measurements on each aliquot to obtain a dose response curve and the natural luminescence intensity measured in the initial cycle of the protocol is then projected to this curve to get the equivalent dose, D_e (Fig. 1.3a, b).

Some internal checks are employed in the SAR protocol to evaluate the validity of the protocol applied for measurement. Preheat is an indispensable part of SAR cycle which helps to empty any light sensitive shallow traps, particularly filled during laboratory irradiations (Wintle and Murray, 2006). The preheat conditions were chosen from a plateau of D_e responses for different preheat temperatures (for quartz, 160-260°C for 10 s each with a fixed cutheat temperature of 160°C). The samples behave differently to the preheat treatments and may cause sensitivity changes and lead to unwanted charge transfer to the light sensitive traps. SAR protocol assumes that the OSL sensitivity of the test dose (T_i) should be directly proportional to the prior natural/regenerative dose (L_i) (Murray and Wintle, 2000, Wallinga et al., 2000). The change in the luminescence sensitivity per unit dose is explicitly monitored by the subsequent test dose (T_x) and a sensitivity corrected luminescence response is obtained by dividing the natural (L_n) and regenerated luminescence curve (L_x) intensities by their respective test dose intensity (T_x) (Murray and Wintle, 2000). A sensitivity corrected SAR growth curve was obtained by plotting the value L_x/T_x against the dose applied in the SAR cycle and the value of L_n/T_n is then interpolated to this growth curve to get D_e (Murray and Wintle, 2000). The protocol requires that the changes in luminescence sensitivity are adequately corrected for a minimum of three measurement cycles (natural dose with two regeneration dose cycles) (Bailey, 2000b). The robustness of the method to accurately date samples are tested by a recycling point (Fig. 1.3b) (the ratio of measurements of the first regenerated dose with that repeated at the end of the cycle), generally 2 and 6 cycles and the zero regeneration dose point (should yield values close to zero during the subsequent treatment). Any non- zero sensitivity corrected signal obtained from the zero regeneration

dose may be expressed in percentage to the natural signal and is termed as recuperation. This is derived as a result of charge transfer from deeper traps due to previous irradiation, optical stimulation and preheats (Wintle and Murray, 2006). SAR protocol provides high precision estimates of D_e , commonly with overall uncertainties of <5% (Bailey, 2000b; Wintle and Murray, 2006). A dose recovery test was performed as a routine test for all samples to ensure the accuracy of D_e values estimated and the efficiency of the protocol to recover a given dose (Roberts et al., 1999; Murray and Wintle, 2003). The test requires resetting the natural signal level to zero by artificial stimulation and gives a known laboratory dose to the sample. For ideal measurement conditions the SAR protocol recovers the given dose close to unity, which underlines the choice of heat treatment and test dose in the measurement cycle.

The protocol estimates individual D_e values for a number of subsamples on different aliquots and provides an accurate outcome from a distribution of D_e values of the same sample. A detailed description of this procedure for quartz and feldspar can be found elsewhere (Murray and Wintle, 2000; Wallinga et al., 2000; 2007; Wintle and Murray, 2006). The protocol is also advantageous as it provides an insight into the bleaching and depositional events of the sediment. This is carried out by analysing the scatter in the distribution of D_e values by with little variance in the D_e distribution of well bleached samples (Stokes et al., 2003). SAR can be applied either to aliquots of multiple grains (Single aliquots, Duller, 1991; 1994; 1995) or single grains (Murray and Roberts, 1997; Duller, 2008) based on the sample properties and latter was found to be preferable for sediment samples of poorly bleached and reworked sediments (Duller, 2008).

1.2.4. Partial bleaching

Incomplete bleaching of luminescence signal prior to deposition is a major hindrance in the application of OSL dating in fluvial environments. Attenuation of light in the water column minimizes signal resetting (Berger, 1990). The major factors which influence the bleaching of fluvial sediments are water depth, suspended sediment concentration in water, mode of transport (by suspension or bed load transport) and transporting distance (Rittenour, 2008). Two types of methods are evolved to extract true burial age from partially bleached samples. One method uses separation of multiple components in luminescence signal by isolating the most bleached fast component in the signal (Tsukamoto et al., 2003; Jain et al.,

2005). The second method reduces number of grains in each aliquot to as small as few tens (Olley et al., 1998) or uses the single grain technique (Duller, 2008). Agersnap Larsen et al., (2000) studied the use of LM-OSL technique for the detection of partial bleaching in quartz. They found that the ratio of the OSL signals due to the beta dose from the partly and fully bleached aliquots is an indicator of the degree of optical resetting of the OSL signal in a mineral grain. Many statistical techniques are proposed (Olley et al., 1998; Galbraith et al., 1999; Fuchs and Lang, 2001; Jain et al., 2002; Lepper and McKeever, 2002) for the extraction of most likely set of D_e values from the scattered population of D_e distribution. This depends on the mechanism that causes the scattering in D_e value such as heterogeneous bleaching, post-depositional reworking and/or beta dose variation in the surrounding sediments (Bailey and Arnold, 2006; Arnold et al., 2007; 2009).

Owing to the sub-aerial transport of aeolian sediments it is reasonable to assume maximum resetting of residual signal to zero prior to deposition. However it is possible that the saltation of sand grains may accompanied by a cloud of fine dust in the dry land and this will attenuate the sum of light reaching the grains (Singhvi and Porat, 2008). Other factors which may contribute to the scattering in D_e values in a desert environment include non-uniform exposure of solar radiation (Lomax et al., 2007), iron oxide coating on grains at varied levels (Singhvi et al., 1983; 1986) and variation in beta dose in the sample (Mayya et al., 2006; Morthekai, 2007).

The concept behind using small aliquots with less number of grains is that in a multigrain aliquot, sediments may consist of grains that have received different light exposure energies, forming grains having variable residual signal during deposition. The measurements using small aliquots with minimum number of grains and single grains have the advantage that variability in the residual level of the grains will be minimum and hence the averaged signal could be close to the true dose.

1.2.5 Anomalous fading in feldspar

Luminescence of feldspar is significantly brighter than that of quartz when optically or thermally stimulated and as its level of luminescence saturation is much higher (Auclair et al., 2003; Huntley and Lamothe, 2001) it can provide a good estimate of burial age even for relatively old sediments (Wallinga et. al., 2007). The beta dose from internal radioactive

elements of ^{40}K and ^{87}Rb from the lattice structure contributes significantly to the total dose rate of the K- feldspar. Thus, the contribution of external nuclear radiation is lower and therefore less vulnerable to environmental dose rate fluctuations (Wintle, 2008b; Li et al., 2008). However feldspar has slow bleaching rate upon exposure to sunlight when compared to quartz (Aitken, 1985; Godfrey Smith et al., 1988; Spooner, 1993; Porat et al., 2008).

It has been reported by many authors (Wintle, 1973; Spooner, 1994; Huntley and Lamothe, 2001; Huntley and Lian, 2006; Wallinga et al., 2007) that feldspar shows the phenomenon of anomalous fading due to the instability of a few electron traps (Aitken, 1985). This results in spontaneous declination of signal intensity which causes significant age underestimation and so correction procedures were proposed for the linear part of the growth curve for this phenomenon (Huntley and Lamothe, 2001). Further detailed description and physical mechanism behind anomalous fading can be found in Aitken (1998 - Appendix D). Anomalous fading can be detected by comparing luminescence intensity of prompt measurement to those of delayed measurement on artificially irradiated aliquots (Auclair et al., 2003).

The time elapsed since irradiation, t^* , is calculated by considering the time from half of samples' irradiation until the beginning of the measurement ($t^* \approx t_1 + (t_2 - t_1) / 2$; Eq. by Auclair et al., 2003). The samples were subjected to measurement after delay in time of various orders of magnitude for prompt to delayed measurement with a respective increase in scale in delayed time since irradiation. It was then plotted on a logarithmic scale with the respective IRSL intensities against the elapsed time since irradiation. Individual fading rates were then calculated using the formula of Huntley and Lamothe (2001). The g value was calculated as a measure of fading rate corresponding to the unit of percentage per decade, which was used to correct the IRSL ages when the D_e values of respective samples falls within the linear part of the dose response curve (Huntley and Lamothe, 2001).

It was observed that the fading rate varied over the IRSL decay curve from the initial part to the latter (Tsukamoto et al., 2006; Thomsen et al., 2008) resulting in a significant difference in g value and hence the corrected age. The steadily declining CW (CW- IRSL) signal from coarse grain feldspar was separated into three different components (A_1, A_2, A_3), using the curve fitting to three exponential functions (Fig. 1.5). The remaining long-lived components of the decay curve were considered as constant for the purpose of fitting (Tsukamoto et al., 2006). The areas of decay curve (0.1-1s and 10-11s) were verified for the

reliability tests of preheat, recycling, recuperation and dose recovery and found to be within the acceptable range of uncertainty, which were used for comparison and age calculation. The rate of fading (g' value % per decade) was calculated for three different components of the IRSL decay curve which eventually showed a very high fading rate for the first A_1 component (18 ± 5 for average of 6 aliquots) and much lesser for A_2 and A_3 (1.6 ± 0.5 and 1.3 ± 0.4 respectively) components (Fig. 1.7). This was reported previously by Novothny et al., (2010a, b) for their studies on cover sands of Hungary.

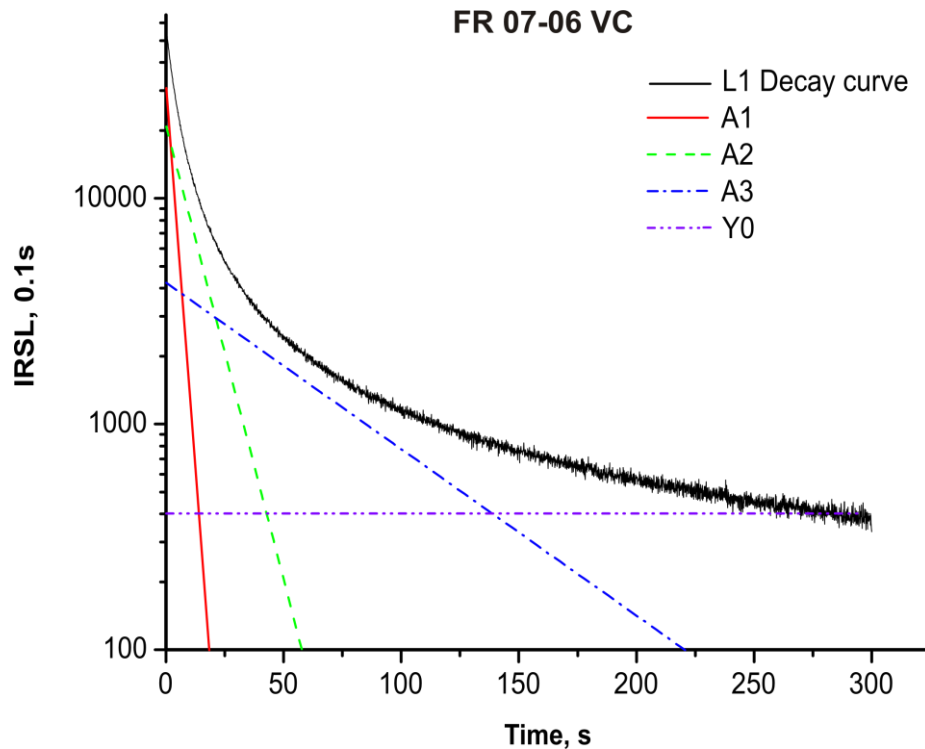


Figure. 1.5. IRSL signal as a function of time showing 3 components A_1 , A_2 , A_3 separated using the curve fitting to three exponential functions. The remaining slower components are considered as a constant shown as Y_0 in the figure.

The sample under study showed a strong fading for the initial part of the signal and less fading towards the later part of the signal (Fig. 1.6; 1.7). The later integrals (10-11s) were used for age calculation in order to avoid the strongly fading A_1 component (Fig. 1.6; 1.7). It was observed that the short lived components (<1 ; 3-4 μ s) which dominate the initial part of the CW IR-OSL decay curve are more likely to be associated with fading (Tsukamoto et al., 2006).

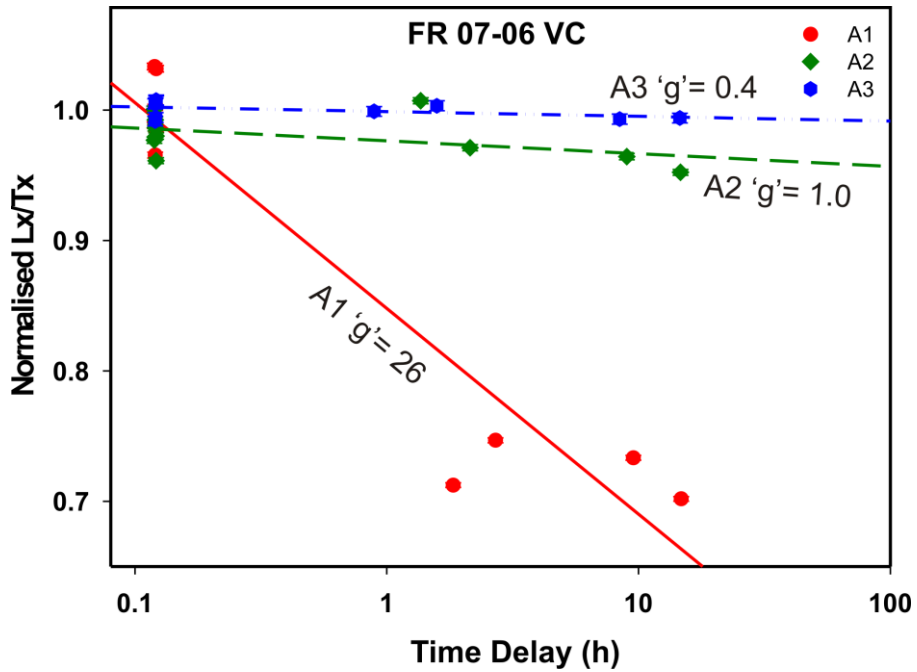


Figure 1.6. Normalised L_x/T_x as a function of time delay in the fading test of one sample. The rates of fading of three different components are shown.

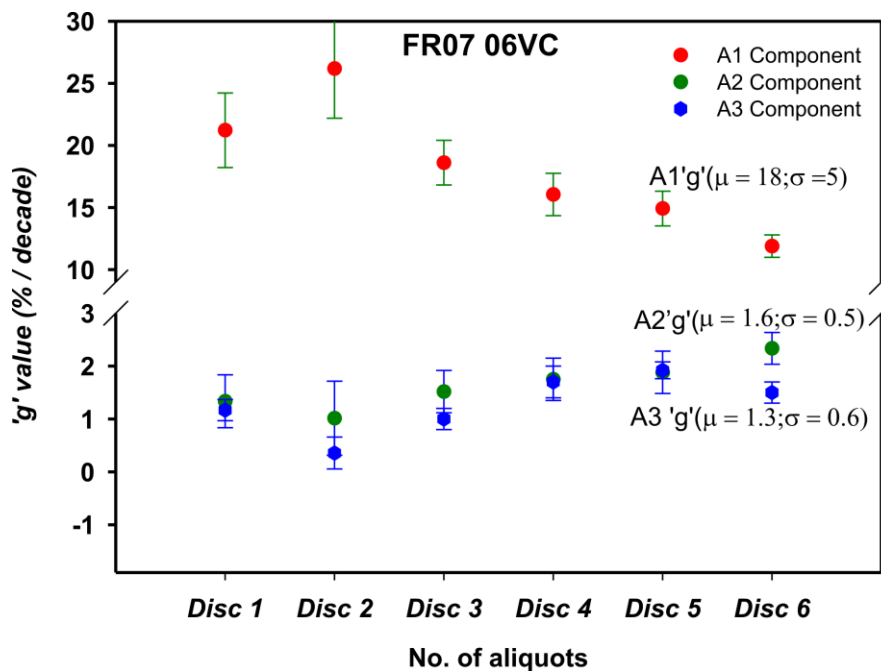


Figure 1.7. Rate of fading ('g', %/ decade) for three components of 6 measured aliquots. Average fading rate for individual components of 6 aliquots are given.

It has been demonstrated by previous findings (Thomsen et al., 2008; Buylaert et al., 2009) that the use of an elevated temperature for IRSL measurements reduces laboratory fading rates considerably compared to the IRSL signal measured at 50°C which was also observed in the present study. The protocol uses an identical heat treatment of 250°C for 60s prior to the regenerated and test dose IRSL measurements and a 40s high temperature (290°C) hot bleach at the end of each cycle. The IRSL signal was first measured at 50°C and then at 225°C for 100s. The D_e values were calculated for both stimulation temperatures by integrating the initial 2s of IRSL signal with the last 10s of signal subtracted as background. The example of fading rate for both IRSL and post-IR IRSL are shown in the figure 1.8 for a sample from Cauvery delta, south east India.

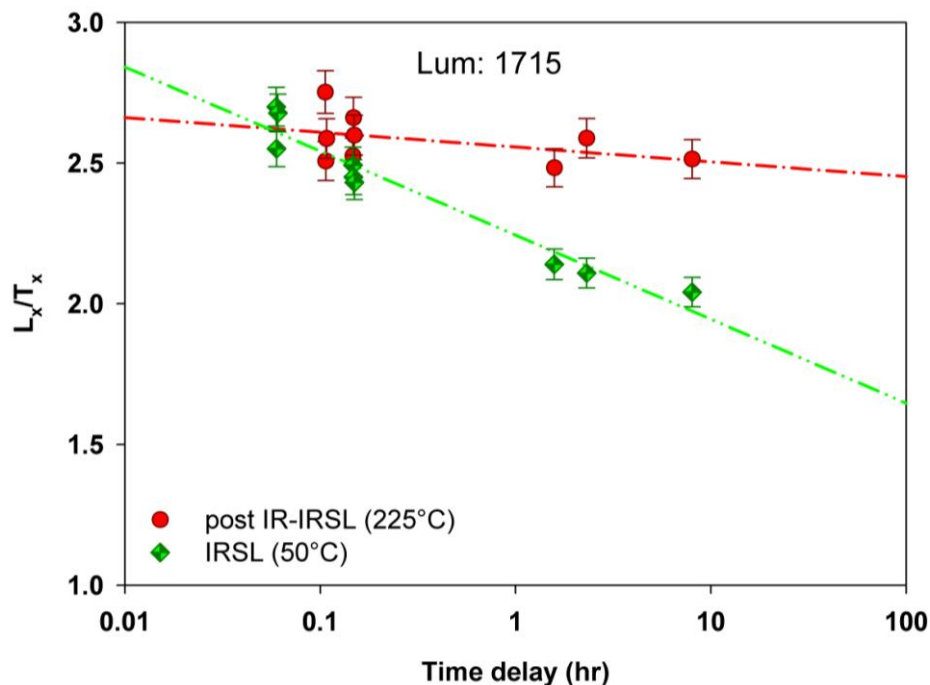


Figure 1.8. Shows the variation in rate of fading (g , %/ decade) for post IR-IRSL (225°C) and IRSL (50°C) for a sample collected from core sediments of Cauvery delta.

1.3. Sample collection

Samples from different parts of the German North Sea were collected using vibrocores (maximum length 6 m) (Fig. 1.10) during a sampling campaign with M/V Franklin in July

2007. Core samples (average depth of ~50m) were recovered from different parts of the Cauvery delta as a part of a shallow subsurface study programme.

In the east and west coast of south India sampling was carried out from clean faces of the profiles made on a vertical wall of the dunes/ beach ridges, which helped to identify different beds and structures. The profiles were made on the stable slopes or most stabilised part of the dune to minimise the possibility that the upper layers collapsed due to slope failure or removal of bottom sands because of human interference. Wherever possible, pits were excavated further down to the ground in order to retrieve sample from the bottommost level feasible. OSL samples were collected by driving 15x 6cm opaque PVC tubes horizontal to the surface (Fig 1.9) from all representative beds and from places where visible unconformities could be identified. Samples for gamma measurements (~700g) were collected from 10cm surroundings of the OSL sample. From samples used for OSL measurements the outer 1.5 cm was discarded to avoid possible contamination of light exposed outer parts while recovering the sample (Fig. 1.9).

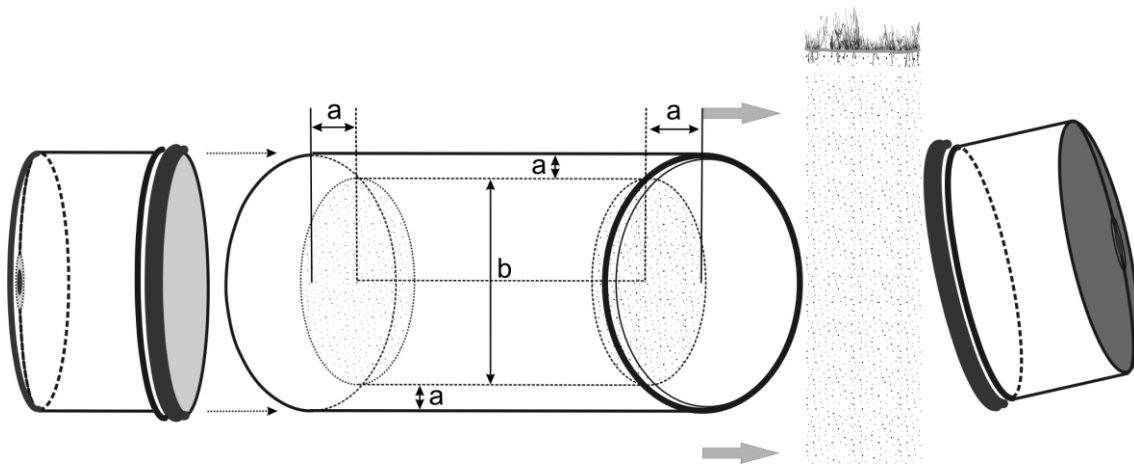


Figure 1.9. Diagram illustrates the sampling apparatus used in luminescence sampling of dunes. The portion of the sample marked (b) inside the tube is used for measurements after discarding disturbed outer part (a).

1.4. Origin and aim of the thesis

Coastal features including coastal dunes (Ballarini et al., 2003; Porat and Botha, 2008; Kunz et al., 2010; Reimann et al., 2010), marine terraces (Choi et al., 2003a, 2003b), beaches

and associated landforms (beach ridges, raised beaches, beach rocks (Berger et al., 2003), aeolianites, palaeosols, tsunami (Murari et al., 2007) and storm deposits (Banerjee et al., 2001), estuarine and tidal-flat sediments (Gerdes et al., 2003) as well as deep and shallow marine sediments (Alappat et al., 2010a) have been subjected to various studies in the past to understand the palaeoclimate and response of world coastline on climate change. A geochronological frame is critical for the proper interpretation of environmental responses to past climatic and sea level changes and precipitation variations and is important to assess and mitigate terrestrial responses to varying climate. The potential of coastal sediments which are currently submerged or formed as shallow sea due to change in global sea level have great potential in studying palaeoclimate by establishing its chronology.

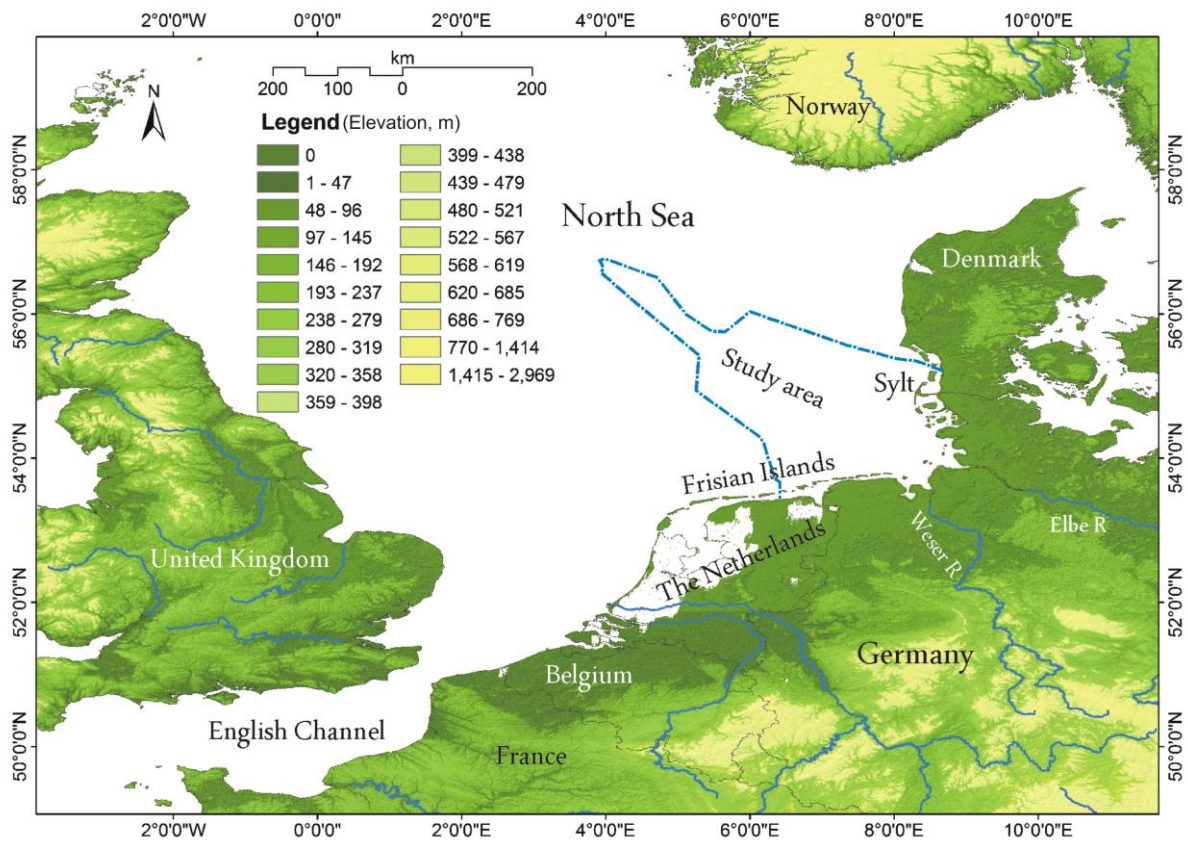


Figure 1.10. Digital elevation map of Southern North Sea area prepared using the DEM images of ASTER-GDEM, a product of METI and NASA.

The first aim of this thesis is to examine the potential and suitability of OSL dating in establishing the chronology and sedimentation history of Upper Pleistocene glacio-fluvial and -lacustrine sands and the overlying Holocene basal peat and/or clastic shallow marine sediments in the German sector of the North Sea (Chapter 2; Fig. 1.10). The outcome of the

study can subsequently be used for subsurface geological mapping and modelling of the analysed area and can further substantiate the proposed relative sea-level curve for the region.

Reconstruction of coastal evolution on a decadal to century resolution provides information about the coastal system processes, which will help in the planning and implementation of coastal management tools and policies and coastal defence planning (Ballarini et al., 2003). There is very little knowledge and no continuous high resolution terrestrial proxy climate records that have been studied in detail for southern peninsular India (Fig. 1.11). Such records are especially scarce for the Cauvery delta (Fig. 1.11) which is one of the major sediment repositories in peninsular India and biggest of such in the east coast of Tamil Nadu. In order to fill these void shallow subsurface sediments of this delta were studied using luminescence dating method (Chapter 3). The second aim of the thesis was therefore to construct a reliable chronological frame for the upper (~50 m) sediments of the Cauvery Delta to get baseline information on the depositional history of sediments.

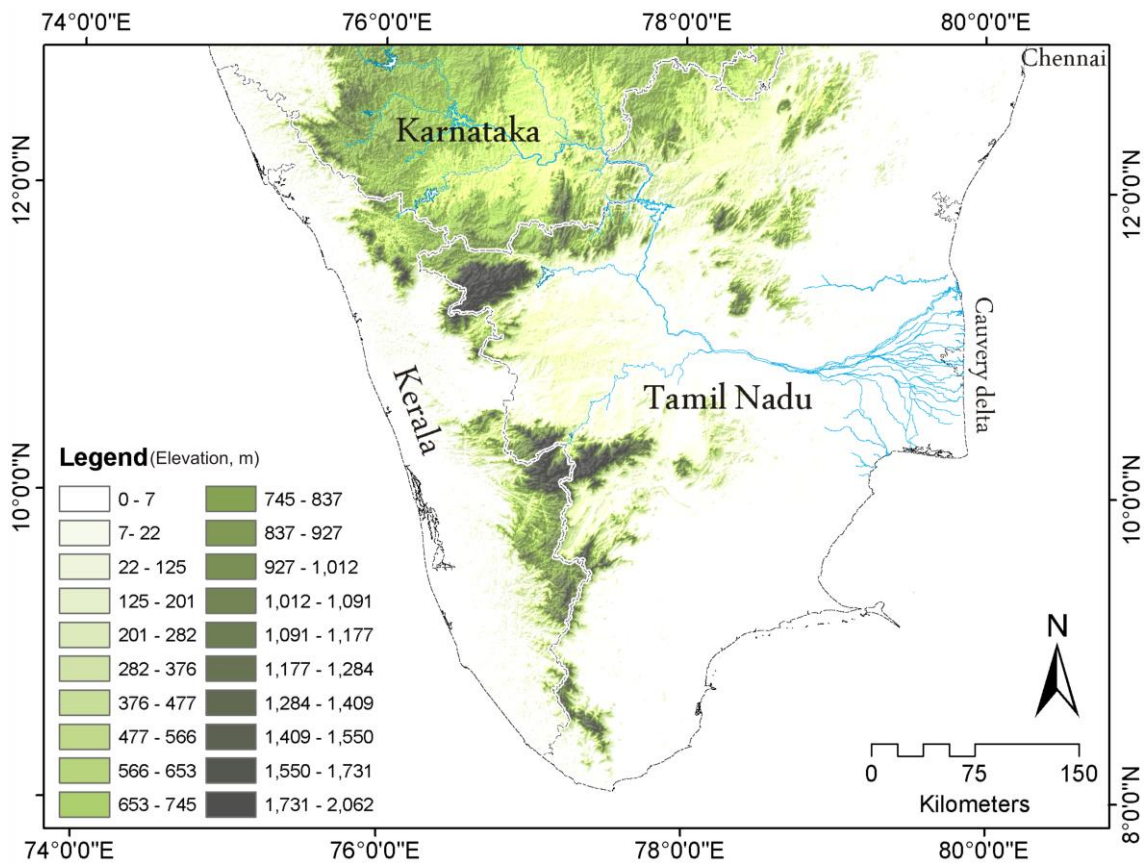


Figure 1.11. Digital elevation map of South India prepared using the DEM images of ASTER-GDEM, a product of METI and NASA, showing both east and west coasts.

Several sites in the east (Tamil Nadu; Fig. 2) of south India were investigated geomorphologically and stratigraphically and samples were recovered from both inland and coastal dunes in the area (Fig. 1.11). Due to discontinuous sedimentation and incomplete preservation of sediments most of the Late Quaternary climatic change and process is fragmented, hence generally a multi disciplinary research is required to get reliable information about the past climate history of the area from sediment records.

The study investigates the use of quartz OSL dating of coastal dunes from less than a decade to few hundred years for the reconstruction of evolution of coastal dunes in the south east coast of India (Chapter 4). The study aims to set up a robust chronological frame to better understand the formation and reactivation history of coastal dunes of Tamil Nadu, in particular to the Cauvery deltaic region using 28 OSL dates from 10 profiles. Sedimentological techniques (grain size analysis, heavy mineral analysis, and Scanning Electron Microscopic (SEM) analysis of quartz surface) were used to examine the possible sediment transport, depositional mechanism and provenance of sediments. An index for 'dune mobility' (Lancaster, 1988), also called 'potential dune surface sand activity' (Bullard et al., 1997) was calculated to assess the dune activity in the region. OSL ages of the youngest sample of ~4 yrs indicate that the sample is well bleached before deposition and the material is suitable for dating. Similar to our study very young ages from < 5- 10 yrs to few hundred years are reported in previous studies (Banerjee et al., 2001; Ballarini et al., 2003; Kunz et al., 2010) on coastal dunes.

On the coast of Kerala (Fig. 1.11), in south west India, coast parallel beach ridges were identified and samples were collected to study their chronology (Chapter 5). The Kerala coast receives a high rate of sediment supply owing to the large number of rivers flowing west in to the Arabian Sea. The steep gradient along with the proximity of the Western Ghats where the rivers originate, to the coast, sediments experience only short transporting distance and grains are sub-angular in nature. The area has a varied land use including coconut, paddy, plantain, cashew plantations along with many other tropical plants and seasonal crops apart from being densely populated.

Beach ridges are found in prograding shoreline having large supply of sand sized clastic sediment available in the littoral zone. Availability of fluvial sediments and large quantity of unconsolidated aeolian sands in the littoral zone contribute to the formation of well developed beach ridges in the area. At present beach ridges along the Kerala coast occur as

isolated outcrops in inland and major roads in the area have been constructed on top of the beach ridge morphology, running parallel to the coast. The land use is highly altered due to the increased pressure of human settlements and agricultural activities. However, seven locations were identified with areas having less habitation and stratigraphically undisturbed. The beach ridge formation in this area provides vital information on the coastal line progradation during late middle Holocene to late Holocene and gives insight in to the response of the coast to varying climate and sea level.

1.5. Outline of thesis

This thesis is aimed at investigating the application of OSL dating on coastal deposits from various landforms. The SAR protocol for quartz and elevated temperature post-IR IRSL SAR protocol for feldspar grains were applied for the study and the results are reported. The principal areas of investigation are described below. Three major proxy deposits were identified to apply OSL dating to reveal the chronology of events associated with the change in climate or geomorphologic features. They are

- Submerged sediments of present day shallow continental shelf of southern North Sea (Chapter 2)
- Subsurface sediments of Cauvery delta, South east coast of India (Chapter 3)
- Surface deposits such as dune/ beach ridges in southern coasts of Bay of Bengal in the east (Tamil Nadu) (Chapter 4) and Arabian sea in the west (Kerala) (Chapter 5) of India

The main conclusions of the study and possible future directions are summarised in Chapter 6.

Chapters 2, 3 and 4 have been published, accepted and submitted for publishing in peer reviewed journals. Chapter 5 is in preparation for submission. The study on continental shelf sediments of North Sea (chapter 2) is published in (Alappat et al., 2010a) in the Proceedings of the Geologists' Association. The study on subsurface sediments of Cauvery delta (Chapter 3) has been accepted for publication (Alappat et al., 2010b) in Geochronometria. The studies on surface deposits of the Tamil Nadu and Kerala coast have been submitted to Journal of Asian Earth Sciences and in preparation for submission to journal, The Holocene.

1.6. References

- Agersnap Larsen, N.A., Bulur, E., Bøtter-Jensen, L., McKeever, S.W.S., 2000. Use of the LM-OSL technique for the detection of partial bleaching in quartz. *Radiation Measurements* 32, 419-425.
- Aitken, M., 1985. *Thermoluminescence Dating*. Academic Press, London, 359 pp.
- Aitken, M.J., 1998. *Introduction to Optical Dating*. Oxford University Press, Oxford.
- Aitken, M.J., Reid, J., Tite, M.S., 1964. Thermoluminescence dating of ancient ceramics. – *Nature*, 202, 1032.
- Alappat, L., Vink A., Tsukamoto S., Frechen M., 2010a. Establishing the Late Pleistocene - Holocene sedimentation boundary in the southern North Sea using OSL dating of shallow continental shelf sediments. *Proceedings of the Geologists' Association* 121, 43-54. doi:10.1016/j.pgeola.2009.12.006.
- Alappat, L., Tsukamoto, S., Singh, P., Srikanth, D., Ramesh, R., Frechen, M., 2010b. Chronology of Cauvery delta sediments from shallow subsurface cores using high-temperature post-IR IRSL dating of feldspar. *Geochronometria*, accepted for publication.
- Arnold, L.J., Bailey, R.M., Tucker, G.E., 2007. Statistical treatment of fluvial dose distributions from southern Colorado arroyo deposits. *Quaternary Geochronology* 2, 162-167.
- Arnold, L.J., Roberts, R.G., 2009. Stochastic modelling of multi-grain equivalent dose (De) distributions: Implications for OSL dating of sediment mixtures. *Quaternary Geochronology* 4, 204-230.
- Auclair, M., Lamothe, M., Huot, S., 2003. Measurement of anomalous fading for feldspar IRSL using SAR. *Radiation Measurements* 37, 487-492.
- Bahadur, H., 2006. Radiation induced modification of impurity-related point defects in crystalline quartz – a review. *Crystal Research and Technology* 41(7), 631-635.
- Bailey, R.M., 2000a. The slow component of quartz optically stimulated luminescence. *Radiation Measurements*, 32, 233-246.
- Bailey, R.M., 2000b. Circumventing possible inaccuracies in the single aliquot regeneration technique. *Radiation measurements* 32, 833-840.

- Bailey, R.M., Arnold, L.J., 2006. Statistical modelling of single-grain quartz D_e distributions and an assessment of procedures for estimating burial dose. *Quaternary Science Reviews* 25, 2475-2502.
- Ballarini, M., Wallinga, J., Murray, A.S., Heteren, S.v., Oost, A. P., Bos, A.J.J., Eijk, C.W.E.v., 2003. Optical dating of young coastal dunes on a decadal time scale. *Quaternary Science Reviews* 22, 1011-1017.
- Banerjee, D., Murray, A.S., Foster, I.D.L., 2001. Scilly Isles, UK: optical dating of a possible tsunami deposit from the 1755 Lisbon earthquake. *Quaternary Science Reviews* 20, 715-718.
- Barletta, F., St-Onge, G., Channell, J.E.T., Rochon, A., 2010. Dating of Holocene western Canadian Arctic sediments by matching paleomagnetic secular variation to a geomagnetic field model. *Quaternary Science Reviews* 29, 2315-2324.
- Berger, G.W., 1990. Effectiveness of natural zeroing of the thermoluminescence in sediments. *Journal of Geophysical Research* 95, 12,375-12,397.
- Berger, G.W., Murray, A.S., Havholm, K.G., 2003. Photonic dating of Holocene back-barrier coastal dunes, northern North Carolina, USA. *Quaternary Science Reviews* 22, 1043-1050.
- Bøtter-Jensen, L., McKeever, S.W.S., Wintle, A.G., 2003. *Optically Stimulated Luminescence Dosimetry*. 355 pp. Elsevier, Amsterdam.
- Büntgen, U., Trouet V., Frank D., Leuschner H.H., Friedrichs D., Luterbacher J., Esper J., 2010. Tree-ring indicators of German summer drought over the last millennium. *Quaternary Science Reviews* 29, 1005-1016. doi:10.1016/j.quascirev.2010.01.003.
- Bullard, J.E., Thomas, D.S.G., Livingstone, I., Wiggs, G.F.S., 1997. Dune field activity and interactions with climatic variability in the southwest Kalahari Desert. *Earth Surface Processes and Landforms* 22 (2), 165-174.
- Buylaert, J.P., Murray, A.S., Thomsen, K.J., Jain, M., 2009. Testing the potential of an elevated temperature IRSL signal from K-feldspar. *Radiation Measurements* 44, 560-565.
- Cann, J.H., Belperio, A.P., Gostin, V.A., Wallace, C.V.M., 1988. Sea-Level History, 45,000 to 30,000 yr B.P., inferred from Benthic Foraminifera, Gulf St. Vincent, South Australia. *Quaternary Research* 29, 153-175.

- Chen, Y.W., Chen, Y.G., Murray, A.S., Liu, T.K., Lai, T.C., 2003. Luminescence dating of neotectonic activity on the southwestern coastal plain, Taiwan. *Quaternary Science Reviews* 22, 1223-1229.
- Cheong, C.S, Hong, D.G., Lee, K.S., Kim, J.W., Choi, J.H., Murray, A.S., Chwae, U., Im, C.B., Chang, C.J., Chang, H.W., 2003. Determination of slip rate by optical dating of fluvial deposits from the Wangsan fault, SE Korea. *Quaternary Science Reviews* 22, 1207-1211.
- Choi, J.H., Murray, A.S., Jain, M., Cheong, C.S., Chang, H.W., 2003a. Luminescence dating of well-sorted marine terrace sediments on the southeastern coast of Korea. *Quaternary Science Reviews* 22, 407-421.
- Choi, J.H., Murray, A.S., Cheong, C.S., Hong, D.G., Chang, H.W., 2003b. The resolution of stratigraphic inconsistency in the luminescence ages of marine terrace sediments from Korea. *Quaternary Science Reviews* 22, 1201-1206.
- Clemmensen, L.B., Murray, A., 2006. The termination of the last major phase of aeolian sand movement, coastal dunefields, Denmark. *Earth Surface Processes and Landforms* 31, 795-808.
- Damm, B., Terhorst, B., Bork, H-R., 2010. Quaternary landscape formation: The key to understand present day morphodynamics. *Quaternary International* 222, 1-2. doi:10.1016/j.quaint.2010.02.021.
- Duller, G.A.T., 1991. Equivalent dose determination using single aliquots. *Nuclear Tracks Radiation Measurements*, 18, 371-378.
- Duller, G.A.T., 1994. A new method for the analysis of infrared stimulated luminescence data from potassium feldspars. *Radiation Measurements* 23(2-3), 281-285.
- Duller, G.A.T., 1995.** Luminescence dating using single aliquots: methods and applications, *Radiation Measurements* 24, 217-226.
- Duller, G.A.T., 2006. Single grain optical dating of glacial deposits. *Quaternary Geochronology*, 1, 296-304.
- Duller, G.A.T., 2008. Single-grain optical dating of Quaternary sediments: why aliquot size matters in luminescence dating. *Boreas* 37, 589-612.

- Farooqui, A., Ray, J.G., Farooqui, S.A., Tiwari, R.K., Khan, Z.A., 2010. Tropical rainforest vegetation, climate and sea level during the Pleistocene in Kerala, India. *Quaternary International* 213, 2-11. doi:10.1016/j.quaint.2009.09.024.
- Frechen, M., Oches, E.A., Kohfeld, K.E., 2003. Loess in Europe - mass accumulation rates during the last glacial period. *Quaternary Science Reviews* 22 (18-19), 1835-1857.
- Frechen, M., Neber A., Tsatskin A., Boenigk W., Ronen A., 2004. Chronology of Pleistocene sedimentary cycles in the Carmel Coastal Plain of Israel. *Quaternary International* 121, 41-52.
- Fuchs, M., Lang, A., 2001. OSL dating of coarse-grain fluvial quartz using Single-Aliquot protocols on sediments from NE-Peloponnese, Greece. *Quaternary Science Reviews* 20, 783-787.
- Galbraith, R.F., Roberts, R.G., Laslett, G.M., Yoshida, H., Olley, J.M., 1999. Optical dating of single and multiple grains of quartz from Jinmium rock shelter, northern Australia. Part I experimental design and statistical models. *Archaeometry* 41, 339-364.
- Gemmell, A.M.D., 1999. IRSL from fine-grained glaciobuvial sediment. *Quaternary Geochronology* 18, 207-215.
- Gerdes, G., Petzelberger, B.E.M., Scholz-Bottcher, B.M., Streif, H., 2003. The record of climatic change in the geological archives of shallow marine, coastal, and adjacent lowland areas of Northern Germany. *Quaternary Science Reviews* 22, 101-124.
- Godfrey-Smith, D.I., Huntley, D.J., Chen, W.H., 1988. Optical dating studies of quartz and feldspar sediment extracts. *Quaternary Science Reviews* 7, 373-380.
- Harrison, S.P., Goñi, M.F., 2010. Global patterns of vegetation response to millennial-scale variability and rapid climate change during the last glacial period. *Quaternary Science Reviews* 29, 2957-2980. doi:10.1016/j.quascirev.2010.07.016.
- Hua, Q., 2009. Radiocarbon: A chronological tool for the recent past. *Quaternary Geochronology* 4, 378-390.
- Huntley, D.J., and Lian, O.B., 2006. Some observations on tunnelling of trapped electrons in feldspars and their implications for optical dating. *Quaternary Science Reviews* 25, 2503-2512.
- Huntley, D.J., Godfrey-Smith, D.I., Thewalt, M.L.W., 1985. Optical dating of sediments. *Nature* 313, 105-107.

- Huntley, D.J., Hutton, J.T., Prescott, J.R., 1993. Optical dating using inclusions within quartz grains. *Geology* 21, 1087-1090.
- Huntley, D.J., Lamothe, M., 2001. Ubiquity of anomalous fading in K-feldspars and the measurement and correction for it in optical dating. *Canadian Journal of Earth Sciences* 38, 1093-1106.
- IPCC, 2007. Contribution of Working Group I to the Fourth Assessment Report of the Intergovernmental Panel on Climate Change. In: Allali, A., Bojariu, R., Diaz, S., Elgizouli, I., Griggs, D., Hawkins, D., Hohmeyer, O., Jallow, B.P., Bogataj, L.K., Leary, N., Lee, H., Wratt, D., (Eds.) *Climate Change 2007: Synthesis Report*. 73 pp.
- Islam, M.S., Tooley, M.J., 1999. Coastal and sea-level changes during the Holocene in Bangladesh. *Quaternary International* 55, 61-75.
- Jain, M., Bøtter-Jensen, L., Murray, A.S., Jungner, H., 2002. Retrospective dosimetry: dose evaluation using unheated and heated quartz from a radioactive waste storage building. *Radiation Protection Dosimetry* 101, 525-530.
- Jain, M., Tandon, S.K., 2003. Fluvial response to Late Quaternary climate changes, western India. *Quaternary Science Reviews* 22, 2223-2235.
- Jain, M., Tandon, S.K., Singhvi, A.K., Mishra, S., Bhatt, S.C., 2005. Quaternary alluvial stratigraphical development in a desert setting: A case study from the Luni River basin, Thar Desert of western India. In: Blum M and Marriott S, (Eds), *Fluvial Sedimentology VII, International Association of Sedimentologists*. Special Publication 35: 349-371.
- Juyal, N., Pant, R.K., Basavaiah, N., Bhushan, R., Jai, M., Saini, N.K., Yadav, M.G., Singhvi A.K., 2009. Reconstruction of Last Glacial to early Holocene monsoon variability from relict lake sediments of the Higher Central Himalaya, Uttarakhand, India. *Journal of Asian Earth Sciences* 34, 437-449.
- Klasen, N., Fiebig, M., Preusser, F., Radtke, U., 2006. Luminescence properties of glaciofluvial sediments from the Bavarian Alpine Foreland. *Radiation Measurements* 41, 866-870.
- Kunz, A., Frechen, M., Ramesh, R., Urban, B., 2010. Luminescence dating of late holocene dunes showing remnants of early settlement in Cuddalore and evidence of monsoon activity in south east India. *Quaternary International* 222, 194-208. doi:10.1016/j.quaint.2009.10.042.

- Lancaster, N., 1988. Development of linear dunes in the southwestern Kalahari, southern Africa. *Journal of Arid Environments* 14, 233-244.
- Lauer, T., Frechen, M., Hoselmann, C., Tsukamoto S., 2010. Fluvial aggradation phases in the Upper Rhine Graben- New insights by quartz OSL dating. *Proceedings of the Geologists' Association*, in press, DOI 10.1016/j.pgeola.2009.10.006.
- Lepper, K., McKeever, S.W.S., 2002. An objective methodology for dose dispersion analysis, *Radiation Protection Dosimetry* 101 (1-4), 349-352.
- Li B, Li SH, and Wintle AG, 2008. Overcoming environmental dose rate changes in luminescence dating of waterlain deposits. *Geochronometria* 30: 33-40. DOI:10.2478/v10003-008-0003-z.
- Lomax, J., Hilgers, A., Twidale, C.R., Bourne, J.A., Radtke, U., 2007. Treatment of broad paleodose distributions from the western Murray Basin, South Australia. *Quaternary Geochronology* 2, 51–56.
- Luoto, T.P., Helama S., 2010. Palaeoclimatological and palaeolimnological records from fossil midges and tree-rings: the role of the North Atlantic Oscillation in eastern Finland through the Medieval Climate Anomaly and Little Ice Age. *Quaternary Science Reviews* 29, 2411-2423. doi:10.1016/j.quascirev.2010.06.015.
- Madsen, A.T., Murray, A.S., Andersen, T.J., Pejrup, M., Breuning-Madsen, H., 2005. Optically stimulated luminescence dating of young estuarine sediments: a comparison with ^{210}Pb and ^{137}Cs dating. *Marine Geology* 214, 251-268.
- Mayya, Y.S., Morthekai, P., Murari, M.K., Singhvi, A.K., 2006. Towards quantifying beta microdosimetric effects in single-grain quartz dose distribution. *Radiation Measurements* 41, 1032-1039.
- McKeever S.W.S., 1985. *Thermoluminescence of Solids*. Cambridge University Press, Cambridge.
- Mörner, N-A., 2010. Some problems in the reconstruction of mean sea level and its changes with time. *Quaternary International* 221, 3-8. doi:10.1016/j.quaint.2009.10.044.
- Morthekai, P., 2007. Investigations on the Radiation Dose Distribution in Natural Environments and their Implications in Luminescence Chronology. *Ph.D. Thesis*, Gujarat University.

- Murari, M.K., Achyuthan, H., Singhvi, A.K., 2007. Luminescence studies on the sediments laid down by the December 2004 tsunami event: Prospects for the dating of palaeo tsunamis and for the estimation of sediment fluxes. *Current Science* 92(3), 367-371.
- Murray, A.S., Roberts, R.G., 1997. Determining the burial time of single grains of quartz using optically stimulated luminescence. *Earth and Planetary Science Letters* 152, 163-180.
- Murray, A.S., Wintle, A.G., 2000. Luminescence dating of quartz using an improved single-aliquot regenerative-dose protocol. *Radiation Measurements* 32, 57-73.
- Murray, A.S., Wintle, A.G., 2003. The single aliquot regenerative dose protocol: potential for improvements in reliability. *Radiation Measurements* 37, 377-381.
- Novothny, Á., Frechen, M., Horváth, E., 2010a. Luminescence dating of sand movement periods from the Gödöllő Hills, Hungary. *Geomorphology* 122 (3-4), 254-263. doi:10.1016/j.geomorph.2010.04.013.
- Novothny, Á., Frechen, M., Horváth, E., Krbetschek, M., Tsukamoto, S., 2010b. Infrared stimulated luminescence and radiofluorescence dating of aeolian sediments from Hungary. *Quaternary Geochronology* 5 (2-3), 114-119.
- Ollerhead, J., Huntley, D.J., Berger, G.W., 1994. Luminescence dating of sediments from Buctouche Spit, New Brunswick. *Canadian Journal of Earth Sciences* 18, 419-432.
- Olley, J.M., Caitcheon, G.G., Murray, A.S., 1998. The distribution of apparent dose as determined by optically-stimulated luminescence in small aliquots of fluvial quartz: Implications for dating young samples. *Quaternary Science Reviews (Quaternary Geochronology)* 17, 1033-1040.
- Olley, J.M., Caitcheon, G.G., Roberts, R.G., 1999. The origin of dose distributions in fluvial sediments, and the prospect of dating single grains from fluvial deposits using optically stimulated luminescence. *Radiation Measurements* 30, 207-217.
- Pellegrini, M., Longinelli, A., 2008. Palaeoenvironmental conditions during the deposition of the Plio-Pleistocene Sedimentary sequence of the Canoa Formation, central Ecuador: A stable isotope study. *Palaeogeography, Palaeoclimatology, Palaeoecology* 266, 119-128.
- Porat, N., Botha, G.A., 2008. The luminescence chronology of dune development on the Maputaland coastal plain, southeast Africa. *Quaternary Science Reviews* 27, 1024-1046.

- Porat, N., Duller, G.A.T., Amit, R., Zilberman, E., Enzel, Y., 2008. Recent faulting in the southern Arava, Dead Sea Transform: Evidence from single grain luminescence dating. *Quaternary International*, doi: 10.1016/j.quaint.2007.08.039.
- Prescott J.R., Stephan L.G., 1982. The contribution of cosmic radiation to the environmental dose for thermoluminescence dating. Latitude, altitude and depth dependences. *PACT* 6, 17-25.
- Prescott, J.R., Hutton, J.T., 1994. Cosmic Ray contributions to dose rates for luminescence and ESR dating: large depths and long- term time variations. *Radiation Measurements* 23, 497-500.
- Preusser, F., Chithambo, M.L., Götze, T., Martini, M., Ramseyer, K., Sendezera, E.J., Susino, G.J., Wintle, A.G., 2010. Quartz as a natural luminescence dosimeter. *Earth-Science Reviews*, doi:10.1016/j.earscirev.2009.09.006.
- Reimann, T., Naumann, M., Tsukamoto, S., Frechen, M., Luminescence dating of coastal sediments from the Baltic Sea coastal barrier-spit Darss–Zingst, NE Germany. *Geomorphology*. doi:10.1016/j.geomorph.2010.03.001.
- Rhodes, E.J., Singarayer, J.S., Raynal, J.P., Westaway, K.E., Sbihi-Alaoui, F. Z., 2006. New age estimates for the Palaeolithic assemblages and Pleistocene succession of Casablanca, Morocco. *Quaternary Science Reviews*, 25, 2569-85.
- Rittenour, T., 2008. Luminescence dating of fluvial deposits: applications to geomorphic, paleoseismic and archaeological research. *Boreas* 37, 613-635.
- Roberts, H.M., 2008. The development and application of luminescence dating to loess deposits: a perspective on the past, present and future. *Boreas* 37, 483-507.
- Roberts, R.G., Galbraith, R.F., Olley, J.M., Yoshida, H., Laslett, G.M., 1999. Optical dating of single and multiple grains of quartz from Jinmium rock shelter, northern Australia. Part II: Results and implications. *Archaeometry* 41, 365-395.
- Scott, L., 1982. A Late Quaternary Pollen Record from the Transvaal Bushveld, South Africa. *Quaternary Research* 17, 339-370.
- Shao, X., Xua, Y., Yin, Z.-Y., Liang, E., Zhu, H., Wang S., 2010. Climatic implications of a 3585-year tree-ring width chronology from the northeastern Qinghai-Tibetan Plateau. *Quaternary Science Reviews* 29, 2111-2122. doi:10.1016/j.quascirev.2010.05.005.

- Singarayer, J., Bailey, R.M., Rhodes, E.J., 2000. Age determination using the slow component of quartz OSL. *Radiation Measurements*, 32: 873-880.
- Singarayer, J.S., Bailey, R.M., 2003. Further investigations of the quartz optically stimulated luminescence components using linear modulation. *Radiation Measurements* 37(4-5): 451-458.
- Singhvi, A.K., Sharma, Y.P., Agrawal, D.P., and Dhir R.P., 1983. Thermoluminescence dating of dune sands: some refinements. *PACT* 9, 499-504.
- Singhvi, A.K., Sengupta, D., Deraniyagala, S.U., 1986. Thermoluminescence Dating of Quaternary red sand beds: a case study of coastal dunes in Sri Lanka. *Earth and Planetary Science Letters* 80, 139-146.
- Singhvi, A.K., Bluszcz, A., Bateman, M.D., Someshwar Rao, M., 2001. Luminescence dating of loess-paleosol sequences-methodological aspects and paleoclimatic implication. *Earth-Science Reviews* 54, 193-211.
- Singhvi, A.K., Porat, N., 2008. Impact of luminescence dating on geomorphological and palaeoclimate research in drylands. *Boreas*, 37, 536-558.
- Spooner, N.A., 1993. The Validity of Optical Dating Based on Feldspar. *Ph.D. Thesis*, Oxford University, 207 pp.
- Spooner, N.A., 1994. The anomalous fading of infrared-stimulated luminescence from feldspars. *Radiation Measurements* 23 (2/3), 625-632.
- Stokes, S., Ingram, S., Aitken, M.J., Sirocko, F., Anderson, R., Leuschner, D., 2003. Alternative chronologies for Late Quaternary (Last Interglacial-Holocene) deep sea sediments via optical dating of silt-size quartz. *Quaternary Science Reviews* 22, 925-941.
- Tegel, W., Vanmoerkerke, J., Büntgen, U., 2010. Updating historical tree-ring records for climate reconstruction. *Quaternary Science Reviews* 29, 1957-1959. doi:10.1016/j.quascirev.2010.05.018.
- Thomas, P.J., Juyal, N., Kale, V., Singhvi, A.K., 2007. Luminescence chronology of late Holocene extreme hydrological events in the upper Penner River basin, South India. *Journal of Quaternary Science* 22: 747-753.
- Thomsen, K.J., Murray, A.S., Jain, M., Bøtter-Jensen, L., 2008. Laboratory fading rates of various luminescence signals from feldspar-rich sediment extracts. *Radiation Measurements* 43, 1474-1486.

- Tsukamoto, S., Denby, P.M., Murray, A.S., Bøtter-Jensen, L., 2006. Time-resolved luminescence from feldspars: New insight into fading. *Radiation Measurements* 41(7-8), 790-795.
- Tsukamoto, S., Rink, W.J., Watanuki, T., 2003. OSL of tephric loess and volcanic quartz in Japan and an alternative procedure for estimation D_e from a fast component. *Radiation Measurements* 23, 593-600.
- Walker, K.J., Surge, D., 2006. Developing oxygen isotope proxies from archaeological sources for the study of Late Holocene human-climate interactions in coastal southwest Florida. *Quaternary International* 150, 3-11.
- Wallinga, J., Murray, A., Wintle, A., 2000. The single-aliquot regenerative-dose (SAR) protocol applied to coarse-grain feldspar. *Radiation Measurements* 32, 529-533.
- Wallinga, J., Bos, A.J.J., Dorenbos, P., Murray, A.S., Schokker, J., 2007. A test case for anomalous fading correction in IRSL dating. *Quaternary Geochronology* 2, 216-221.
- Wintle, A.G., 1973. Anomalous fading of thermoluminescence in mineral samples. *Nature* 245, 143-144.
- Wintle, A.G., 2008a. Luminescence dating: where it has been and where it is going. *Boreas* 37, 471-482.
- Wintle, A.G., 2008b: Fifty years of luminescence dating. *Archaeometry* 50, 276-312.
- Wintle, A.G., Murray, A.S., 2006. A review of quartz optically stimulated luminescence characteristics and their relevance in single aliquot regeneration dating protocols. *Radiation Measurements* 41, 369-391.
- Wolff, E.W., Chappellaz, J., Blunier, T., Rasmussen, S.O., Svensson, A., 2010. Millennial-scale variability during the last glacial: The ice core record. *Quaternary Science Reviews* 29, 2828-2838. doi:10.1016/j.quascirev.2009.10.013.
- Zimmerman, D.W., 1967, Thermoluminescence from fine grains from ancient pottery, *Archaeometry*, 10, 26-28.
- Zimmerman, D.W., Huxtable, J., 1971. Thermoluminescence dating of Upper Palaeolithic fired clay from Dolni Vestonice. *Archaeometry*, 13, 53-57.

Proceedings of the Geologists' Association

(<http://dx.doi.org/10.1016/j.pgeola.2009.12.006>)

Establishing the Late Pleistocene-Holocene sedimentation boundary in the Southern North Sea using OSL dating of shallow continental shelf sediments

L. Alappat ^{*a}, A. Vink ^{**}, S. Tsukamoto ^{*}, M. Frechen ^{*}

**Leibniz Institute for Applied Geophysics, Section S3: Geochronology and Isotope Hydrology, Stilleweg 2, 30655, Hannover, Germany.*

***Federal Institute for Geosciences and Natural Resources, Stilleweg 2, 30655, Hannover, Germany*

^aCorresponding author: (Linto.Alappat@liag-hannover.de; lintoalappat@yahoo.co.uk)

Abstract

This paper provides insight into the fate of Late Weichselian and Early Holocene sediments accumulated in the German sector of the Southern North Sea. A combination of Optically Stimulated Luminescence (OSL) dating and radiocarbon dating was applied to set up the chronology. Seven cores were studied to obtain ten quartz OSL samples and ten radiocarbon samples. The core locations were chosen along a southeast to northwest transect along the western side of the Elbe palaeovalley, giving a good coverage of the entire German North Sea area. All samples for OSL dating showed a significant scatter in the equivalent dose (D_e) distribution of quartz due to heterogeneous bleaching. The Minimum Age Model (MAM-3) was found to be the most suitable to extract true burial ages. It was inferred from the study that sedimentation did still occur during the late deglaciation period in many areas. These are mainly Late Weichselian glacio-fluvial or glacio-lacustrine sediments directly overlain by early Holocene fluvial and/or transgressive

deposits and followed by modern marine sands. However, considerable late Weichselian erosion or a possible period of non-deposition was observed in the highland area to the northeast of the Dogger Bank and a small discontinuity in the near-shore region was noticed, probably due to early Holocene fluvial erosion. Relicts of a palaeo-river bank or terrace were identified in core 14VC to the east of the Dogger Bank. A possible interpretation of the Pleistocene-Holocene interface along the core transect is provided based on lithology and measured OSL and radiocarbon ages.

Key words: North Sea, Weichselian deglaciation, Quaternary, Optically Stimulated Luminescence, Holocene

2.1 Introduction

The shallow continental shelf of the German sector of the southern North Sea with a maximum depth of 60 m below sea level is being increasingly used for commercial activities such as the installation of pipelines, offshore wind parks, cable lines, underground storage caverns, and sand and gravel extraction. However, detailed comprehensive geological information on the intricately structured (sub) surface sediments and a thorough knowledge of the nature and timing of the geological processes involved in their deposition are still largely lacking, although such information is a prerequisite for the long-term planning and management of the region. The area has experienced continuous modifications of landscape during the past, due to the interactions of glacial and interglacial periods with associated lower and higher stands of sea level.

The southern North Sea area is considered to be a major sediment repository of the past, containing up to 1 km of Quaternary sediments deposited mainly during glacial periods (Caston, 1979; Gibbard, 1988). The commencement of the current interglacial following the Weichselian glacial maximum (22-18 ka) initiated a eustatic sea-level rise of about 130 m, and caused a coast line displacement of about 600 km towards the inland (Gerdes et al., 2003; Hoselmann and Streif, 2004; Streif, 2004). The onset of the Flandrian transgression at approximately 10 ka BP resulted in a concurrent rise of ground water level in the coastal regions. River water could no longer drain off, leading to swampy conditions and the development of basal peat (cores 35VC, 49VC and 06VC in the present study) in a

belt along the coastal area (Streif, 2004) which moved inland with increase in sea level. The basal peat is characteristically eutrophic peat with remains of *Phragmites*, *Carex* and trees and appears as thin beds in places where rapidly rising sea level quickly drowned the peat (e.g. Bijlsma, 1982; Vink et al., 2007). Such basal peats are excellent sea level indicators when an uninterrupted transition of sediments from a non-marine to brackish and marine environment is observed (e.g. Baetman and Strijdonck, 1989). Far offshore from the present coastline basal peat beds started to form during the earliest Holocene, but these have largely been removed due to intensive tidal erosion and wave action and are now difficult to find (Cameron et al., 1987).

The existing Holocene chronology in the German coastal area is mainly based on peat (Streif, 2004), which formed between 8 ka and 3 ka BP when the relative sea-level rise slowed down to less than 50 cm per century (Behre, 2004). The basal peat and/or basal shell layers have traditionally been considered as the base of the Holocene, where they formed in response to relative sea-level and/or ground water rise and are considered to be unconformably underlain by Late Pleistocene glaciofluvial, glaciolacustrine and/or aeolian deposits (Behre, 2004, 2007). The idea of Holocene peats and brackish-marine sediments resting with an erosional contact on older Pleistocene deposits was tested with a combined radiocarbon and luminescence dating approach in this study, as it is possible that the base of the Holocene is further down in the core, where Early Holocene fluvial processes may have deposited reworked glacio-fluvial sediments on the Late Pleistocene sandy palaeosurface.

Understanding the geomorphic response to rapid sea-level change in the past in these currently submerged regions is crucial to predict the future reaction to climate change and the associated effect of coastal landscape alterations (Fitch et al., 2005). Thus establishing a chronology of the shallow terrestrial and marine deposits of the North Sea can well contribute to palaeoenvironmental reconstruction and aid in understanding the current landscape evolution. Optically Stimulated Luminescence (OSL) dating is a direct method to develop numerical chronologies in sedimentology, especially in sandy terrestrial deposits where few or no alternative dating methods are available. However, incomplete resetting of the OSL signal in fluvio-glacial and shallow marine environments of the continental shelf region may be of concern, leading to an age overestimation due to

residual signals. This makes it important to study all possible means of extracting the most reliable age and establishing a model criterion for such sediments.

The aim of the present study is to examine the potential and suitability of OSL dating in establishing the chronology and sedimentation history of Upper Pleistocene glacio-fluvial and -lacustrine sands and the overlying Holocene basal peat and/or clastic shallow marine sediments in the German sector of the North Sea. The outcome of the study can subsequently be used for subsurface geological mapping and modelling of the analysed area, and can further substantiate the proposed relative sea-level curve for the region.

2.2 Geological setting

The German North Sea sector (Fig. 2.1) extends between 53° and 56°N latitude, and 3° and 9°E longitude. Except for a thin layer of Holocene top sediments, varying in thickness between 0 and 10 m with a maximum of about 16 m in the north-western part of the Weichselian Elbe palaeovalley infill (e.g. Figge, 1980), the vast majority of uppermost sediments in the German sector of the North Sea are considered to have been deposited during the cold (glacial) climatic phases of the Pleistocene (e.g. Gibbard, 1988). Three main phases of Pleistocene landscape evolution were proposed by Streif (2004) for the southern North Sea basin; i) a stage characterised by marine to fluvio-deltaic sedimentation during the Early Pleistocene, ii) a stage which was characterised by repeated ice advances and intervened by marine transgressions during the Middle and Late Pleistocene, iii) the final stage of melting of ice and the development of present-day landscape and sedimentary environments in the Weichselian late glacial and the Holocene.

During cold phases, the area was laid dry due to the drop in sea level and was either covered by the Scandinavian ice sheet (e.g. during the main ice advances of the Elsterian and Early Saalian (Drenthe) (Figs. 3b, 4b and 5 of Ehlers, 1990; Ehlers et al., 2004; Ehlers and Gibbard, 2007)), or was crossed by a complex system of periglacial braided or meandering, multi-channel rivers (e.g. during the Late Saalian-, Early Weichselian, Late Weichselian and Early Holocene) (e.g. Fitch et al., 2005). Deeply incised subglacial valleys into the underlying Pleistocene and Tertiary deposits were formed due to ice scouring and/or high melt water discharge or fluvial erosion during the main ice advances (Cameron et al., 1987; Huuse and Lykke-Andersen, 2000; Ehlers et al., 2004; Kuhlmann

and Wong, 2008; Lutz et al., 2009). These valleys were later filled with melt water deposits, gravel, sands and silts of predominantly terrestrial origin (Streif, 2004).

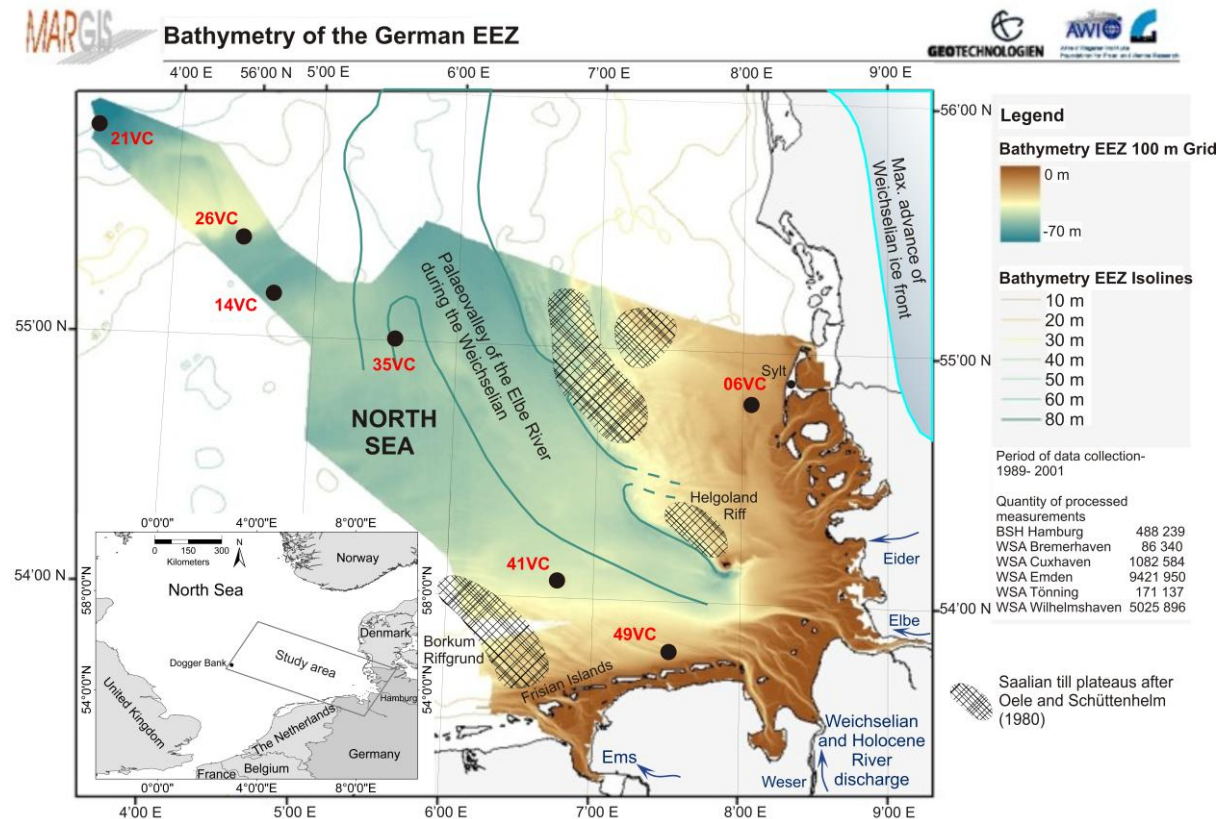


Figure. 2.1. Map showing the core positions and bathymetry of the German sector of the North Sea (source: MARGIS/Digital atlas of the North Sea, DANS-Vo.9), http://www.awi.de/en/research/researchdivisions/geosciences/marine_geochemistry/marinegis/digital_atlas_of_the_north_sea/. The inset map shows the geographical location of the study area.

A comparative observation by Ehlers (1990) between Saalian and Weichselian glacial advances suggests that the glaciers reached farther to the south during the Saalian to cover the majority of North German lowlands, whereas the Scandinavian ice sheet did not reach the southern North Sea region in the Weichselian (Cameron et al., 1987). Occasional occurrences of stiff greyish-brown marls with a high gravel and stone content found relatively close to the sea bed represent glacial tills that are considered to be of Saalian (Drenthe) origin (e.g. Laban, 1995). During the Weichselian, the southern North Sea shelf (above the present 100 m bathymetric contour) was instead exposed to

periglacial conditions (Cameron et al., 1987; Zeiler et al., 2000). Rivers extended far seaward and subsequent erosion and glaciofluvial to glaciolacustrine deposition altered the morphology that was left by the previously prevailing marine conditions. The rivers Ems, Weser, Elbe and Eider continued flowing towards the coast during the sea-level low stand, sometimes through 30-40 km-wide shallow valleys (e.g. the Elbe palaeovalley (see Fig. 2.1)). Weichselian glacio-fluvial deposits in the southern North Sea generally consist of light grey to grey unfossiliferous, micaceous, fine to medium-grained sand with or without reworked plant remains (e.g. Laban, 1995; Kudraß et al., 2004). In contrast, glacio-lacustrine deposits are often laminated and have much greater clay content.

Due to the complex processes involved in the evolution of the area and the general lack of datable, well-preserved interglacial/marine sediments in the German Bight, the stratigraphic position and/or approximate age of most of the available glacio-fluvial and glaciolacustrine deposits are especially difficult to determine. Seismic/structural geological data in combination with sedimentological data can support chronological interpretation, e.g. deep, boat-shaped subglacial valleys of >100 m depth filled by outwash gravels and sands, thick lacustrine clays (“Lauenburger Ton”) and fluvial sands are generally representative of the Elsterian, whereas the Saalian is rather characterised by shallower and significantly fewer subglacial valleys and the widespread occurrence of till and periglacial fluvial gravels (e.g. Laban, 1995). However, it is extremely difficult to distinguish lithologically between Early Saalian and Weichselian glacio-fluvial and glacio-lacustrine deposits in the absence of clear seismic and/or stratigraphic indications.

The main characteristic of the postglacial southern North Sea is the Holocene marine transgression, which started in the Elbe palaeovalley at around 11 ka BP (Özer, 2009) and consecutively reached the other regions of the German sector starting at around 9.5 ka BP (the marine transgression did not occur instantaneously in the whole area, but varied spatially with depth and time). The opening of the English Channel via the Dover Strait also occurred at around 9.5 ka BP which introduced strong tidal currents into the area. The transition from a terrestrial to a marine environment is often marked by a lagoonal and/or tidal flat horizon on top of the sandy terrestrial palaeosurface, which may be underlain by or intervened by peat layers. Such tidal flat deposits are generally grey to dark grey in colour, occurring mainly as distinct layers of clay and silt with occasional lenses of sandy silt or reworked peat. These also contain plant remains, molluscs and mollusc fragments,

and are often bioturbated. Streif (2004) reported a widespread formation of tidal flat sediments in the southern North Sea basin between 9 and 8 ka BP.

Complete marine conditions existed in the region after 7 ka BP (Eisma et al., 1981; Lambeck, 1995; Zeiler et al., 2000; Behre, 2007). This phase is represented sedimentologically by unconsolidated sea-bed sediments consisting of fine to medium-grained sand with numerous shell fragments. In some instances beds of coarse shelly sand are also present.

2.3 Materials and Methods

2.3.1 Samples

Seven vibrocores (maximum length 6 m) were collected from different parts of the German North Sea (Fig. 2.1) during a sampling campaign with M/V Franklin in July 2007 (Reinhardt et al., 2007). Six of the seven core locations were chosen in a way that they form a southeast to northwest transect on the western side of the Elbe palaeovalley and give good coverage of the entire German North Sea area (49VC, 41VC, 35VC, 14VC, 26VC and 21VC: see Fig. 2.1). The water depths in which these cores were taken vary between 23 m and 57 m below NN (German Ordnance Datum, Normal Null (NN) which is close to mean sea-level (MSL)), with generally increasing water depth towards the north-western part of the study area. The seventh core (06VC) was obtained from the north-eastern part of the sector, from a water depth of 19 m below NN off the barrier island Sylt. Ten fine to medium-grained homogeneous sands deposited in glaciofluvial or -lacustrine terrestrial environments were sampled from the cores. In cores 21VC, 35VC and 41VC, two luminescence sand samples were taken directly next to each other in order to determine the depositional frequency and also to test the reproducibility of the dating results. Wherever available, wood fragments, shells and/or peat layers were sampled for radiocarbon dating at or around the OSL sample locations in order to obtain an independent age control.

2.3.2 Optically Stimulated Luminescence (OSL) dating

OSL is the only currently available numerical dating method which can be used to determine the timing of events or sediment dynamics in organic-poor, well-sorted, fossil-depleted sands including those from coastal and shallow marine environments. It has been applied to a wide range of sedimentary archives, mainly to glacial, fluvial, aeolian and lacustrine deposits and archaeological materials for dating where conventional dating techniques are inadequate due to the lack of proper dating materials or time-specific dating limits. For example, radiocarbon dating is restricted to the material that was once formed as a part of living organisms, can be applied only if well-preserved organic materials are incorporated into the strata, and has a maximum age range of about 50,000 years (~9 to 10 half lives of ^{14}C) (Hua, 2009). It is always possible that older materials are deposited into younger sediments, leading to significant age overestimation. Carbonate samples can easily be contaminated via bicarbonate in ground water or accretion may occur, adding more recent carbon (Burleigh, 1974). There is a greater risk of contamination for small fragments. Shells of terrestrial and fresh water molluscs are usually not a reliable material when the age exceeds about 25 ka as the ages tend to be too old (Olsson, 1968) whereas marine shells are considered more suitable for dating. In the case of wood fragments, the radiocarbon age can only be considered as the upper age limit, as these fragments are usually redeposited into a younger sequence except for in-situ woods. ^{14}C dating of peat is generally preferred, as its in-situ formation can be verified and it is highly organic, with whole remains of leaves and twigs even allowing a contamination-free dating of the local vegetation.

Unlike most of the other dating techniques, luminescence dating dates the material of interest directly and is useful for a broad range of time from a few years (Ollerhead et al., 1994; Ballarini et al., 2003; Madsen et al., 2005) to more than a hundred thousand years (Stokes et al., 2003; Frechen et al., 2004). The OSL dating technique uses common minerals like quartz and feldspar as natural dosimeters. The exposure to natural radioactivity accumulates energy into defect centres in the crystal lattice of the mineral grain when it is buried and sealed off from light. The natural ionising radiation ionises or detaches the electrons and the electrons were accumulated in defects in the mineral grains. The total amount of dose the sample has been received can be determined by stimulating

the grains with a light source, which empties the traps and the resultant energy releases a luminescence signal. The natural luminescence signal is then compared with the laboratory-induced beta dose (from $^{90}\text{Sr}/^{90}\text{Y}$) response of the same sample which can be plotted as a dose response curve (Fig. 2.2a) in order to obtain the total absorbed radiation from the flux of nuclear radiation during the whole span of burial. This is quantified as the equivalent dose D_e , which is a measure of time since the last depositional event, if dose rate D is known. Equivalent dose D_e is expressed in „Gray’ (1 Gy = 1 J kg⁻¹) which represents the amount of radiation required to trap 1 joule of energy in 1 kg of sample. The rate of accumulation of dose (dose rate) is calculated from the concentration of radionuclides in the surrounding bulk sediment and from the cosmic dose considering the moisture content and burial depth of the sediment. Dose rate is expressed in Gy/ka. The detailed physical and methodological background of the technique is described elsewhere (Aitken, 1985; Wintle, 1997; Aitken, 1998; Lian and Roberts, 2006; Preusser et al., 2008).

The development of the single aliquot regenerative dose (SAR) procedure improved the accuracy and precision due to extensive tests incorporated into every step of the measurement (Murray and Wintle, 2000). The protocol estimates individual D_e values for a number of aliquots and provides an accurate outcome from a distribution of D_e values of the given sample. A detailed description of this procedure for quartz can be found elsewhere (Murray and Wintle, 2000; Wintle and Murray, 2006; Preusser et al., 2008). The protocol is also advantageous as it provides an insight into the completeness of bleaching prior to burial when analysing the scatter in the distribution of D_e values (Stokes et al., 2003). SAR can be applied either to aliquots of multiple grains or single grains based on the sample properties. The latter has been found to be preferable for poorly bleached or reworked sediment samples (Duller, 2008).

2.3.3 Experimental details

The selected cores were sampled under subdued red light laboratory conditions to obtain appropriate material for the luminescence studies. The outer 1.5 cm was not sampled to avoid possible contamination of bleached and/or disturbed outer parts while recovering the core. The quartz grain fractions of 100-150 μm or 150-200 μm were used from each sample, separated by dry sieving and using the standard laboratory preparation

procedure (Aitken, 1998). After extracting the grain size of 100-200 μm , the samples were treated with 0.1 N hydrochloric acid (HCl) to dissolve carbonates and to partly remove any iron oxides, 0.01 N sodium oxalate ($\text{C}_2\text{Na}_2\text{O}_4$) to remove the clay coatings as well as to segregate the grains, and 30% hydrogen peroxide (H_2O_2) to remove the organic matter from the samples. The quartz- rich fraction ($< 2.70\text{-}2.62 \text{ g cm}^{-3}$) was separated by density separation using an aqueous solution of sodium poly-tungstate ($3\text{Na}_2 \text{WO}_4 \cdot 9\text{WO}_3 \cdot \text{H}_2\text{O}$). The quartz fraction was etched using 40% hydrofluoric acid (HF) for 60 minutes to remove feldspar contamination and K-feldspar with inclusions of ferromagnesian minerals. The HF etching also removed the outer layer of the quartz grains to avoid the influence of alpha particles in the coarse grain sand. Samples were then washed and neutralised with distilled water and sieved again through the respective mesh to remove grains that had become smaller. The grains were mounted on steel aliquots as a uniform thin layer and fixed with silicon spray shortly prior to the measurement.

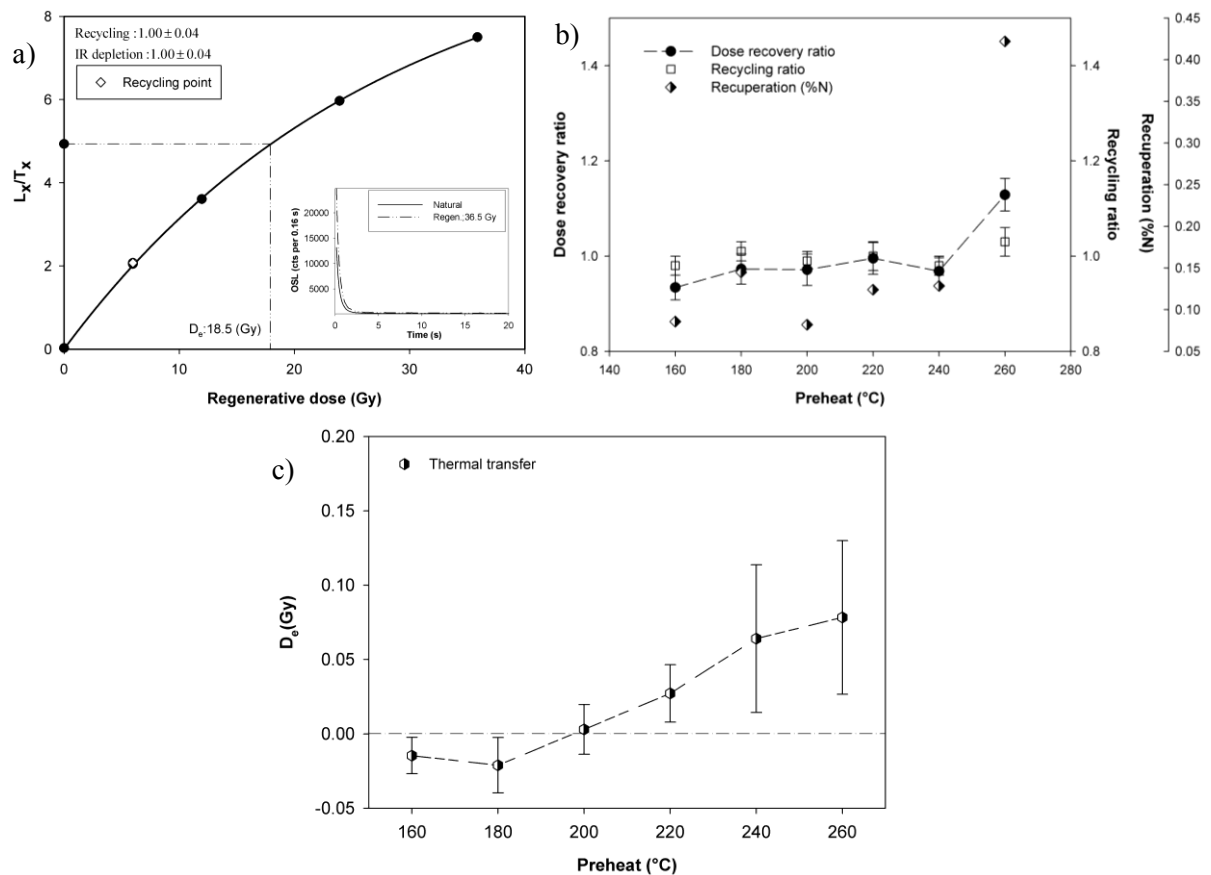


Figure 2.2. Quality-checking criteria tested for sample 26VC: a) Dose response curve using SAR protocol. Inset shows the decay curve for natural and regeneration dose. A preheat of 200°C and cut heat of 160°C were used

and early background subtraction was applied to extract the fast component of the quartz decay curve. b) Dependence of dose recovery, recycling and recuperation ratios on various preheat temperatures. c) OSL signal as a function of preheat shows the rate of thermal transfer at different preheat temperatures.

The single aliquot regenerative dose (SAR) protocol for quartz (Murray and Wintle, 2000; Wintle and Murray, 2006) was used to determine the equivalent dose of each sample (Table 2.1). An automated Riso TL/OSL DA 20 reader attached with a $^{90}\text{Sr}/^{90}\text{Y}$ beta source which delivers a dose rate of 0.12 Gy/s was used for the measurements. Blue light emitting diodes (LED) of 470 ± 30 nm were used for the optical stimulation of quartz. A Hoya U-340 (7.5 mm) filter was used for quartz measurements.

Table 2.1. *Modified SAR procedure used for OSL quartz measurements.*

Step	Treatments	Observation
1	Natural dose (R_n) / Laboratory dose (R_i)	
2	Preheat (PH_1): 200°C, 10s	
3	$R_{\text{IR}} - \text{IRSL}$ 125°C, 40 s, 90% diode power	L_{IR}
4	OSL measurement Blue LED 125°C, 40 s, 90% power	L_n / L_x
5	Test dose	
6	Cut heat (PH_2): 160°C, 0s	
7	OSL measurement Blue LED 125°C, 40 s, 90% power	T_x
8	Hot bleach OSL 280°C Blue LED, 40 s, 90% power	
9	Return to step 1	

Dose rates were calculated from the concentration of radioactive isotopes of K, Th and U (Table 2.2) measured using a high resolution gamma spectrometer (High Purity Germanium (HPGe) n-type detector). The quartz grains were considered to have gained dose from beta and gamma radiation from the radioactive isotopes of the uranium and thorium decay chains along with the gamma dose rate from the decay of ^{40}K in the environment and the cosmic dose and a minor contribution of radioactivity from within the quartz grains (Jacobs et al., 2008). The samples for the gamma measurements were collected within 10 cm surroundings of the luminescence samples. The bulk of the collected sample was dried at 50°C and crushed to achieve a homogeneous grain size. The samples were then filled into 50 g plastic containers for gamma measurements. The prepared samples were sealed air tight and stored for one month to gain the ^{222}Rn - ^{226}Ra equilibrium condition and then used for measurements. Each sample was measured for 36 hrs to obtain optimum counts for the required radionuclide peaks.

The dose rate conversion factors of Adamiec and Aitken (1998) and beta attenuation factors of Mejdahl (1979) were applied for calculation. A reduction in the average cosmic dose rate from 0.3 mGy a⁻¹ at mean sea level to 0.2 mGy a⁻¹ occurs within the first one meter of the water column due to the absorption of the soft component of cosmic rays by sea water. The remaining hard component is absorbed much less and penetrates to the sediment with a reduced intensity (Prescott and Hutton, 1988; Madsen et al., 2005). The cosmic dose rate was calculated based on the method proposed by Prescott and Stephan (1982) and Prescott and Hutton (1994). Changes in sediment density due to high water content were incorporated into the dose rate calculation. This is achieved by considering the water saturation percentage in the sediment and the thickness of the water column between the sea surface and the sediment surface (i.e. between 17.7 m and 57.2 m below NN), by including a percentage fraction of sea water density to incorporate the attenuation of cosmic rays through water. The sum of the percentage density of the sea water column (for example 80% of sea water density to the total) with the percentage density of sediment (for example 20% sediment density to the total) to the total depth was taken as the final density for the given sample. An average moisture content of 40 ± 10 % was applied for the calculation of dose rate from the measured water content calculated to the percentage of dry sediment weight for random samples (assuming complete water saturation during the entire period of burial).

Table 2.2. Summary of data showing the radionuclide concentration, beta, gamma and cosmic-ray dose rate in the sample. Total dose rate is also given in mGy/a. A measured water content of $40\pm 10\%$ was applied in the calculation.

Core	Water depth (m;NN)	Sample ID	Sample depth (m;NN)	Uranium (ppm)	Thorium (ppm)	K (%)	Beta dose rate (mGy/a)	Gamma dose rate (mGy/a)	Cosmic- ray dose rate (mGy/a)	Total Dose rate (D) (mGy/a)
FR07 21 VC	57.17	LUM-1410	59.93	0.51±0.02	1.52±0.05	0.74±0.02	0.42±0.06	0.20±0.05	0.018±0.002	0.64±0.10
FR07 21 VC	57.17	LUM-1411	60.24	0.4 ±0.02	1.28±0.04	0.73±0.01	0.40±0.06	0.18±0.05	0.018±0.002	0.61±0.10
FR07 35 VC	39.51	LUM-1412	44.77	0.27±0.02	0.95±0.04	0.60±0.01	0.33±0.06	0.14±0.05	0.022±0.002	0.49±0.10
FR07 35 VC	39.51	LUM-1413	44.91	0.32±0.02	0.91±0.04	0.65±0.01	0.35±0.06	0.15±0.05	0.022±0.002	0.53±0.10
FR07 06 VC	17.72	LUM-1414	22.19	0.96±0.02	2.66±0.04	0.95±0.01	0.57±0.06	0.30±0.05	0.044±0.004	0.91±0.12
FR07 41 VC	34.52	LUM-1415	37.57	0.56±0.03	1.60±0.05	0.72±0.01	0.41±0.06	0.20±0.05	0.027±0.003	0.64±0.10
FR07 41 VC	34.52	LUM-1416	38.11	0.73±0.02	1.83±0.04	0.76±0.01	0.45±0.06	0.22±0.05	0.026±0.003	0.70±0.11
FR07 14 VC	43.24	LUM-1439	45.22	0.49±0.03	1.57±0.04	1.17±0.01	0.63±0.06	0.27±0.05	0.023±0.002	0.92±0.12
FR07 26 VC	43.32	LUM-1440	48.51	1.19±0.03	4.08±0.06	1.28±0.02	0.77±0.06	0.40±0.05	0.020±0.002	1.19±0.14
FR07 49 VC	22.35	LUM-1441	27.82	0.43±0.02	1.05±0.04	0.87±0.01	0.47±0.06	0.20±0.05	0.035±0.003	0.71±0.11

The coarse grain (100-150 μm : 06VC, 41VC, 14VC, 26VC and 49VC; 150-200 μm : 21VC and 35 VC) quartz samples were mounted on stainless steel small size aliquots (2 mm diameter) with \sim 100 grains on each aliquot (Duller, 2008) and 48 aliquots per sample were used for each measurement. In addition to the vital assumptions of OSL dating, the SAR protocol assumes that the OSL sensitivity of the test dose (T_i) should be directly proportional to the prior natural/regenerative dose (L_i) (Murray and Wintle, 2000; Wallinga et al., 2000). This can be tested by employing a recycling ratio test, where one of the early regeneration doses is repeated to obtain a sensitivity-corrected dose response curve, and a recuperation test, which measures the OSL response of the zero dose and monitors the charge transfer from deep traps due to irradiation and preheat (Wallinga et al., 2000, Wintle and Murray, 2006).

To ensure the efficiency of the protocol to recover a given dose, a dose recovery test (Roberts et al., 1999; Murray and Wintle, 2003) was performed. The SAR protocol which was applied for D_e determination of quartz in the present study is shown in Table 2.1. The preheat conditions were chosen from a plateau from D_e responses for different preheat temperatures (160-260°C for 10 s each with a fixed cutheat temperature of 160°C). Dose recovery experiments revealed the efficiency of the applied protocol with a recovery ratio close to unity when it successfully recovered a given dose close to the expected natural dose (Fig. 2.2b). A thermal transfer test was carried out for selected quartz samples to find out the possible charge transfer from light insensitive thermally shallow traps to the light sensitive OSL traps due to the effect of high temperature treatments. The samples were bleached using blue light stimulation for 100 s at 125°C two times with a pause of 5000 s. The measured D_e values were plotted against the respective preheat temperatures and the optimum combinations with no significant increase in signal were selected as preheat temperature (Fig. 2.2b). The OSL signal after bleaching and preheating was indistinguishable from the background signal, which was consistent with zero up to the temperature of 200°C and showed a negligible increase towards higher temperature. The OSL-IR depletion test provides a measure of feldspar contamination in the sample, calculated from the ratio of OSL response of a beta dose of 6 Gy with preheat of 200°C for 10 s to that of a subsequent step of measurement with the same beta dose and preheat after exposing the sample for 40s of IR stimulation at 125°C (Duller, 2003). The acceptance criteria (Fig. 2.2b,c) of the measured D_e values for quartz were considered as i) the

recycling ratio (Wallinga et al., 2000) within the range of 0.90-1.10, ii) recuperation of <5% of natural signal (Murray and Wintle, 2000; Wallinga et al., 2000), iii) dose recovery ratio close to unity (0.95-1.05) (Wintle and Murray, 2006), iv) OSL-IR depletion ratio between 0.85-1.15 (Duller, 2003) and v) thermal transfer <5% of the natural signal. Measurement uncertainty of 1.5 % was incorporated for the D_e calculation. A few aliquots of sample 21VC and sample 35VC displayed a poor OSL-IR depletion and recycling ratios and these aliquots were excluded from the final D_e calculation. The total numbers of accepted aliquots in relation to those measured (in brackets) are shown in Table 2.3. The sensitivity-corrected natural luminescence signal (L_x/T_x) was then projected to the exponential growth curve of regenerated data points and the equivalent dose was estimated from the curve to the corresponding part of the x-axis (Fig 2.2a).

The use of small aliquots was preferred based on the fact that a greater number of grains in the aliquot average out any possible variability in the individual grains of the given aliquot (Olley et al., 1999). It has also been observed that different grains within the same sample have different luminescence sensitivities giving a spread in the measured D_e values when only a very small portion (~5 %) of the grains are responsible for the total luminescence emitted by a given aliquot (Huntley and Baril, 1997; Jacobs et al., 2003; Duller et al., 2000; Duller, 2008). As we used small aliquots (2 mm diameter) with ~100 grains on each aliquot for quartz measurements, only ~5 grains (Duller, 2008) were considered as active grains which contributed to the total emitted signal.

The fast components of the luminescence signal reset within a few seconds of sunlight exposure. As the initial part of the Continuous Wave-OSL (CW-OSL) signal, the first 1 s of 100 s blue LED stimulation is dominated by fast and medium components (Murray and Olley, 2002; Wintle and Murray, 2006), and the relatively poorly bleached slow component can be nearly eliminated by the early background subtraction (EBG) (Ballarini et al., 2007). The luminescence signals were collected for 250 data points and determination of D_e was carried out using signals integrated over the first three channels, giving signals of initial 0.48 s and an early background subtracted from the subsequent channels corresponding to 1.12 - 2.4 s. It was then considered that the background subtraction removed medium and slow quartz components and the D_e values were solely from the quartz fast component luminescence signal. Exponential fitting was applied to the natural and regenerated OSL signal for D_e value determination.

Table 2.3. Summary of data showing the sample details, single aliquot D_e distribution characteristics and statistics of the measured OSL quartz samples in the study. The number of accepted aliquots 'n' using the acceptance criteria are given with the total measured aliquots in the brackets. Sample ages obtained using different age models are shown. The favoured age model using the single aliquot decision-making process is highlighted in bold.

Core	Sample ID	Sample depth (m; NN)	n	D_e distribution characteristics							Age model selection		
				D_e (Gy)	Skewness (c)	$1\sigma_c$	Kurtosis (k)	$1\sigma_k$	D_e - RSD (%)	Wt. D_e - RSD (%)	Mean age (ka)	CAM age (ka)	MAM age (ka)
FR07 21 VC	LUM-1410	59.93	13(24)	46.2±9.3	0.33	0.68	-0.21	1.36	20.2	18.8	72.6±18.8	71.2±12.2	54.2±10.3
FR07 21 VC	LUM-1411	60.24	42(48)	45.2±12.2	2.17	0.38	7.01	0.76	27.0	22.3	74.6±23.7	79.4±14.4	54.2±9.5
FR07 35 VC	LUM-1412	44.77	37(44)	8.0±1.7	0.87	0.40	1.23	0.81	21.2	22.1	16.3±4.7	15.7±3.1	12.2±2.5
FR07 35 VC	LUM-1413	44.91	40(48)	8.2±2.4	2.89	0.39	11.06	0.77	29.8	25.0	15.4±5.4	14.9±2.8	11.0±2.1
FR07 06 VC	LUM-1414	22.19	47(48)	16.4±2.5	1.08	0.36	1.20	0.71	15.5	14.3	18.0±3.7	17.8±2.4	14.7±2.1
FR07 41 VC	LUM-1415	37.57	48(48)	8.6±1.2	0.48	0.35	0.92	0.71	13.5	13.0	13.5±2.8	13.3±2.2	11.3±1.9
FR07 41 VC	LUM-1416	38.11	47(48)	10.1±1.3	0.60	0.36	0.41	0.71	13.1	13.0	14.4±2.9	14.3±2.2	12.1±1.9
FR07 14 VC	LUM-1439	45.22	46(48)	23.7±6.1	1.43	0.36	2.19	0.72	25.8	18.9	25.7±7.4	24.9±3.4	19.0±2.6
FR07 26 VC	LUM-1440	48.51	48(48)	19.1±4.3	1.26	0.35	1.38	0.71	22.5	18.0	16.0±4.1	15.6±2.0	12.1±1.6
FR07 49 VC	LUM-1441	27.82	44(48)	16.4±9.0	3.19	0.37	10.72	0.74	55.0	23.2	23.1±13.2	21.1±3.4	14.3±2.3

Radiocarbon measurements were carried out using a conventional ^{14}C dating method for selected samples of wood, molluscs and peat at the Leibniz Institute for Applied Geophysics (LIAG). The ^{14}C ages were calibrated using the CALIB-5.0 ^{14}C Age Calibration Programme (Stuiver and Reimer, 1993) and presented within the uncertainty range of 1σ of the calibrated age. Sample details and results of the measurements are summarised in Table 2.4.

Table 2.4. Summary of data showing the results of ^{14}C dating in the study. Non-calibrated and calibrated ages are shown. Calibrated ages are given in age BP.

Core	Lab Code, Hv	Sample depth (m;NN)	Sample material	^{14}C -Age (ka, B.P.)	Calibrated Age (ka, B.P.) (2σ)
FR07 21 VC	25759	60.20	Wood	28.65±1.58	—
FR07 35 VC	25767	44.12	Peat	9.97±0.14	11.75-11.26
FR07 35 VC	25768	44.97	Wood	13.01±0.25	16.18-14.54
FR07 06 VC	25753	21.47	Peat	7.40±0.07	8.39-8.17
FR07 06 VC	25754	21.93	Wood	8.00±0.10	9.07-8.72
FR07 41 VC	25772	38.26	Wood	10.39±0.13	12.68-12.01
FR07 14 VC	25757	45.68	Wood	28.42±1.30	—
FR07 26 VC	25788	48.02	Mollusc (<i>C.edule</i>)	9.02±0.08	10.30-9.98
FR07 49 VC	25777	27.09	Peat	7.93±0.10	9.04-8.67
FR07 49 VC	25778	27.16	Peat	8.49±0.13	9.68-9.35

2.4 Age model decision-making process

The North Sea area can generally be characterised as an area of dynamic sediment reworking due to climatically-induced variations in sea level, ice coverage, meltwater discharge, river architecture and incision. Sand and gravel may have experienced multiple

cycles of erosion and redeposition. Heterogeneity in the physical processes involved in sedimentation (e.g. in sediment transporting agents such as wind, rivers, glaciers etc. and/or redeposition in sub-aerial, muddy or turbid conditions) induces differences in the basic assumptions of the dating procedure (i.e. amount of bleaching) which in turn displays inequalities in the D_e distribution characteristics. One can expect a normal distribution with a tight Gaussian curve for the population of D_e values of well-bleached samples, with no reworking once deposited, and a steady dose rate from a uniform radiation field. Often this is not the case in natural environments, especially within the regime of glacial, fluvial, deltaic and lacustrine environments in which sediments are more vulnerable to post-depositional reworking, heterogeneous or partial bleaching due to the very short light exposure, glacial or subglacial mass transport of sediments and heterogeneity in the radiation field due to the change in prevailing geomorphology. Deposition of sediments within (partly) underwater conditions has greater probability of incomplete bleaching due to the attenuation of solar radiation by absorption and turbidity. The study area experienced numerous glacial and interglacial cycles, resulting in a complex active braided-fluvial network, ice scouring and coverage and multiple stages of long-term sea-level changes (Streif, 2004, Fitch et al., 2005). This gives a clear implication for a possible heterogeneity in the sediment source and variation in the luminescence behaviour of individual sample.

Analysing the dose distribution of a sample can provide some evidence about the extent of bleaching and post-depositional reworking and also the variation in the radiation field. Incomplete bleaching can be attributed when the measured D_e values from an aliquot comprise not only the signals of the latest event of daylight exposure, but also a considerable amount of the residual signal from the previous event. This will result in a higher dose for the measured aliquot and scatter of the D_e distribution due to the differences in the D_e values of the same sample for different aliquots. Fuchs et al. (2007) observed a tight normal distribution of D_e values for a well-bleached artificially simulated reference sample with a relatively small coefficient of variance ($v = 8\%$), whereas a positively skewed distribution or broad normal distribution ($v > 18\%$) was found for the insufficiently bleached simulated samples of the same type. Apart from heterogeneous bleaching other factors influencing the dose distributions are the β -dose variation arising from the proximity of the grain to a β -hot spot (^{40}K β -emitters) (Mayya et al., 2006),

differences in the luminescence properties of individual grains in the aliquot and instrumental factors (Thomsen et al., 2005; Juyal et al., 2006; Arnold and Roberts, 2009).

The single aliquot decision-making procedure proposed by Bailey and Arnold (2006) and Arnold et al. (2007) was used as the standard criterion to derive the D_e values from the scattered D_e distributions in the present study. The assumptions for the decision-making process were satisfied during the measurement, such as i) the exponential form of dose response which is independent of dose rate for both the natural and regenerative dose, ii) the sensitivity-corrected OSL signal with no effects of thermal transfer, and iii) early background subtraction which successfully isolated the fast component of the quartz OSL (Bailey and Arnold, 2006). Considering the depositional history of the samples, it was proposed that the distribution could be attributed to heterogeneous bleaching, post-depositional reworking and temporal variation in the beta dose (Arnold et al., 2007). Statistical models have been proposed to identify the outliers of the D_e distribution, allowing choice of the optimum D_e values (Olley et al., 1998; Galbraith et al., 1999; Fuchs and Lang, 2001; Lepper and McKeever, 2002; Jain et al., 2002). The D_e distribution was then analysed using statistical age models such as the Central Age Model (CAM) and the Minimum Age Model (MAM) proposed by Galbraith et al. (1999) to extract the most likely D_e values for the age calculation. The CAM uses the weighted mean as the measure of central tendency to choose the appropriate D_e value from the population. The MAM uses the lower end of the D_e population, assuming that the well-bleached population falls in to the lower end of the D_e distribution due to almost complete resetting of the latent luminescence signal, whereas the additional residual dose in the sample causes higher D_e values (Fuchs et al., 2007; Duller, 2008; Fuchs and Owen, 2008).

The D_e distribution showed a considerable scatter in the D_e values (Fig. 2.3), having a clear asymmetry with significant positive skewness (skew, $c > 1\sigma_c$; kurtosis, $k > 1\sigma_k$) (Table 2.3) which is similar to those of type 1 and type 3 of the Colorado arroyo samples presented by Arnold et al. (2007). The D_e distribution of samples 35VC (Fig. 2.3c), 26VC (Fig. 2.3b) and 49 VC gave a scatter of values from 6.0 ± 0.4 Gy to 19.4 ± 0.6 Gy, 12.7 ± 0.6 Gy to 32.6 ± 1.1 Gy and 9.3 ± 0.4 Gy to 52.8 ± 6.7 Gy respectively, with a relative standard deviation (RSD) of 30%, 23% and 55%. The calculated ages for different age models are shown in Table 2.3.

Application of OSL dating on coastal sediments...

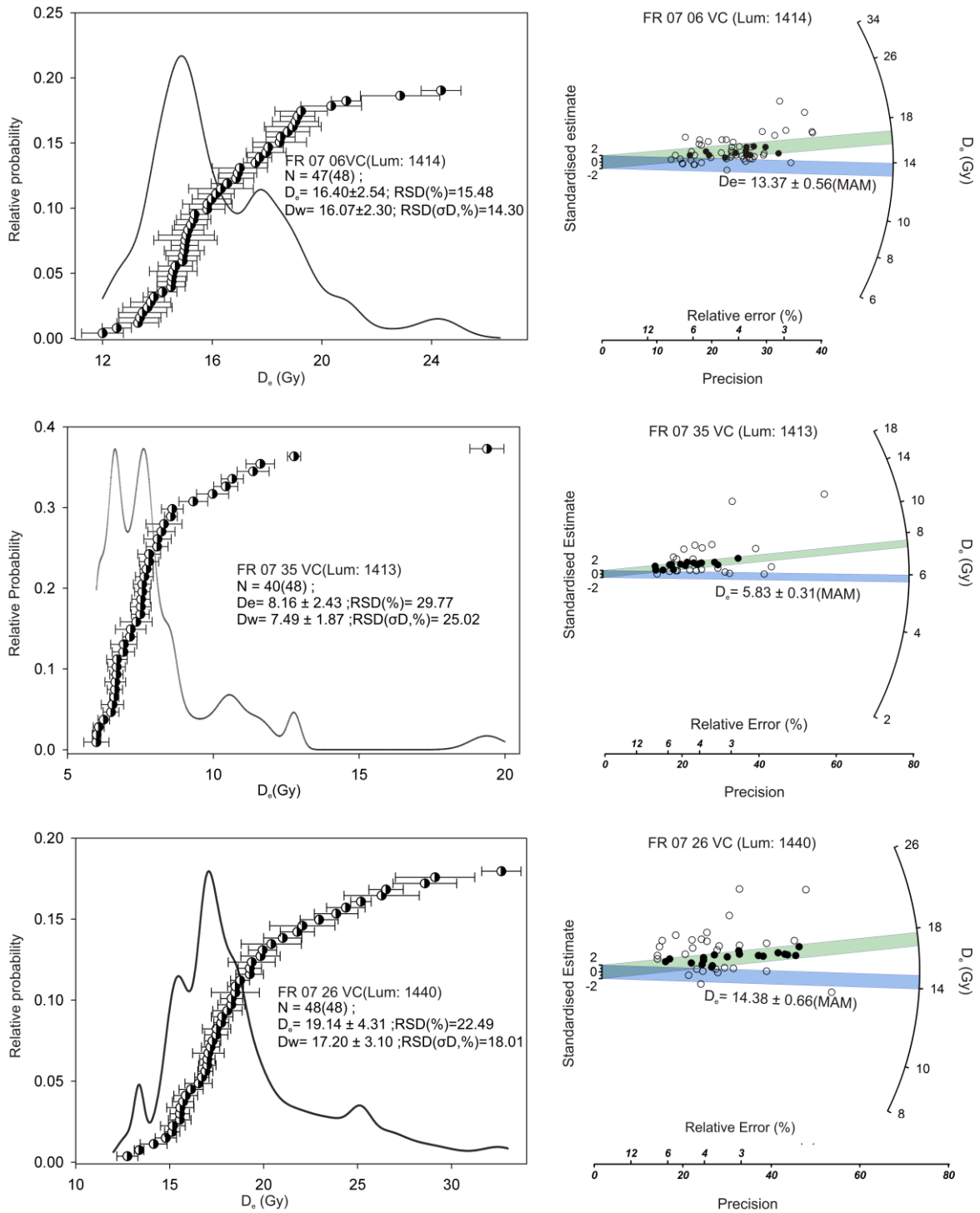


Figure 2.3. Types of single aliquot D_e distribution observed in the study as shown by the scatter of measured D_e values for three samples (a (06VC), b (26VC) and c (35VC)). The Gaussian curve shows the relative probability of D_e values of individual aliquots to the weighted mean of the distribution. Dispersion values (RSD %) to that of the mean and weighted mean D_e

distribution are also shown. The radial plot shows the weighted D_e distribution (filled circle in the shaded region) and D_e using the selected age model (blue shading) within two standard deviations of the distribution.

A statistically significant asymmetric distribution is distinguished when the values of skewness and kurtosis of the dose distribution exceeds one standard deviation ($c > 1\sigma_c$; $k > 1\sigma_k$) (Bailey and Arnold, 2006). The values of σ_c and σ_k were calculated following the equations (16) and (17) of Bailey and Arnold (2006):

$$(\sigma_c = \sqrt{6/n} \text{ and } \sigma_k = \sqrt{24/n}).$$

For all samples, final OSL D_e values calculated using the MAM as the measure of dispersion were significantly higher. For sample Lum-1410 (21VC), the number of aliquots accepted were too low ($n = 13$) to apply any kind of age model. Here it was inferred that the MAM gives the best fit as this age shows better agreement to the adjacent sample.

2.5 Sedimentological and chronological results

All of the analysed cores contain only a relatively thin 1 to 4.5-m-thick marine sedimentary sequence resting on terrestrial glacio-fluvial or glacio-lacustrine sediments (Fig. 2.4). The glacio-fluvial sediments generally consist of well-sorted fine to medium micaceous sands, often with cm-layering and/or with intercalations of woody particles or Tertiary brown coal pieces (06VC, 14VC, 21VC, 35VC, 41VC, 49VC). In contrast, glacio-lacustrine sediments consist of silt with fine sand and clay intercalations (26VC). Both types of glacial sediments are assumed to have been deposited in a periglacial setting and correlate to the Twente Formation in the Dutch North Sea sector (e.g. Laban, 1995). The transition from terrestrial to marine sediments is usually characterised either by a shell-rich debris layer, which was probably deposited below the wave base and may reflect the first preserved near-coastal storm surge in the area (14VC, 21VC, 41VC), or by in situ lagoonal or tidal flat sediments (26VC), sometimes on top of preserved basal peat (06VC, 35VC, 49VC). The marine sedimentary sequences in the cores for the most part reflect increasing sea level upcore; no indications for periodic regressions or phases of sea level stagnancy as

described from coastal sequences were found (e.g. Streif, 2004; Bungenstock, 2005; Behre, 2007).

A summary of the sample positions within the cores and their deduced final OSL and ^{14}C ages is provided in tables 2.3 and 2.4, and in figure 2.4. The results for each individual core will be presented separately in the remainder of this section.

Core 21VC is located in the north-western part of the German North Sea sector, on the northern side of a topographical high which represents the north-eastward extension of the Dogger Bank (shown in the bathymetric map in Fig. 2.1). A 2.7-m thick layer of homogeneous fine to medium-grained glacio-fluvial sand was found between the marine top layer and a lowermost stiff marl representing a glacial till (see Fig. 2.4). Due to its proximity to the surface, this till will not be of Elsterian age, but is most likely part of the Saalian Cleaver Formation as defined for the northern Dutch North Sea sector (e.g. Oele and Schüttelhelm, 1979; Laban, 1995). In our study, two subsequent samples collected from the sandy, fluvial layer of this core gave OSL-MAM ages of 54.2 ± 10.3 ka and 54.2 ± 9.5 ka at a sample depth of 59.93 and 60.24 m below NN, respectively (water depth 57.17 m below NN). A radiocarbon sample of wood collected between the two OSL samples at a sample depth of 60.20 m below NN gave an uncalibrated ^{14}C age of 28.6 ± 1.5 ka BP. Assuming that the till deposit represents a Saalian till, a constraint on the possible age of the analysed glacial sands above was provided.

The OSL-MAM age of the sample of core 26VC collected to the southeast of core 21VC on the other side of the Dogger Bank extension (Fig. 2.1) is 12.1 ± 1.6 ka at a depth of 48.51 m below NN. This Late Pleistocene glacio-lacustrine silt with fine sand and clay intercalations is overlain by tidal flat sediments with a shell layer at the base. This shell layer contains many specimens of bivalved *Cerastoderma edule* which are still present in their living positions. Radiocarbon dating of these in situ shells at a depth of 48 m below NN provided a calibrated age of 10.3-9.98 ka BP. Above this a layer of tidal flat clay with a thickness of 3 m contains lenses of fine sand and silt with intermittent layers containing peat fragments and plant remains. The upper 1.5 m of the core consists of fine-grained marine sand with intermingled molluscs, lumps of peat and shell fragments.

Application of OSL dating on coastal sediments...

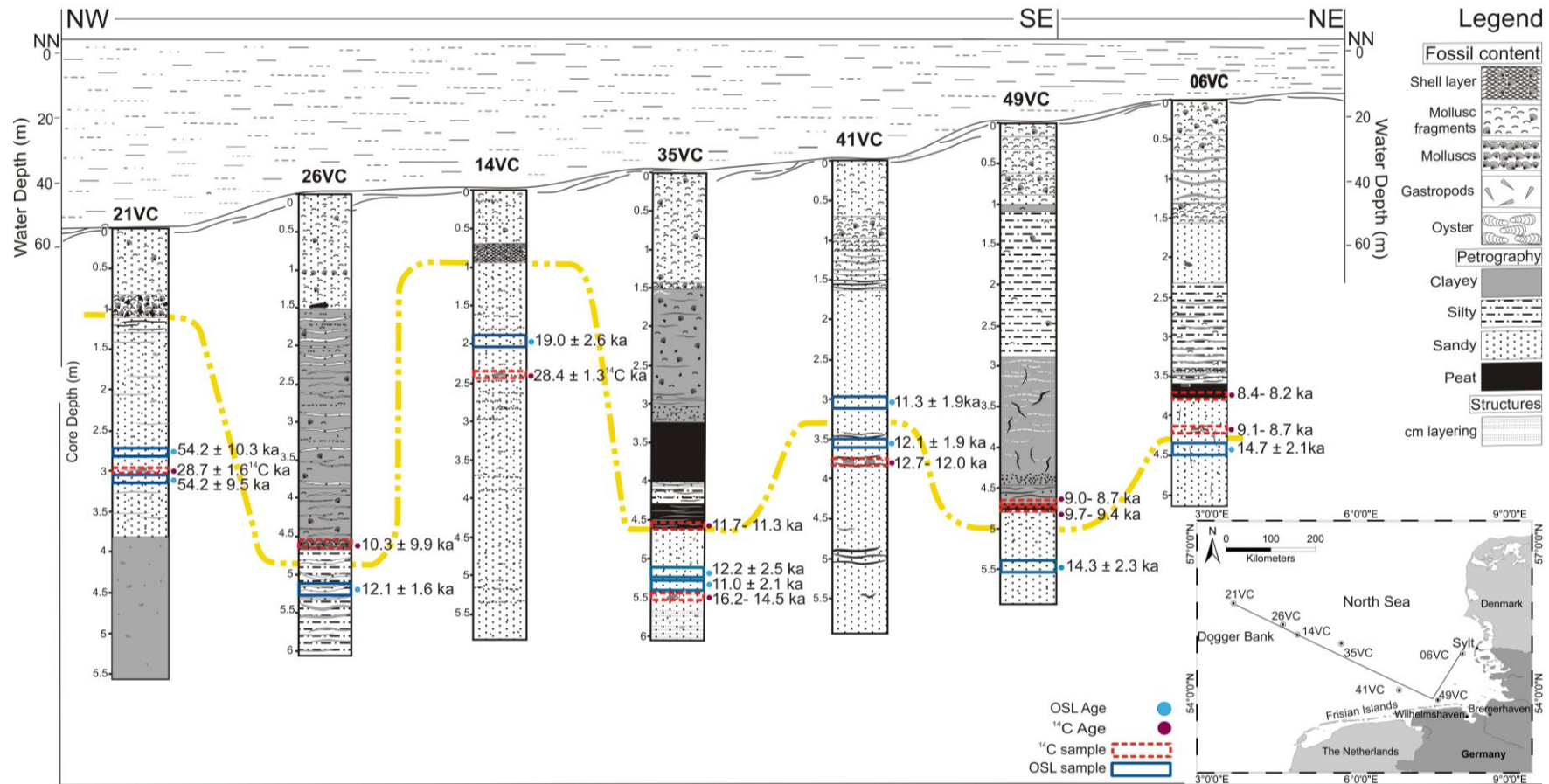


Figure 2.4. Schematic representation of core lithology and depth along the analysed transect (see inset). OSL and radiocarbon ages are shown. The estimated Pleistocene-Holocene 11.7 ka interface (yellow line) is based on lithology and the chronology derived from the current study.

Core 14VC was retrieved about 50 km southeast of 26VC. The sediments analysed for luminescence dating from a depth of 45.22 m below NN yielded an OSL age of 19.0 ± 2.5 ka. This core is characterised by a relatively thin upper layer of fine-grained marine sand (69 cm) with a layer of molluscs and shell debris at the base (24 cm), underlain by glacio-fluvial fine sands. A radiocarbon sample of wood fragments collected below the luminescence sample at a depth of 45.7 m below NN gave an uncalibrated ^{14}C age of 28.4 ± 1.3 ka BP, thus providing a much greater age for the underlying layer in comparison with the OSL age.

Two OSL samples were collected from core 35VC recovered from the middle of the NW-SE transect from depths of 44.77 and 44.91 m below NN. These two subsequent sandy samples provided MAM ages of 12.2 ± 2.4 ka and 11.0 ± 2.1 ka, respectively. A radiocarbon sample of wood fragments collected below (44.97 NN) the OSL samples yielded a calibrated age of 16.18-14.54 ka BP. Two layers of peat, separated by a 0.27 m thick silty layer, were observed on top of these Late Weichselian sands. The lower peat contains layers of clay, whereas the upper peat is very dense and contains remains of reed (*Phragmites*). A radiocarbon sample collected from the base of lower peat layer at a depth of 44.1 m below NN gave a calibrated radiocarbon age of 11.7-11.2 ka BP, which is in agreement with the OSL age within the given uncertainty. The upper peat probably marks the onset of the postglacial marine transgression and is overlain by a clayey layer of intertidal flat sediments intercalated with wood, plant remains and peat lenses. The uppermost part of the core consists of marine, fine sandy-silty sediments with fragments of molluscs.

Core 41VC was collected much closer to the coast on the western side of the Elbe palaeovalley. Two successive samples collected from this core at 38.11 m and 37.57 m below NN provided MAM ages of 11.3 ± 1.9 ka and 12.1 ± 1.9 ka, respectively, which are in agreement with each other. Independent age control from a radiocarbon sample of wood collected from the same core immediately below the lower OSL sample at a depth of 38.26 m below NN yielded a calibrated age of 12.68-12.0 ka BP, indicating a good stratigraphic agreement within the range of uncertainty. The lower layer in the core comprises micaceous fine-grained glacio-fluvial sand with thin peaty layers and intercalated wood fragments. Core 41VC reflects a steady accumulation of fluvial sediments up to a core

depth of 1.5 m, after which it shows layers of peat and clay incorporated within the matrix of shell-bearing marine fine sand.

Core 49VC was taken from the near-shore region off the Frisian Islands. The lowermost layer consists of glacio-fluvial fine sand with centimetre layering and intercalated with plant remains. This fine sand yielded an OSL age of 14.3 ± 2.3 ka at a depth of 27.8 m below NN. A thin layer of basal peat preserved in the core on top of this unit yielded calibrated radiocarbon ages of 9.0-8.7 ka BP and 9.7-9.4 ka BP for the two samples collected from the top and bottom of the layer, respectively. This peat was overlain by a 2-m-thick sequence of brackish lagoonal sediments followed by typical tidal flat deposits of clay with incorporated thin layers of fine sand. The youngest deposits in the core contain molluscs and shell fragments within a matrix of fine-grained sand.

The core 06VC was recovered from the near-shore region off the island of Sylt (Fig. 2.1). The lowermost layer comprises Pleistocene glacio-fluvial fine sand with reworked plant remains, wood fragments and woody roots, giving an OSL age of 14.7 ± 2.1 ka at a depth of 22.19 m below NN. A layer of Holocene basal peat was found at a depth of 21.47 m below NN and yielded a calibrated radiocarbon age of 8.4-8.2 ka BP. A wood sample collected from the sands below the basal peat from a depth of 21.93 m below NN gave a radiocarbon age of 9.1-8.7 cal. ka BP. As this sample lies only 0.26 m above the OSL sample, it probably marks the base of the Holocene within this core. The peat layer is covered by calcareous silt intercalated with thin clay layers (shell-bearing tidal flat deposits) and overlain by a medium to fine-grained marine sand with an intermediate layer of coarse to medium-grained sand containing shell fragments.

2.6 Discussion

The comparison of our determined OSL ages with ^{14}C ages and with the lithologies of our analysed cores shows that OSL generally provides reliable results within the studied area. The degree of over-dispersion and the measure of skewness and kurtosis of dose distribution reveals the incompleteness of bleaching of sediments before burial. It is obvious from the shape of the dose distribution that CAM cannot be applied for our samples as this model is only suitable for well bleached samples. The use of MAM will be more appropriate as it identifies the true dose population from insufficiently bleached,

scattered distribution, in which the D_e values corresponding to latest exposure normally lies in the first quartile of the distribution. The proposed age model decision making process was used as a criterion to select appropriate age models for individual samples. Though the age model decision making process is not considered as a robust criterion for all the sedimentary environments, it is relatively safe to apply it in such a highly varying depositional system like southern North Sea. The factors which make the OSL dates more or less reliable in our study are; i) its applicability of age model decision making process to chose among different models, ii) use of MAM based on the D_e distribution characters such as value of over dispersion (>20%) and/or statistically significant positive skewness and kurtosis. This in turn is substantiated by the knowledge of different physical processes and depositional environments that prevailed in the region which might have lead to incomplete bleaching of sediments before burial and iii) relatively good stratigraphic correlation of OSL dates with ^{14}C dates. The latter gives effective age control for the cores where in situ peats and shells are available.

The inherent problems with available ^{14}C samples in the area have to be considered. In core 26VC, shells of *Cerastoderma edule* were collected from a layer containing both complete shells and shell debris, which may imply remobilisation and high hydrodynamics. Radiocarbon dating of these shells provided a calibrated age of 10.3-9.9 ka BP, which is chronologically in agreement with the luminescence age of the lower sand unit which is around 12.1 ± 1.6 ka. As the shells collected for radiocarbon dating were still paired and in live position, and were obtained from the base of a low-dynamic tidal flat sediment, we assume that they were formed autochthonously and reflect the timing of the marine transgression in this area. In cores 14VC and 35VC, the wood samples analysed for radiocarbon dating may give an age overestimation, as older fragments of wood might have been reworked into younger glacio-fluvial sand deposits. In contrast, ^{14}C -dating of basal peat is considered much more reliable as reworking of such layers is less likely. Furthermore, the dates deriving from the basal peats in cores 35VC and 06VC fit well with the OSL dates, providing a good constraint on the luminescence chronology.

Core lithologies and our determined OSL and radiocarbon dates show that all seven cores contain a topmost 1 to 5 m of Holocene sediments (Fig. 2.4; Table 2.4). The base of the marine sedimentary succession generally lies on terrestrial sand, at times with a peat layer in between, and is often informally described as the base of the Holocene (e.g. for

mapping purposes). However, this sedimentological transition is not necessarily based on absolute age, but is rather dependent on elevation and the local time of transgression. Radiocarbon and OSL samples allow us to determine an improved yet still approximate Pleistocene-Holocene interface in the core transect (yellow line in Fig. 2.4). The Pleistocene boundary apparently varies in depth as a function of distance from the shore, accommodation space and palaeo-elevation. The marine transgression and associated beginning of marine sedimentation often occurred relatively late in the Early Holocene, especially in the shallower depositional areas (e.g. in cores 41VC, 49VC and 06VC). In core 49VC, for example, the calibrated radiocarbon age of the top of the peat layer proved it to be of Boreal age (9.0-8.7 ka BP), which is in good agreement with the coastal evolution suggested by Streif (2004) and fits well with the sea-level curve of the Southern North Sea estimated by Vink et al. (2007). Another sample collected from the bottom of the basal peat provided a Pre-boreal age, showing that the onset of peat formation, which is not necessarily sea-level related, also occurred well into the Early Holocene. In core 06VC, the onset of peat formation was even later (8.4-8.2 ka BP). Our dates show that fluvial sedimentation did still occur in these areas during the Early Holocene, right up to the time of peat formation and, consequently, marine inundation.

The oldest Weichselian sands were registered in core 21VC, close to the Dogger Bank. In this core OSL dates may be erroneous (if the radiocarbon age of wood is true) due to the inherent problem of optical dating, i.e. the sediments in this region may have been reworked in a glacio-fluvial system and could have been deposited under poor bleaching conditions. However, it still remains uncertain which dates are more likely to be correct as the two luminescence samples collected above and below the radiocarbon sample did provide similar ages and are in good agreement with each other. Geologically there are several possible reasons why these sands are older than the others in the study. The Dogger Bank itself consists of Weichselian and older Pleistocene deposits that are overlain by Holocene sands and modern sand waves and still forms a raised platform within the southern North Sea (e.g. Cameron et al., 1992; Laban, 1995; Fitch et al., 2005). During the Weichselian, the topographic high from which the core 21VC was obtained had probably been a land tongue extending from the Dogger Bank, cutting the area of the core position off from the generally abundant sediment supply deriving from river runoff through the Elbe palaeovalley and a series of other braided drainage channels in the

German Bight (e.g. Figge, 1980; Gibbard, 1988). Their melt and river waters were probably discharged to a freshwater lake located to the southeast of the Dogger Bank (Streif, 1990). Thus, sedimentation rates at core site 21VC on the other side of the land tongue and melt-water lake were likely to have been a lot lower, or sediment starvation may even have (episodically) occurred in the area. This would have resulted in a relatively thin layer of Weichselian fluvial sand between Saalian till material and Holocene marine sediments, and Weichselian sediments which are significantly older than those from the other analysed cores. Alternatively, no Late Weichselian deposition took place on the topographical high in the first place, due to its greater elevation. As a third scenario wave erosion of the postglacial transgressive sea on the Upper Pleistocene surface may have removed much of the Late Weichselian glacio-fluvial sand, and deposited a thin layer of Holocene sediments after sea level rose. Postglacial fluvial channels were still active in the area during the Early Holocene (Fitch et al., 2005), which may also have contributed to the erosion of late glacial sediments from the surface and redeposited them elsewhere.

Core 14VC was recovered from a small-scale Pleistocene glacial topographical high (e.g. a fossil river bank or terrace) further east of the Dogger Bank. The analysed OSL sample of this core dates somewhat older (Glacial maximum), and like 21VC the core only contains a thin layer of Holocene top sediments. Cores 15VC and 16VC obtained in the direct vicinity of core 14VC also contain only 50 cm and 70 cm of Holocene sediments, respectively (Reinhardt et al., 2007). Core AU04-12-VC taken from almost the same position during an earlier cruise in 2004 (Kudraß et al., 2004) contained no Holocene top sediments. Ten industrial vibrocores were taken on a transect over the core position of 14VC in 2005, which again showed only a thin Holocene sediment succession varying in thickness between 0 and 60 cm (A. Vink, unpublished data). Presumably, no sediments accumulated at this location during the Late Weichselian due to its topography. Instead, it could be a relict Pleistocene sand ridge of which much of the upper sediments were eroded during Early Holocene fluvial action and/or marine transgression. Hence the transition from Pleistocene to Holocene is most likely erosional and discordant which is also visible in the lithology.

Core 35VC, located on the western flank of the Elbe palaeovalley, comprises the most complete sedimentary record of Late Weichselian to Early Holocene landscape evolution including the deposition of two peat layers intercalated by a terrestrial silty sand

layer and the consecutive deposition of low-energy tidal flat deposits. The formation of the lower peat cannot be attributed to the direct effect of sea-level rise, as the commencement of the Holocene transgression in the region was much later (Lambeck, 1995; Vink et al., 2007; Behre, 2007). It is likely that changes in local hydrographic conditions, perhaps forced by changes in the fluvial system, triggered the formation of the lower peat. However the upper peat is considered to have been formed under the direct influence of rising sea level.

2.7 Conclusion

In accordance with our aim to examine the potential of OSL dating of continental shelf sediments from the North Sea, it is possible to establish an OSL chronology of sediments which is in agreement with ^{14}C dating as an independent age control. Adjacent samples collected from the same core yielded similar age, which reassures the consistency of the age and the ability of the OSL protocol to provide real depositional age where radiocarbon age shows limitations due to reworking of older organic detritus. The use of different statistical age models allowed extraction of the possible depositional age from a set of highly varied D_e distributions.

The combined OSL and radiocarbon ages of the (glacio-)fluvial and lacustrine sands deposited between 2 m and 0.5 m below the terrestrial-to-marine transition show that, in general, sedimentation in a predominantly periglacial, fluvial environment continued to occur throughout the latest Weichselian and Early Holocene (approximately 16-8 ka BP), right up to the elevation-dependent time of transgression (e.g. in cores 26VC, 35VC, 41VC). The absence of large unconformities suggests that the earliest Holocene period was not as strongly erosive in the present continental shelf area as it was in the coastal areas of Schleswig- Holstein (eastern German Bight) (e.g. Behre et al., 1979).

Small discontinuities in sedimentation were observed in the near-shore regions of this study (06VC and 49VC). These can be attributed to the relatively high elevation which caused less accumulation space for sediments close to the present day coastline, and/or due to episodic fluvial and eolian erosion (or a combination of these factors). Relatively large unconformities were observed in the north-eastward extension of the Dogger Bank (21VC) and on what may have been a Weichselian sand ridge or river bank (14VC). Weichselian

sedimentation rates at 21VC are likely to have been much lower or sediment starvation may even have (episodically) occurred in the area, resulting in a relatively thin layer of Weichselian fluvial sand between Saalian till material and Holocene marine sediments, and Weichselian sediments which are significantly older than those in the other studied cores.

In summary, quartz OSL dating show that there was still sufficient accumulation space left within the generally subsiding North Sea Basin for terrestrial deposition to occur in offshore areas until the time of marine transgression. This is in general agreement with the results from a high resolution seismic survey of the western part of the Dogger Bank (Fitch et al., 2005), where a large-scale, proglacial meandering fluvial channel network was thought to have existed between the end of the last glaciation and the Holocene marine transgression. The prevailing fluvial channel was considered to be the main source of sedimentation in the region, and deposited reworked sediments from the Pleistocene hinterland on top of the Late Pleistocene sandy palaeo-surface. Though our study can only be considered as providing fragmentary evidence for the understanding of Late Pleistocene and Early Holocene landscape evolution in the region, it does provide a solid framework for further detailed OSL studies with high-resolution sampling in fossil-depleted glacial sediments.

2.8 Acknowledgements

This research has been supported by Leibniz DAAD fellowship funded by the German Academic Exchange Service (DAAD) and the Leibniz Institute for Applied Geophysics, Hannover (LIAG), which is greatly acknowledged. The authors are thankful to the anonymous reviewers who provided thoughtful suggestions and detailed review on this manuscript. L.A. is grateful to Dr. Agnes Novothny for untiring help and discussions in the beginning, which enhanced understanding of the technique. The authors are thankful to Gudrun Drewes and Petra Posimowski, technicians of LIAG-Section S3 for the preparation and measurements of radiocarbon samples.

2.9 References

- Adamiec, G., Aitken, M.J., 1998. Dose-rate conversion factors: update. *Ancient TL* 16, 37-49.
- Aitken MJ, 1998. *Introduction to Optical Dating*. Oxford, Oxford University Press, 262 pp.
- Aitken MJ, 1985. *Thermoluminescence Dating*. London, Academic Press, 359pp.
- Arnold, L.J., Bailey, R.M., Tucker, G.E., 2007. Statistical treatment of fluvial dose distributions from southern Colorado arroyo deposits. *Quaternary Geochronology* 2, 162-167.
- Arnold, L.J., Roberts, R.G., 2009. Stochastic modelling of multi-grain equivalent dose (D_e) distributions: Implications for OSL dating of sediment mixtures. *Quaternary Geochronology* 4, 204-230.
- Baeteman, C., Van Strijdonck, M., 1989. Radiocarbon dates on peat from the Holocene coastal deposits in West Belgium. In: Baeteman, C. (Ed.), *Quaternary sea-level investigations from Belgium*, Ministerie van Economische Zaken, Geologische Dienst van België, Brussel, pp. 59-91.
- Bailey, R.M., Arnold, L.J., 2006. Statistical modelling of single-grain quartz D_e distributions and an assessment of procedures for estimating burial dose. *Quaternary Science Reviews* 25, 2475-2502.
- Ballarini, M., Wallinga, J., Murray, A.S., Heteren, S.v., Oost, A.P., Bos, A.J.J., Eijk, C.W.E.v., 2003. Optical dating of young coastal dunes on a decadal time scale. *Quaternary Science Reviews* 22, 1011-1017.
- Ballarini, M., Wallinga, J., Wintle, A.G., Bos, A.J.J., 2007. A modified SAR protocol for optical dating of individual grains from young quartz samples. *Radiation Measurements* 42, 360-369.
- Behre, K.E., 2004. Coastal development, sea-level change and settlement history during the later Holocene in the Clay District of Lower Saxony (Niedersachsen), northern Germany. *Quaternary International* 112, 37-53.
- Behre, K.E., 2007. A new Holocene sea-level curve for the southern North Sea. *Boreas* 36, 82-102.

- Behre, K.E., Menke, B., Streif, H.J., 1979. The Quaternary geological development of the German part of the North Sea. In: Oele, E., Schüttenhelm, R.T.E., Wiggers, A.J. (Eds.), *The Quaternary History of the North Sea. Acta Universitatis Upsaliensis, Symposium Universitatis Upsaliensis Annum Quingentesimum Celebrantis*, vol. 2. University of Uppsala, Uppsala, pp. 85-113.
- Bijlsma, S., 1982. Geology of the Holocene in the Western part of the Netherlands, In: de Bakker, H., van den Berg, M.W. (Eds), *Proceedings of the symposium on peat lands below the sea level, International Institute for land Reclamation and Improvement ILRI, Wageningen, The Netherlands*, pp.11-41.
- Burleigh, R., 1974. Radiocarbon dating: some practical considerations for the archaeologist. *Journal of Archaeological Science* 1, 68-97.
- Bungenstock, F., 2005. Der holozäne Meeresspiegelanstieg südlich der ostfriesischen Insel Langeoog, südliche Nordsee - hochfrequente Meeresspiegelbewegungen während der letzten 6000 Jahre. *Ph.D. thesis*, University of Bonn, 184 pp.
- Cameron, T.D.J., Stocker, M.S., Long, D., 1987. The history of Quaternary sedimentation in the U.K. Sector of the North Sea Basin. *Journal of the Geological Society* 144, 43-58.
- Cameron, T.D.J., Crosby, A., Balson, P.S., Jeffery, D.H., Lott, G.K., Bulat, J., Harrison, D.J., 1992. *United Kingdom Offshore Regional Report: The Geology of the Southern North Sea*. HMSO for the British Geological Survey, 152 pp.
- Caston, U.N.D., 1979. A new isopachyte map of the Quaternary of the North Sea. In: Oele, E., Schüttenhelm, R.T.E., Wiggers, A.J. (Eds.), *The Quaternary History of the North Sea. Acta Universitatis Upsaliensis, Symposium Universitatis Upsaliensis Annum Quingentesimum Celebrantis*, vol. 2. University of Uppsala, Uppsala, pp. 23-28.
- Duller, G.A.T., 2003. Distinguishing quartz and feldspar in single grain luminescence measurements. *Radiation Measurements* 37, 161-165.
- Duller, G.A.T., 2008. Single-grain optical dating of Quaternary sediments: why aliquot size matters in luminescence dating. *Boreas* 37, 589-612.
- Duller, G.A.T., Bøtter-Jensen, L., Murray, A.S., 2000. Optical dating of single sand-sized grains of quartz: sources of variability. *Radiation Measurements* 32, 453-457.

- Eisma, D., Mook, W.G., Laban, C., 1981. An early Holocene tidal flat in the Southern Bight. *International Association of Sedimentologists*. Special Publication, 5, 229-237.
- Ehlers, J., 1990. Reconstructing the dynamics of the north-west European Pleistocene ice sheets. *Quaternary Science Reviews* 9, 71-83.
- Ehlers, J., Gibbard, P.L., 2007. The extent and chronology of Cenozoic Global Glaciation. *Quaternary International* 164-165, 6-20.
- Ehlers, J., Eissmann, L., Lippstreu, L., Stephan, Hans-J., Wansa, S., 2004. Pleistocene glaciations of North Germany. In: Ehlers, J., Gibbard, P.L., (Eds.), *Quaternary Glaciations- Extent and Chronology* 12, 135-146.
- Figge, K., 1980. Das Elbe-Urstromtal im Bereich der Deutschen Bucht (Nordsee). *Eiszeitalter und Gegenwart* 30, 203-211.
- Fitch, S., Thomson, K., Gaffney, V., 2005. Late Pleistocene and Holocene depositional systems and the palaeogeography of the Dogger Bank, North Sea. *Quaternary Research* 64, 185-196.
- Frechen, M., Neber A., Tsatskin A., Boenigk W., Ronen A., 2004. Chronology of Pleistocene sedimentary cycles in the Carmel Coastal Plain of Israel. *Quaternary International* 121, 41-52.
- Fuchs, M., Lang, A., 2001. OSL dating of coarse-grain fluvial quartz using Single-Aliquot protocols on sediments from NE-Peloponnese, Greece. *Quaternary Science Reviews* 20, 783-787.
- Fuchs, M., Owen, L.A., 2008. Luminescence dating of glacial and associated sediments: review, recommendations and future directions. *Boreas* 37, 636-659.
- Fuchs, M., Woda, C., Burkert, A., 2007. Chronostratigraphy of a sedimentary record from the Hajar mountain range in north Oman: Implications for optical dating of insufficiently bleached sediments. *Quaternary Geochronology* 2, 202-207.
- Galbraith, R.F., Roberts, R.G., Laslett, G.M., Yoshida, H., Olley, J.M., 1999. Optical dating of single and multiple grains of quartz from Jinmium rock shelter, northern Australia: Part I experimental design and statistical models. *Archaeometry* 41, 339-364.

- Gerdes, G., Petzelberger, B.E.M., Scholz-Bottcher, B.M., Streif, H., 2003. The record of climatic change in the geological archives of shallow marine, coastal, and adjacent lowland areas of Northern Germany. *Quaternary Science Reviews* 22, 101-124.
- Gibbard, P.L., 1988. The history of the great north-west European rivers during the past three million years. *Philosophical Transactions of the Royal Society of London B* 318, 559-602.
- Hoselmann, C., Streif, H., 2004. Holocene sea-level rise and its effect on the mass balance of coastal deposits. *Quaternary International* 112, 89-103.
- Hua, Q., 2009. Radiocarbon: a chronological tool for the recent past. *Quaternary Geochronology* 4, 378-390.
- Huntley D.J., Baril, M.R., 1997. The K content of the K-feldspars being measured in optical dating or in thermoluminescence dating. *Ancient TL* 15 (1), 11-13.
- Huuse, M., Lykke-Andersen, H., 2000. Overdeepened Quaternary valleys in the eastern Danish North Sea: morphology and origin. *Quaternary Science Reviews* 19, 1233-1253.
- Jacobs, Z., Duller, G.A.T., Wintle, A.G., 2003. Optical dating of dune sand from Blombos Cave, South Africa: II- single grain data. *Journal of Human Evolution* 44, 613-625.
- Jacobs, Z., Wintle, A.G., Roberts, R.G. and Duller, G.A.T., 2008. Equivalent dose distributions from single grains of quartz at Sibudu, South Africa: Context, causes and consequences for optical dating of archaeological deposits. *Journal of Archaeological Science* 35, 1808-1820.
- Jain M., Bøtter-Jensen L., Murray A.S., Jungner H., 2002. Retrospective dosimetry: dose evaluation using unheated and heated quartz from a radioactive waste storage building. *Radiation Protection Dosimetry* 101, 525-530.
- Juyal, N., Chamyal, L.S., Bhandari, S., Bhushan R., Singhvi, A.K., 2006. Continental record of the southwest monsoon during the last 130 ka: evidence from the southern margin of the Thar Desert, India. *Quaternary Science Reviews* 25, 2632-2650.
- Kudraß, H.-R., and cruise participants, 2004. *Cruise Report: North Sea BGR04-AUR / Leg 2*. Internal report, pp. 93.

- Kuhlmann, G., Wong, T.E., 2008. Pliocene paleoenvironment evolution as interpreted from 3D-seismic data in the southern North Sea, Dutch offshore sector. *Marine and Petroleum Geology* 25, 173-189.
- Laban, C., 1995. The Pleistocene glaciations in the Dutch sector of the North Sea: A synthesis of sedimentary and seismic data. *Ph.D. thesis*, University of Amsterdam, pp.194.
- Lambeck K. 1995. Late Devensian and Holocene shorelines of the British Isles and North Sea from models of glacio-hydro-isostatic rebound. *Journal of the Geological Society of London* 152, 437-448.
- Lepper, K., McKeever, S.W.S., 2002. An objective methodology for dose dispersion analysis, *Radiation Protection Dosimetry* 101 (1-4), 349-352.
- Lian, O.B., Roberts, R.G., 2006. Dating the Quaternary: Progress in luminescence dating of sediments. *Quaternary Science Reviews* 25, 2449-2468.
- Lutz, R., Kalka, S., Gaedicke, C., Reinhardt, L., Winsemann, J., 2009. Pleistocene tunnel valleys in the German North Sea: Spatial distribution and morphology. *Zeitschrift der Deutschen Gesellschaft für Geowissenschaften* 160 (3), 225-235.
- Madsen, A.T., Murray, A.S., Andersen, T.J., Pejrup, M., Breuning-Madsen, H., 2005. Optically stimulated luminescence dating of young estuarine sediments: a comparison with ^{210}Pb and ^{137}Cs dating. *Marine Geology* 214, 251-268.
- Mayya, Y.S., Morthekai, P., Murari, M.K., Singhvi, A.K., 2006. Towards quantifying beta microdosimetric effects in single-grain quartz dose distribution. *Radiation Measurements* 41, 1032-1039.
- Mejdahl, V., 1979. Thermoluminescence dating: beta-dose attenuation in quartz grains. *Archaeometry* 21, 61-72.
- Murray, A.S., Wintle, A.G., 2000. Luminescence dating of quartz using an improved single-aliquot regenerative-dose protocol. *Radiation Measurements* 32, 57-73.
- Murray, A.S., Olley, J.M., 2002. Precision and accuracy in the optically stimulated luminescence dating of sedimentary quartz: a status review. *Geochronometria* 21, 1-16.
- Murray, A.S., Wintle, A.G., 2003. The single aliquot regenerative dose protocol: potential for improvements in reliability. *Radiation Measurements* 37, 377-381.

- Oele, E., Schüttenhelm, R.T.E., 1979. Development of the North Sea after the Saalian glaciation. In: Oele, E., Schüttenhelm, R.T.E., Wiggers, A.J. (Eds.), *The Quaternary History of the North Sea*. Acta Universitatis Upsaliensis, Symposium Universitatis Upsaliensis Annum Quingentesimum Celebrantis, Vol. 2. University of Uppsala, Uppsala, pp. 191-215.
- Ollerhead, J., Huntley, D.J., Berger, G.W., 1994. Luminescence dating of sediments from Buctouche Spit, New Brunswick. *Canadian Journal of Earth Sciences* 18, 419-432.
- Olley, J.M., Caitcheon, G.G., Murray, A.S., 1998. The distribution of apparent dose as determined by optically-stimulated luminescence in small aliquots of fluvial quartz: Implications for dating young samples. *Quaternary Science Reviews (Quaternary Geochronology)* 17, 1033-1040.
- Olley, J.M., Caitcheon, G.G., Roberts, R.G., 1999. The origin of dose distributions in fluvial sediments, and the prospect of dating single grains from fluvial deposits using optically stimulated luminescence. *Radiation Measurements* 30, 207-217.
- Olsson, I.U., 1968. Modern aspects of radiocarbon datings. *Earth Science Reviews* 4, 203-218.
- Özer, C., 2009. Geologische Erkundung des Elbeurstromtals basierend auf flachseismischen und sedimentologischen Daten. *B.Sc. Thesis*, Leibniz University of Hannover, 57pp.
- Prescott, J.R., Stephan, L.G., 1982. Contribution of cosmic radiation to environmental dose. *PACT* 8, 205-213.
- Prescott, J.R., Hutton, J.T., 1988. Cosmic ray and gamma ray dosimetry for TL and ESR. *Nuclear Tracks and Radiation Measurements* 14, 223-227.
- Prescott, J.R., Hutton, J.T., 1994. Cosmic ray contributions to dose rates for luminescence and ESR dating: large depths and long-term time variations. *Radiation Measurements* 23, 497-500.
- Preusser, F., Degering, D., Fuchs, M., Hilgers, A., Kadereit, A., Klasen, N., Krbetschek, M., Richter D., Spencer, J., 2008. Luminescence dating: basics, methods and applications, *Quaternary Science Journal (Eiszeitalter and Gegenwart)* 57, 95-149.

- Reinhardt, L., and cruise participants, 2007. *Cruise Report: BGR cruise BGR07 FRANKLIN Leg 2 Geology and Geophysics 10.07. - 28.07.2007*. Internal Report, pp.121.
- Roberts, R.G., Galbraith, R.F., Olley, J.M., Yoshida, H., Laslett, G.M., 1999. Optical dating of single and multiple grains of quartz from Jinmium rock shelter, northern Australia: Part II, results and implications. *Archaeometry* 41, 365-395.
- Stokes, S., Ingram, S., Aitken, M.J., Sirocko, F., Anderson, R., Leuschner, D., 2003. Alternative chronologies for Late Quaternary (Last Interglacial-Holocene) deep sea sediments via optical dating of silt-size quartz. *Quaternary Science Reviews* 22, 925-941.
- Streif, H., 1990. Das ostfriesische Küstengebiet. *Sammlung geologischer Führer* 57, Gebr. Borntraeger, 376 pp.
- Streif, H., 2004. Sedimentary record of Pleistocene and Holocene marine inundations along the North Sea coast of Lower Saxony, Germany. *Quaternary International* 112, 3-28.
- Stuiver, M., Reimer, P.J., 1993. Extended ^{14}C data base and revised CALIB 3.0 ^{14}C age calibration program. *Radiocarbon* 35, 215-230.
- Thomsen, K.J., Murray, A.S., Bøtter-Jensen, L., 2005. Sources of variability in OSL dose measurements using single grains of quartz. *Radiation Measurements* 39, 47-61.
- Vink, A., Steffen, H., Reinhardt, L., Kaufmann, G., 2007. Holocene relative sea-level change, isostatic subsidence and the radial viscosity structure of the mantle of northwest Europe (Belgium, the Netherlands, Germany, southern North Sea). *Quaternary Science Reviews* 26, 3249-3275.
- Wallinga, J., Murray, A., Wintle, A., 2000. The single-aliquot regenerative-dose (SAR) protocol applied to coarse-grain feldspar. *Radiation Measurements* 32, 529-533.
- Wintle, A.G., 1997. Luminescence dating: laboratory procedures and protocols. *Radiation Measurements* 27, 769-817.
- Wintle, A.G., Murray, A.S., 2006. A review of quartz optically stimulated luminescence characteristics and their relevance in single aliquot regeneration dating protocols. *Radiation Measurements* 41, 369-391.

Application of OSL dating on coastal sediments...

Zeiler, M., Schulz-Ohlberg, J., Figge, K., 2000. Mobile sand deposits and shoreface sediment dynamics in the inner German Bight (North Sea). *Marine Geology* 170, 363-380.

Geochronometria

(<http://dx.doi.org/10.2478/v10003-010-0025-1>)

**Chronology of Cauvery delta sediments from shallow subsurface cores
using high-temperature post- IR IRSL dating of feldspar**

L. Alappat^{*a}, S. Tsukamoto^{*}, P. Singh^{**}, D. Srikanth^{**}, R. Ramesh^{***}, M. Frechen^{*}

**Leibniz Institute for Applied Geophysics (LIAG), Section S3: Geochronology and Isotope
Hydrology, Stilleweg 2, 30655 Hannover, Germany*

***Department of Earth Sciences, School of Physical Chemical and Applied Sciences,
Pondicherry University, Puducherry - 605 014, India*

****Institute for Ocean Management, Anna University, Chennai 600 025, India*

^aCorresponding author: Linto.Alappat@liag-hannover.de, lintoalappat@yahoo.co.uk

Abstract

We present the results of luminescence dating of sediments from two cores from the Cauvery Delta in south-east India. Since all natural quartz OSL signals except one sample were in saturation, the elevated temperature post- IR IRSL protocol for K-feldspar was applied to establish a chronology. Internal dose rate of K-feldspar grains were calculated from the measured internal content of potassium, uranium, thorium and rubidium from the bulk K-feldspar grains using solution ICP-OES and ICP-MS analysis. A substantial scatter in single-aliquot D_e values was observed which is most probably due to the effect of incomplete bleaching of fluvial sediments before burial. A minimum age model was applied to extract possible depositional ages. It was revealed in the study that except an upper layer of Holocene sediments (< 5m), the majority of the upper ~50m of Cauvery delta sediments were deposited between marine isotope stage (MIS) -5 and MIS-10 or

Application of OSL dating on coastal sediments...

older. The feldspar luminescence ages also indicate the existence of a period of non deposition or erosion in the upper part of the cores.

Key words: Cauvery delta; fluvial sediments; OSL dating; elevated temperature IRSL; K-feldspar.

Due to copyrights this manuscript is not included in the online version.

Please see the printed version or check the following webpage:

http://www.geochronometria.pl/pdf/geo_37/Geo37_06.pdf

Chronology of Cauvery delta sediments from shallow subsurface cores using high-temperature post-IR IRSL dating of feldspar. Alappat, L., Tsukamoto, S., Singh, P., Srikanth, D., Ramesh, R., Frechen, M., 2010. *Geochronometria*. Vol. 37, 37-47p.

Journal of Asian Earth Science (in press)

(<http://dx.doi.org/10.1016/j.jseaes.2011.05.019>)

Evolution and chronology of late Holocene coastal dunes in the Cauvery delta region of Tamil Nadu, India.

L. Alappat^{*a}, M. Frechen^{*}, R. Ramesh^{**}, S. Tsukamoto^{*}, S. Srinivasalu^{***}

**Leibniz Institute for Applied Geophysics (LIAG), Section S3: Geochronology and Isotope Hydrology, Stilleweg 2, 30655 Hannover, Germany*

***Institute for Ocean Management, Anna University, Chennai 600 025, India*

****Department of Geology, Anna University, Chennai 600 025, India*

^aCorresponding author: Linto.Alappat@liag-hannover.de, lintoalappat@yahoo.co.uk

Tel. 0049-5116433487; 0091-4802701311; Fax 0049-5116433665

Abstract

Widespread occurrences of coastal dunes are observed in the Cauvery delta region of Tamil Nadu in Vedaranniyam in the south east coast of India. These dunes were studied to establish the chronology of their formation and to understand their evolution using optically stimulated luminescence (OSL) dating in combination with sedimentological studies (quartz grain surface morphology using scanning electron microscope, grain size and heavy mineral analysis). The study shows that on the south-east coast of India widespread periodic dune formation/ reactivation has taken place during the Late Holocene to very recent times due to a variety of reasons such as climatic variation and land use changes. The sand mobility index shows that the dunes in the area have been largely active during the past century in the southern part in Nagapattinam region and many of the crests were active in the northern Cauvery delta in Cuddalore region. The angularity and fresh appearance of sand in the inland dunes suggest a short distance of sand transport and a

source proximal sand deposition was proposed for the dune formation. The study demonstrates the sensitivity of sand dunes on the south east coast of India to varying climatic conditions and changes in regional land use.

Key words: Coastal sand dune; Cauvery delta; optically stimulated luminescence dating; quartz; climatic variability

4.1 Introduction

Coastal dunes are important landform which may record information on alternate events of dune activity and stabilisation over a prolonged period of time, and provides information about coastal evolution, palaeoclimate as well as sea level changes (Porat and Botha, 2008; Banerjee et al., 2003). Coast parallel dunes are also important as it forms an effective barrier against natural disasters such as storms and Tsunamis. The formation and reactivation of dunes are mostly related to supply of sand, wind parameters such as direction, strength, frequency and duration as well as moisture content and grain size of the sediment (e.g., Pye and Tsoar, 1990; Tsoar, 2001; Thomas and Wiggs, 2008). Wind plays an important role in stabilising a dune by allowing vegetation growth on dune surface (winds having higher drift potential hinders the plant growth over dune surface) (Tsoar, 2002, 2001; Yizhaq et al., 2009) apart from moisture content of sand, and winds that exceed the velocity threshold will initiate movement of sand with certain grain size (Bagnold, 1941). The east coast of Tamil Nadu, southern India contains numerous vegetated and non-vegetated coast parallel to sub-parallel dunes which occur as discontinuous ridges all along the coast. Among the dunes observed in the east coast of Tamil Nadu, the Vedaranniyam region (between Nagapattinam and Point Calimere) (Fig. 1) possesses a remarkable occurrence of wide, successive dunes, varying in width from few meters to several tens of meters, which may give information on the chronology of coastal development in the region and different stages of emergence. The Vedaranniyam region is a fast emerging cusped foreland located in the south of Cauvery delta formed primarily by the southward drift of sediments by long shore currents (Sundararajan et al., 2009). In general the dunes occur with heights ranging from 0.5 to 7 m. There are only a

few studies that have been carried out to understand the chronology of dune formation in east coast of India (e.g., Kunz et al., 2010 a, b).

Luminescence dating is proved to be an efficient tool to find chronology of coastal sediments and has been successfully applied to inland and coastal dunes (eg., Reiman et al., 2010; Kunz et al., 2010 a, b; Quang-Minh et al., 2010; Tsoar et al., 2009; Clemmensen et al., 2009; Porat and Botha, 2008; Bateman and Godby, 2004; Frechen et al., 2004; Ballarini et al., 2003). Radiocarbon dating has only limited use due to fewer occurrences of organic material in the sand units. The chronological results from the dunes in the north (Cuddalore region) of the study area revealed evidence of early settlements and variation in monsoon activities in the region (Kunz et al., 2010a). Late Holocene to modern ages were proposed for various stages of dune formation in this area using optically stimulated luminescence (OSL) dating of dune sand. Other studies that used OSL dating for coastal deposits in the east coast of India include Murray and Mohanthi (2006) and Thomas (2009).

This study aims to set up a detailed chronological frame to understand the formation and reactivation history of coastal dunes of Tamil Nadu, in particular to the Cauvery delta region. Establishing the chronology of dune formation in the east coast of India may be of help in understanding the response of this landscape to climatic variability and anthropogenically induced activities such as settlements, change in agriculture and land use pattern. Dunes may be used as a proxy to extend the record of terrestrial climate variability and variation in precipitation for the periods beyond instrumental records. Studies on coastal evolution on a decadal time scale also provides information about the sand accretion and will help in the planning of coastal management, land use tools and policies and protection strategies with respect to modern wind climate. We present 28 OSL dates from 10 profiles to establish the chronology of dune formation and use sedimentological techniques (grain size analysis, heavy mineral analysis, and Scanning Electron Microscopic (SEM) analysis of quartz surface) to examine the possible sediment transport, depositional mechanism and provenance of sediments. An index for 'dune mobility' (Lancaster, 1988), also called 'potential dune surface sand activity' (Bullard et al., 1997) was calculated to assess the dune activity in the region. The index was also compared with the recently published OSL ages (Kunz et al., 2010 a, b) from the north of the study.

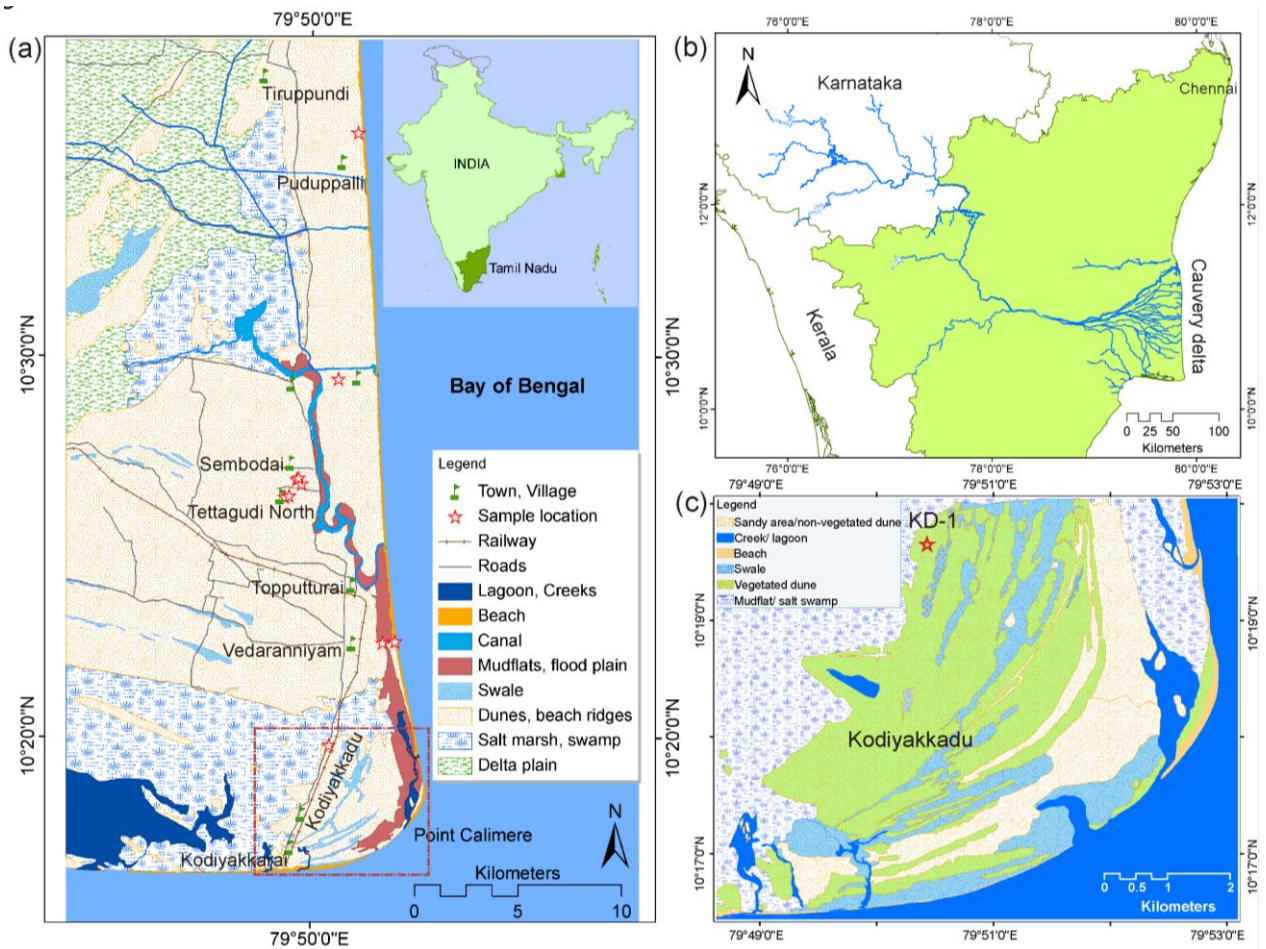


Figure 4.1. Map showing the sampling locations and basic geomorphology of the study area. Inset, map of India shows the location of Tamil Nadu where the Cauvery delta is located (Fig. 4.1a). The drainage basin of Cauvery River is spread across parts of Karnataka and Tamil Nadu, from where it brings sediments to the coast (Fig. 4.1b). A detailed geomorphology map of the southern tip of Cauvery delta in Kodiyakkurai region showing successive development of beach ridges parallel and sub-parallel to the coast (Fig. 4.1c).

4.2 Study area and samples

The study area (Fig. 1) is located in the southern part of Cauvery delta between the latitudes and longitudes of N10°16' to 10°40' and E 79°45' to 79°54'. The Point Calimere region is characterised by moderate to low energy coast, where as the coast in the north of Vedaranniyam is a wave dominated microtidal coast (Sundararajan et al., 2009). The dunes in the area occur as isolated outcrops in the inland area and as linear dune ridges

parallel to the coast towards shore region. The vegetation cover varies from sparse (Sembodai region) to very dense, (in Kodiyakkadu region) dominated by palm trees, tamarind, cashew and coconut trees in the inland region and by casuarinas, eucalyptus and other shrubs and creepers in the coastal region. The southern part in Kodiyakkadu (Fig.1c) is part of a wild life sanctuary and is located within the Kodiyakkarai reserve forest. In the inter-dunal depressions (swales) the soil is fertile, rich in clay and silt, and is widely converted to agricultural lands for paddy, vegetables and aquaculture ponds.

The highest temperature in the study area occurs during the pre-monsoon period (March-May) between 28°C-40°C. The region experiences a semi-arid to dry sub-humid climate and has a mean annual precipitation of 1030 mm for Nagapattinam district (Indian Meteorological Department (IMD)). Majority of the rainfall in the study area is received during the NE monsoon (October- December) with lesser rain during the SW monsoon.

The major wind directions for the study area, as observed in Madras observatory (Chennai) during the months of March to October are SE to W/SE and during November to February it is towards W/NE to NW/NE with maximum wind speeds of 4.5 m/s during the month of June. (Pant and Rupa Kumar, 1997).

4.2.1 Geology and geomorphology of the area

The Cauvery River originates in the Western Ghats and flows east over the Mysore plateau to the Bay of Bengal through the state of Tamil Nadu with an approximate aerial coverage of 87,900 sq. km. (Fig. 1b; Ramanathan et al., 1996; Singh and Rajamani, 2001). Geologically the river basin encounters various lithologies (Fig. 4.2), such as Archean granitoid gneisses (Peninsular gneiss) and intrusives, Closepet granite, Precambrian granulites and supracrustal belts (Bababudan and Sargur schist belt) in the upper reaches. The Bhavani, one of the major tributaries of river Cauvery in the south passes through charnockite massif forming the Nilgiri range, which include garnetiferous enderbites and basic granulites (gabbro to anorthosite) (Pattanaik et al.,2007). Towards the east, the area also features exposures of Cretaceous sediments (Uttatur, Ariyallur, Niniyur and Tiruchirrapalli formation), sandstone (Cuddalore formation) of Mio- Pliocene age and recent alluvium. The study area is covered by fluvio-marine and aeolian sediments such as coastal sand sheets, dunes and mudflats or salt swamps of recent age. The geomorphology of the area is

Application of OSL dating on coastal sediments...

mainly represented by vegetated and non vegetated dunes and beach ridge complexes, swales, spits, barriers, lagoons, palaeo river channels, natural levees, delta plains, mud flats and salt marshes.

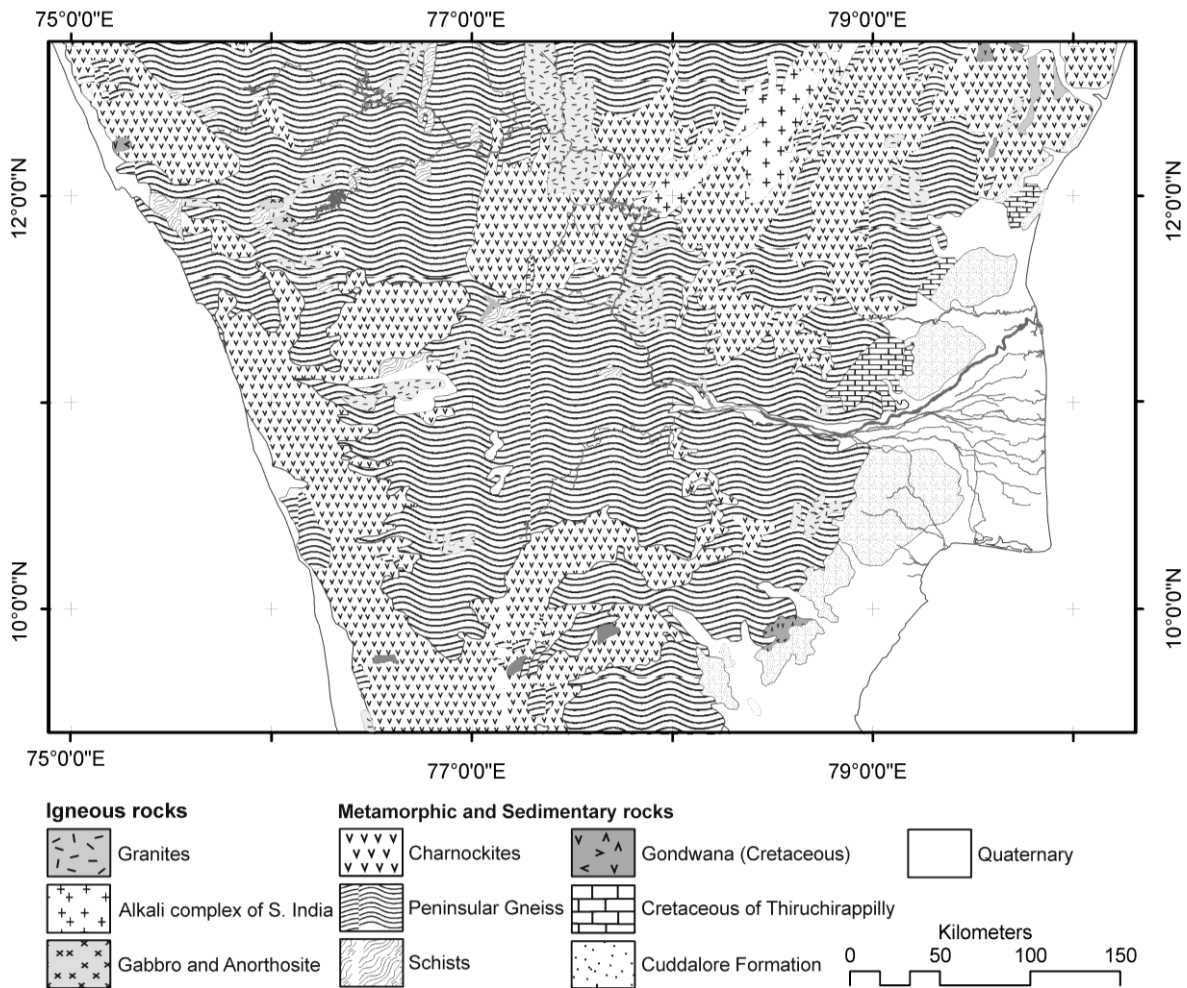


Figure 4. 2. General geology map of the Cauvery river basin (Modified from Geological Society of India map appended to the textbook on the Geology of India by Vaidyanadhan and Ramakrishnan, 2008)

4.2.2 Samples

Three sets of coast parallel dune/ beach ridge complexes were identified during field survey and representative profiles were excavated to collect samples from dunes in the coast to maximum extent towards inland (Fig. 4.1). Sampling was carried out from the vertical wall made from crust to bottom of the dune, which helped to see different beds and structures. Wherever possible, pits were excavated further down to the ground in order to retrieve samples from the lowest level feasible.

Tettagudi North village (TKN-1(10°36'18''N; 79°49'18''E); TKN-2 (10°26'20''N; 79°49'18''E)) forms the western-most part of the investigated dunes. Sections made in Sembodai region (SBD-1(10°26'46''N; 79°49'37''E); SBD-2 (10°26'39''N; 79°49'45''E) and SBD-3 (10°26'48.4''N; 79°49'40.20''E)) represented the second ridge towards east. The lateral distance between Tettagudi and Sembodai dunes was only ~1 km. In both villages, settlements were erected on top of the dune morphology. The eastern most coastal dunes were sampled from Puduppalli (PP-1; 10°35'52''N; 79°51'13''E) in the north and Vedaranniyam coast (VDC-1; 10°22'29''N; 79°51'54''E) in the south. . One sample was collected from the backshore region (VDB-1A; 10°22'31''N; 79°52'15''E) at a depth of 30 cm from surface as a reference sample to identify the degree of zeroing of luminescence signal.

Two profiles (TKN-1 and TKN-2) were excavated in Tettagudi area, second with a lateral distance of approximately 300 m towards northeast of the profile TKN-1. The upper part of the dune was organic rich and relatively stabilised with grass and creeper plants. Gradual soil development was evident with increased silt and clay content in this part. Profile TKN-1 (Fig. 3a) was excavated as three benches up to a depth of 4.7 m from the surface of the dune. Three samples were collected from TKN-1 profile (TKN-1A, B, C) and five samples from TKN-2 profile (TKN-2A, B, C, D and E) (Fig. 3b). In TKN-2 profile, a 3.2 m wall was made from the surface of the dune. Four different layers were identified including a clay-rich dark yellow to light brown upper bed, followed by a light grey sandy bed. This layer was underlain by dark yellow massive sand bed with a 0.15 m thick grey fine sand layer inter-bedded at a depth of 2 m.

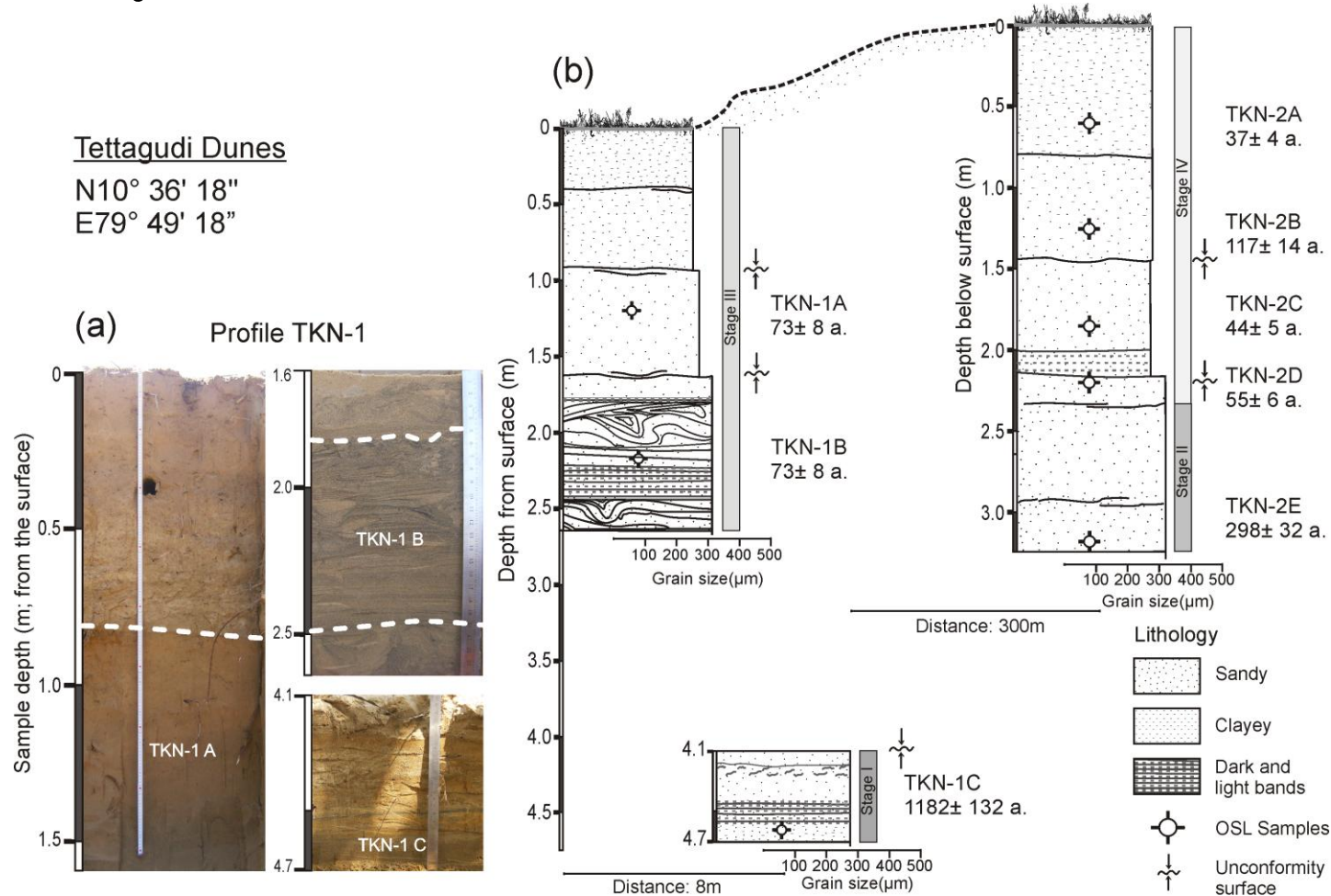


Figure 4.3a. Picture showing the vertical profile of Tettagudi area (TKN-1) with different sand units and depth marked. Three OSL samples were collected from the profile (TKN-1A, TKN-1B and TKN-1C). **3b.** Diagrammatic representation of profiles in Tettagudi area (TKN-1 and TKN-2). Visible unconformities, stages of sand accumulation, grain size and measured OSL ages are shown.

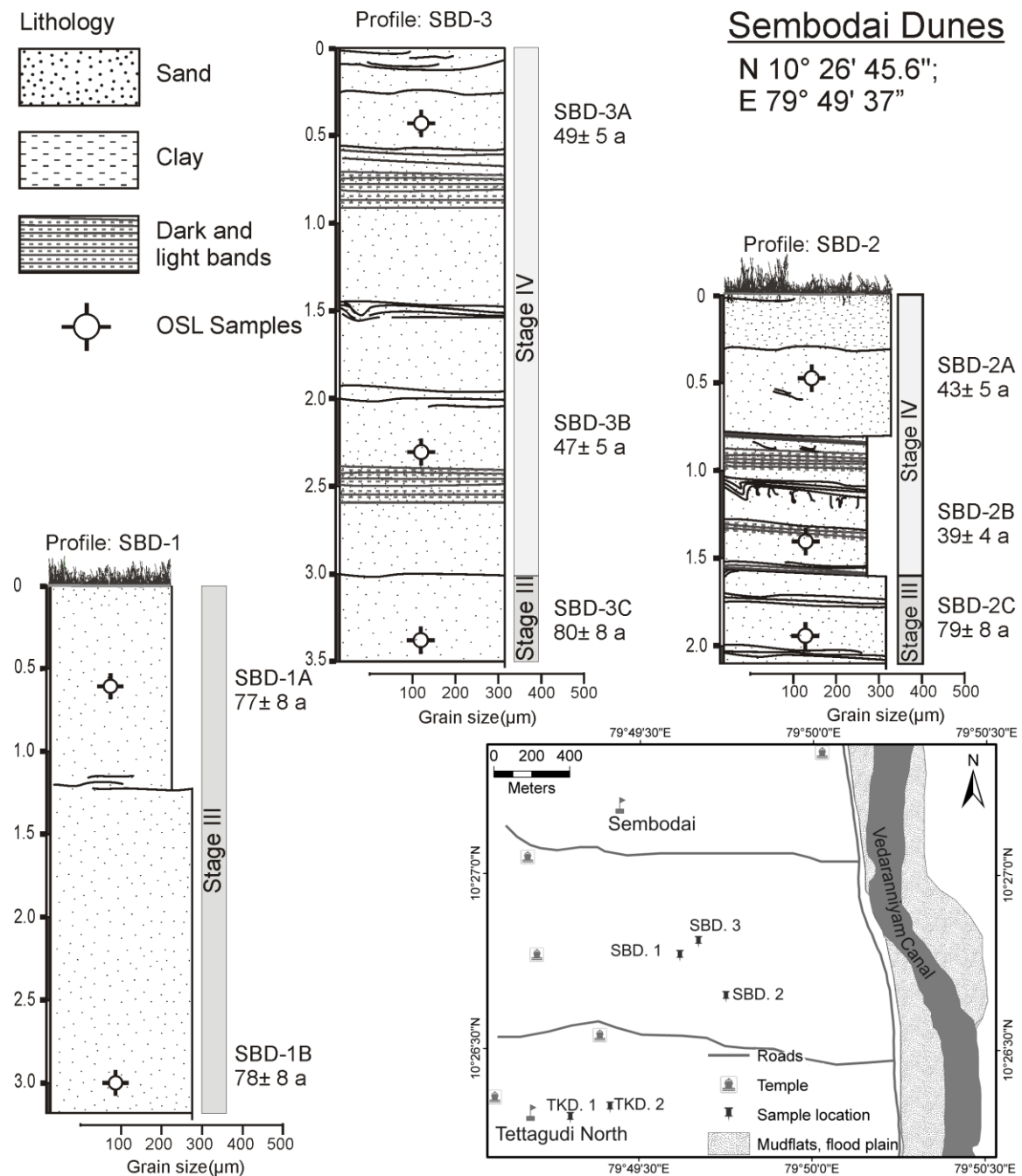


Figure 4.4. Diagrammatic representation of profiles in Sembodai area (SBD-1, SBD-2 and SBD-3). Visible unconformities, stages of sand accumulation, grain size and measured OSL ages are shown. The inset map shows the lateral distribution of sample profiles with locations marked.

In Sembodai region three profiles SBD-1, SBD-2 and SBD-3 were investigated. SBD-1 illustrates a continuous accumulation of sand without any visible unconformities up to a depth of 3.2 m below the surface and two samples (SBD-1A, B) were collected from this profile (Fig. 4.4). SBD-2 shows three distinct beds, a loose massive upper bed, thin dark and light parallel layers with burrow marks and bioturbation in the second bed and a bottommost bed of massive light yellow sand. SBD-3 exhibited a light yellow massive dune showing continuous accumulation of sand with few alternate dark and light heavy mineral layers intercalated. Three samples from each were collected at SBD-2 (SBD-2A, B, and C) and SBD-3 (SBD-3A, B, C) profiles (Fig. 4). In Kodyakkadu area one sample (KD-1A; N10°19'47.4"; E 79°50'29.6" (Fig. 1c)) was collected from a pit dug 1m below surface. In this region the ridges are curvilinear due to the shape of the coastline (Fig. 1c). The investigated dune was largely devoid of any structures and was stabilised by trees and shrubs.

The Puduppalli dune (Fig. 5a) is located ~1 km away from the coast with sparse or no vegetation. A 2.5 m profile was prepared in the dune and three distinct sand beds were identified for sampling (PP-1A, B, C). The upper bed was largely devoid of any sedimentary structures and layers, the middle bed showed dark and light alternating thin layers and the lowermost bed showed some irregular structures (Fig. 5a) possibly formed from animals grazing over the dunes.

Vedaranyam dune (Fig. 5b) is a fore dune located ~300 m away from the modern shoreline. The profile was made perpendicular to the coast parallel dune and five distinct depositional layers were identified and sampled (VDC-1 A, B, C, D, E). A 3 cm thick layer of coarse grained shell bearing sand was observed at a depth of 0.25 m between two uppermost layers (VDC-1A and B), representing a high energy storm event (Fig. 5b). Two inclined layers were observed between 0.5 and 1.1 m depth, sloping towards the coast indicating the change in dune axis and deposition of sand in the eastern flank of the dune. Samples for gamma measurements (~700 g) were collected from 10 cm surroundings of the OSL sample.

Puduppalli Dune (N10° 35' 51.7"; E79° 51' 13") Vedaranniyam dune (N10° 22' 29"; E79° 51' 54")

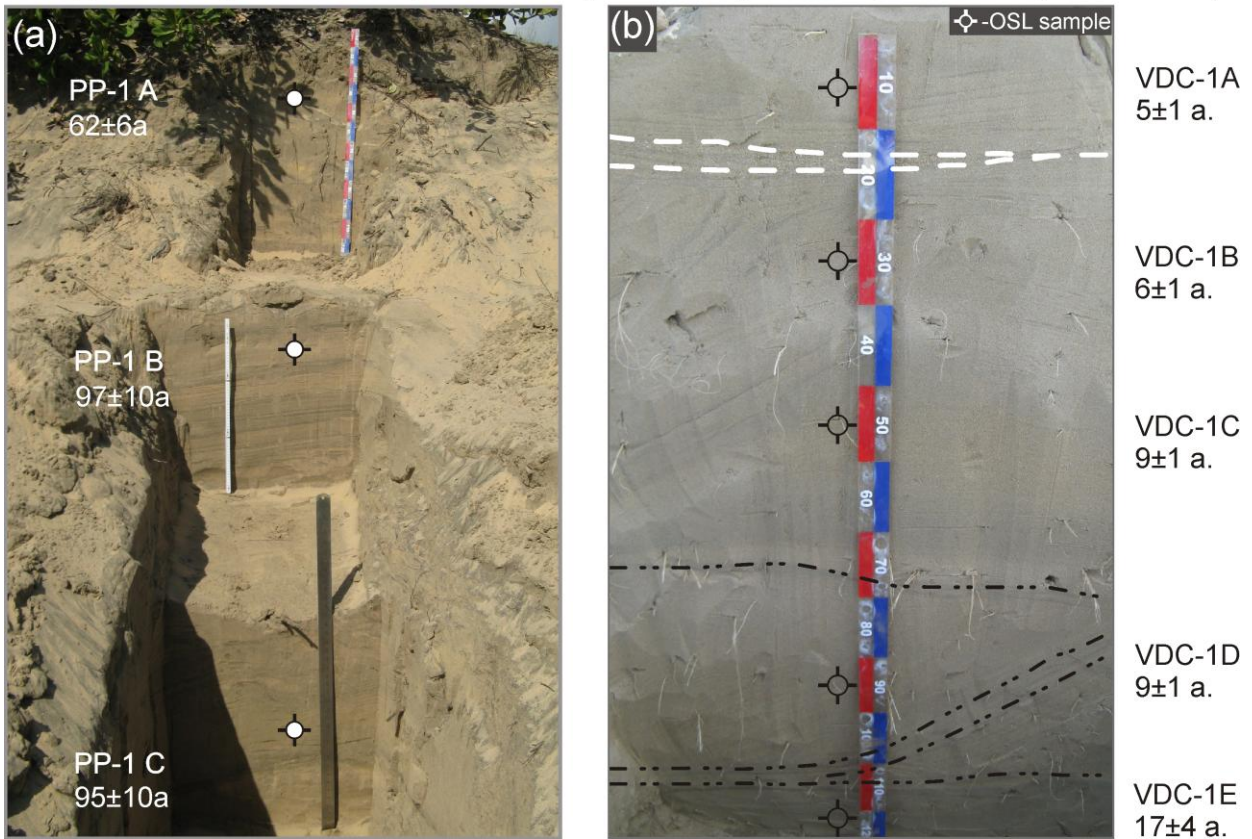


Figure 4.5a. Picture showing the sampling profile in Puduppalli area (PP-1) in the eastern most coastal dune belt with different sand units marked. Three OSL samples were collected from the profile (PP-1A, PP-1B and PP-1C) and the measured OSL ages are given. **4.5b.** Picture showing the sampling profile of Vedaranniyam foredune (VDC-1) with different sand layers marked. Five OSL samples were collected from the profile (VDC-1A, VDC-1B, VDC-1C, VDC-1D and VDC-1E) and the measured OSL ages are given. The coarse grained shell bearing high energy event layer (most likely from the 2004 December Indian Ocean Tsunami) is marked with white hatched line.

4.3 Methods

4.3.1 Luminescence dating

The sample tubes were opened in the laboratory under subdued red light. The grain size fractions of 100-150 μm or 150-200 μm of sample were separated by dry sieving using the standard laboratory sample preparation procedure (Aitken, 1998). After sieving the samples the selected fractions were treated with 0.1 N hydrochloric acid (HCl) to dissolve carbonates and iron oxides, 0.01 N sodium oxalate ($\text{Na}_2\text{C}_2\text{O}_4$) to remove the clay coatings, and 30% hydrogen peroxide (H_2O_2) to remove the organic matter from the samples. The quartz- rich fraction ($\sim 2.65 \text{ g cm}^{-3}$) was separated by density separation using an aqueous solution of sodium poly-tungstate ($3\text{Na}_2 \text{WO}_4 \cdot 9\text{WO}_3 \cdot \text{H}_2\text{O}$) and subsequently etched using 40% hydrofluoric acid (HF) for 60 minutes to remove feldspar contamination.

The grains were mounted on steel discs (9.8 mm) as a uniform thin layer of either 6 mm or 2 mm diameter and fixed with silicon spray. An automated Riso TL/OSL DA 20 reader attached with a $^{90}\text{Sr}/^{90}\text{Y}$ beta source which delivers a dose rate of 0.12 Gy/s was used for the measurements. Blue light emitting diodes (LED) ($470\pm 30 \text{ nm}$) were used for the optical stimulation of quartz and a Hoya U-340 (7.5 mm) filter was used to stop unwanted signal.

For dose rate measurements the bulk of the collected sample was dried at 50°C . The samples (700 g) were then filled into Marinelli beakers and sealed air tight to avoid radon loss. The prepared samples were stored for one month to gain ^{222}Rn - ^{226}Ra equilibrium. External dose rate for the samples were calculated from the activity concentrations of decay chains ^{238}U , ^{232}Th and ^{40}K measured using a high resolution gamma spectrometry (High Purity Germanium (HPGe) N-type coaxial detector) (Tables 1 and 2). The dose rate conversion factors of Adamiec and Aitken (1998) and beta attenuation factors of Mejdahl (1979) were applied for calculation. The cosmic dose rate was calculated based on the method proposed by Prescott and Stephan (1982) and Prescott and Hutton (1994) considering the sample's geographic location, altitude and depth. A moisture content of $6\pm 3\%$ (Kunz et al., 2010 a, b) was used in the dose rate calculation and a moisture content

of $20\pm 10\%$ (Murray and Mohanti, 2006) was applied for sample (VDB-1-A) collected in the intertidal zone.

Medium size aliquots (6 mm) were preferred for most of the measurements as the samples were young and signal to noise ratio was good enough to identify the D_e for most of the samples only when medium aliquots were used. Measurements were repeated with small aliquots (48 nos) when the D_e exhibited significant scattering while using medium aliquots and statistical age models were applied for D_e calculation. For all remaining samples only 24 aliquots were used for measurements and weighted mean of the D_e values were used for final D_e estimation. The uncertainties in D_e values are expressed as standard error of D_e estimates.

The single aliquot regenerative dose (SAR) protocol (Murray and Wintle, 2000; Wintle and Murray, 2006) was applied with additional measurement of the OSL- IR depletion ratio (Duller, 2003) to check feldspar contamination in the sample. Prior to D_e measurements all the samples were subjected to a dose recovery test (Murray and Wintle, 2003) at different preheat conditions from 160- 260°C with a fixed cut heat of 160°C. For dose recovery, two sets of tests were carried out. One test employing high temperature (280°C) hot bleach at the end of each SAR cycle and another one without hot bleach. It was found that the high temperature treatment was neither necessary nor suitable for young samples of few tens to hundred years (e.g. Ballarini et al., 2003) as it underestimate the given dose, whereas tests without hot bleach gave results identical to unity. The dose recovery test provided the ideal preheat- cutheat combination for the measurement of SAR protocol, where dose recovery shows unity with the given dose (Fig. 6a, c). The samples were also tested for possible thermal transfer of signals (Fig. 7) into the OSL traps due to high temperature treatments. The measured D_e values of quartz were evaluated and rejected if poor recycling ratio ($\pm 10\%$), high recuperation ($>5\%$ of natural) or poor IR depletion ratio ($\pm 15\%$) was identified (Fig. 6b, d). Measurement uncertainty of 1.5% was incorporated in the D_e calculation. The total numbers of accepted aliquots in relation to those measured (in brackets) are shown in Table 2.

For the thermal transfer test, the OSL signal measured after bleaching and preheating was indistinguishable from the background signal, which was consistent with zero up to a temperature of 220°C and showed an increasing trend towards higher temperature (Fig. 7).

The D_e determination was carried out using signals integrated over the first three channels, giving signals of initial 0.48 s stimulation and an early background subtracted (Ballarini et al., 2007) from the subsequent channels corresponding to 1.12- 2.4 s.

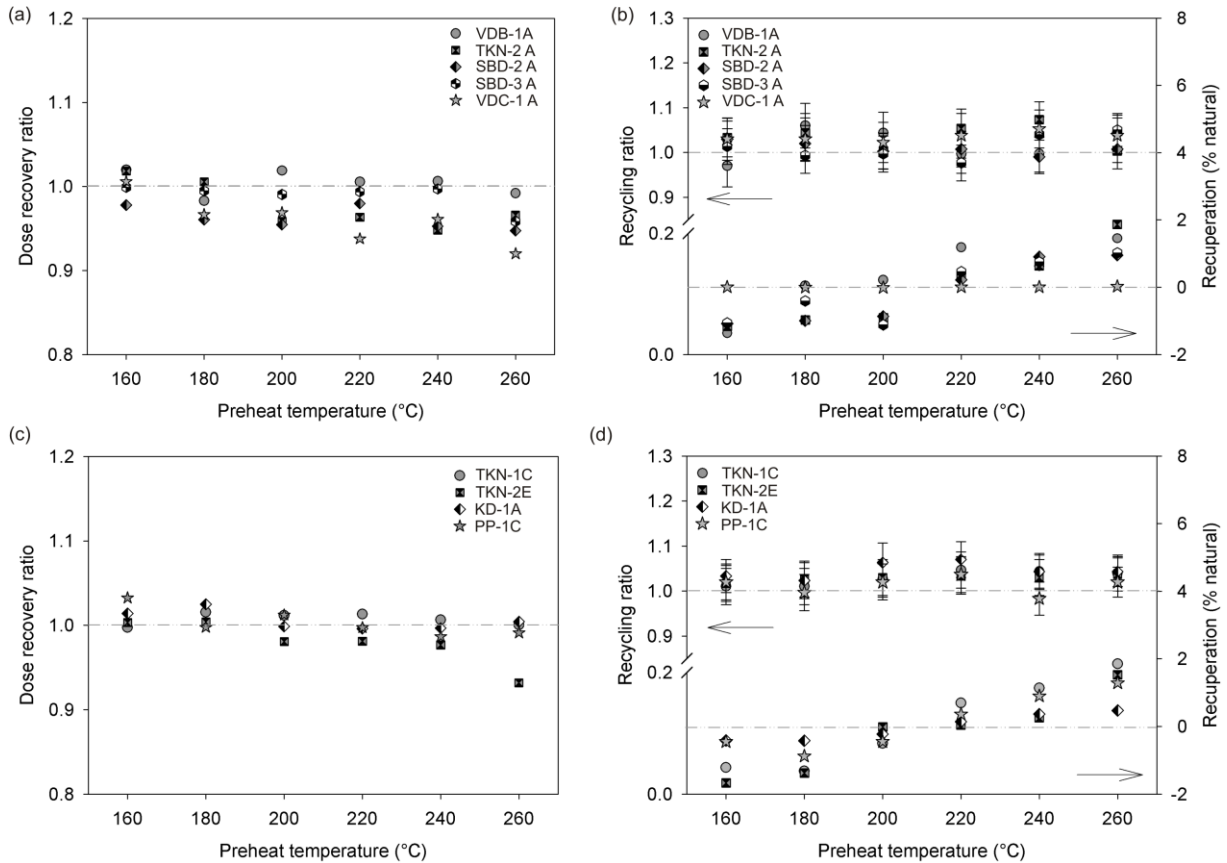


Figure 4.6 Diagram showing the details of quality checking criteria tested for all the samples in the study. Test results of selected younger samples in the profile (VDB-1A, TKN-2A, SBD-2A, SBD-3A and VDC-1A) and older (TKN-1C, TKN-2E, KD-1A and PP-1C) samples are shown. A final preheat temperature of 160/180° C was selected for measurements and early background subtraction was applied to extract the fast component of the quartz decay curve. The plot shows the dependence of dose recovery, recycling and recuperation ratios on various preheat temperatures for the young (a, b) and old (c, d) samples. A fixed cut heat of 160° C was used for all the tests. For each temperature the mean of three aliquots and the standard deviation are shown.

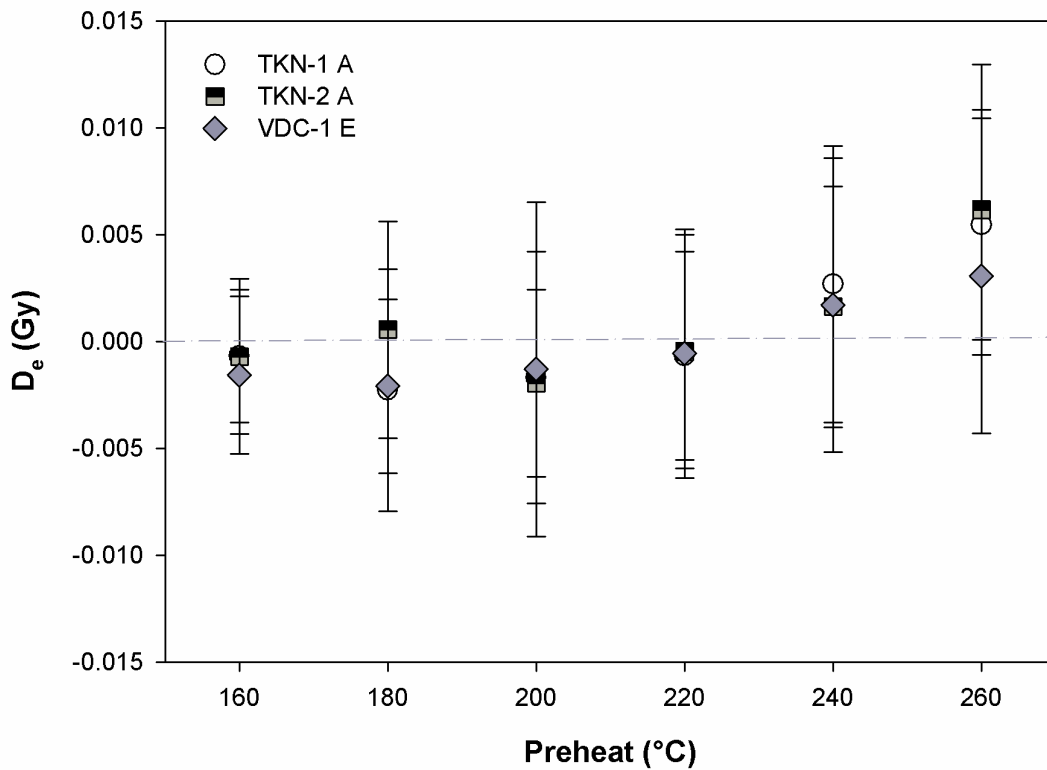


Figure 4.7. OSL signal (D_e in Gy) measured after completely bleaching the sample plotted against different preheat temperature showing the rate of thermal transfer of charge at different preheat temperatures for selected samples. It is observed that there is a slight increase in OSL signal at higher temperatures (>240°C) due to thermal transfer.

4.3.2 Sedimentological studies

The grain size analysis of selected samples from each bed in all the profiles were carried out to determine the distribution of particle size and the degree of sorting. The analyses were carried out using Retsch Camsizer on 50 g of untreated sand for selected samples from the profile to know the vertical variation in grain size. The results were calculated using the method of Folk and Ward (1957) employing the Gradistat programme (Blott and Pye, 2001) for the analysis of grain size statistics.

For scanning electron microscope (SEM) analysis we utilized the identical fraction of separated, non-etched quartz grain extracts that were used for OSL dating. Heavy minerals were separated from the same fraction using heavy liquid with densities $>2.7 \text{ g/cm}^3$. The heavy and light fractions were adhered to the stub and prepared for surface texture analysis and mineral identification. Quantitative assessment of surface textures were carried out by means of visual onscreen identification of various mechanical and chemical features and frequency of occurrence of those features in the given sample were noted. Samples analysed for quartz grain surface textures analysis used a FEI- Quanta 600 SEM equipped with a back scatter electron (BSE) detector having integrated sample tilt rotate stage and electron beam control.

The samples were analysed using standard optical microscopy to identify the heavy mineral constituents. Heavy mineral grains of 100-150 μm were mounted on glass slides with approximately 300 grains on each and were counted in a petrological microscope. The total number of identical mineral grains in each sample was counted and the number percentages of the same were calculated.

4.3.3 Dune mobility Index

One of the major parameters that determine the reactivation of dunes is climate related. The climate of a region is reflected in the vegetation cover which is related to the wind, precipitation and evaporation. When the wind speed exceeds a certain threshold velocity the sand grains of particular size sets to motion. This threshold shear velocity of dry sand can be calculated using the equation given by Bagnold (1941)

$$u_{(t)} = A \sqrt{(\rho_s - \rho_a)gD/\rho_a}$$

in which ρ_s is the density of sand, ρ_a is the density of the air, D is diameter of the grain, 'g' is gravity constant and A is a constant ($A = 0.12$).

Many indices have been proposed (Chepil et al., 1963; Fryberger, 1979; Ash and Wasson, 1983; Talbot, 1984; Wasson, 1984; Lancaster, 1988) to assess sand dune mobility based on the principle that dune activity increases with wind vector and decreases with increasing sand moisture. One of the most widely applied (Lancaster, 1988; Muhs and

Maat, 1993; Kar, 1993; Bullard et al., 1997; Lancaster and Helm, 2000) and relatively simple indexes is Lancaster's mobility index (*M*-index) (Lancaster, 1988), which was applied in this study to compare OSL ages with the periods of sand mobility during the last century. Lancaster's mobility index (Lancaster, 1988),

$$M = W / (P/PE),$$

estimates the mobile and stable phases of a dune field. The equation uses the ratio *W* (the percentage of time during the year with wind blowing above threshold velocity for sand transport) to *P/PE* (ratio of precipitation to potential evapotranspiration). The threshold wind speed is calculated for a height of 2m (U_{2m}) using the equation from Hsu (1977),

$$u_{(r)} = 0.070U_{2m}.$$

This value is substituted in the equation of Hsu and Weggel (2002) to calculate the threshold wind speed at varying heights. Based on the field observations by Lancaster (1988) the *M*-index represents the critical values in which dunes are fully active for $M > 200$, inter dunes are stabilised and flanks are active for $200 > M > 100$, only crests are active when $100 > M > 50$ and $M < 50$ for inactive vegetated dunes.

The Lancaster's sand mobility index (Lancaster, 1988) was calculated for the North (Cuddalore region) and South (Nagapattinam area) of the delta region. The daily wind speed data for variable periods (May 1961- April 2010) for three stations (Cuddalore, Karaikkal and Nagapattinam) in the region were obtained from the data archive of National Climatic Data Centre (NCDC) and data for the average monthly precipitation (1901-2008) for Cuddalore and Nagapattinam districts were obtained from Indian Meteorological Department (IMD). The meteorological stations of IMD generally measures wind speed at various heights between 10-30 m (Lakshmanan et al., 2009) and there was no information available about the height of anemometers for the stations wind data collected. A minimum standard height of 10 m was assumed based on previous studies (Muhs and Maat, 1993) in the calculation of threshold wind speed.

4.4 Luminescence dating results

Tests performed as a part of OSL measurements revealed good sample properties and most of the samples were well bleached prior to deposition (Fig. 8). General luminescence behaviour (natural and regenerated decay curve and dose response curve of an aliquot, and D_e distribution of 23 accepted aliquots) of a representative sample from Tettagudi profile (TKN- 1A; 73 ± 8 a) is shown in figure 8. Samples TKN-2A, B, and SBD-1B, were analysed using small aliquots due to the apparent scattering in the measured D_e values. For these samples, the D_e values were then calculated using Minimum Age Model (Galbraith et al., 1999). The details of dose rate calculation and OSL measurements are given in Table 1 and 2.

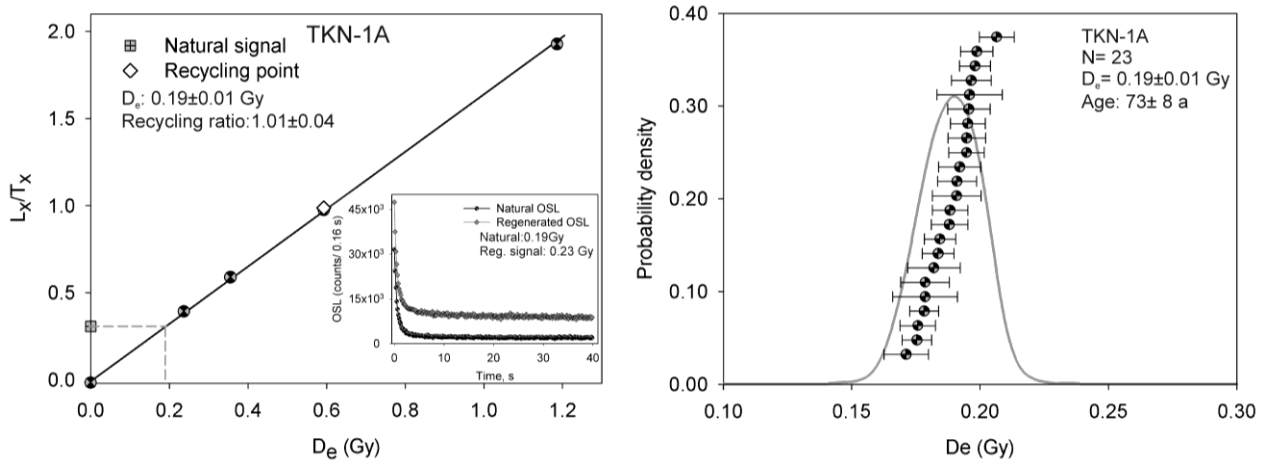


Figure 4.8a SAR growth curve from a young sample (TKN- 1A ; 73 ± 8 a) in the Tettagudi profile with an equivalent dose of 0.19 ± 0.01 Gy, showing OSL signals from regenerated laboratory doses as filled circles and that from a recycled dose as an open diamond. The sensitivity corrected natural OSL signal shown as filled square is interpolated onto the growth curve to give the equivalent dose ($D_e : 0.19 \pm 0.01$ Gy). Inset is the natural OSL decay curve together with the OSL signal from a regenerated laboratory dose 0.23 Gy. **b)** The D_e distribution of 23 accepted aliquots showing a tight Gaussian curve indicating that the samples were well bleached prior to deposition and exposed to a uniform radiation dose.

Table 4.1. Details of quartz OSL measurements of Vedaranniyam foredunes along with the zero dose sample (VDB-1A) collected from intertidal zone. The ^{40}K , Uranium and Thorium concentrations in the sediment was measured using high-resolution gamma spectrometer. An average water content of $6 \pm 3\%$ (Kunz et al, 2010 a, b) ($20 \pm 5\%$ for intertidal sample; VDB-1A) was applied in the dose rate calculation. The calendar years are calculated based on the sampling date in 2008 January. Over dispersion, σD represents the relative standard deviation of the measured single aliquot D_e distribution obtained using the ‘central age model’. The number of accepted aliquots ‘n’ using the acceptance criteria are given with the total measured aliquots in the brackets.

Location	Sample ID	Depth (cms)	K (%)	Th (ppm)	U (ppm)	D_e (Gy)	n	σD (%)	Cosmic dose (mGy a^{-1})	Dose rate (mGy a^{-1})	Age (a)	Age (AD)
Vedaranyam Beach	VDB-1A	30	1.61± 0.01	2.6± 0.03	0.3± 0.01	0.01± 0.01	19(20)	33	0.20± 0.02	1.65± 0.21	4± 1	2003- 2005
	VDC-1 A	20	1.6± 0.01	3.4± 0.03	0.4± 0.01	0.009± 0.005	22(24)	0	0.26± 0.03	1.98± 0.21	5± 1	2003- 2004
	VDC-1 B	40	1.61± 0.01	3.7± 0.02	0.4± 0.01	0.013± 0.009	16(24)	49	0.24± 0.02	1.99± 0.21	6± 1	2000- 2003
Vedaranyam Coast	VDC-1 C	60	1.6± 0.01	3.1± 0.03	0.4± 0.01	0.016± 0.010	21(24)	36	0.22± 0.02	1.92± 0.20	9± 1	1998-2001
	VDC-1 D	100	1.64± 0.01	1.6± 0.03	0.2± 0.01	0.016± 0.008	21(48)	34	0.19± 0.02	1.81± 0.19	9± 1	1998± 2001
	VDC-1 E	130	1.63± 0.01	2.7± 0.02	0.3± 0.01	0.032± 0.025	19(24)	60	0.18± 0.02	1.88± 0.20	17± 4	1987- 1994

Table 4.2. Summary of quartz measurement details (depth, radionuclide concentration, number of aliquots accepted/measured (n), De, dose rate, and OSL age) of inland and coastal dunes in Nagapattinam district. The 40K, Uranium and Thorium concentrations in the sediment was measured using high-resolution gamma spectrometer. An average water content of $6 \pm 3\%$ (Kunz et al, 2010a) was applied in the dose rate calculation. The calendar years are calculated based on the sampling date in 2008 January. The over dispersion, $\square D$ represents the relative standard deviation of the measured single aliquot De distribution obtained using the ‘central age model’. The number of accepted aliquots ‘n’ using the acceptance criteria are given with the total measured aliquots in the brackets. MAM was applied for few samples which showed significant scatter in their De values. The inferred final ages are given in bold. Errors here and in Table 1 are $\pm 1\sigma$.

Location	Sample ID	Depth (cms)	K (%)	Th (ppm)	U (ppm)	De (Gy)	n	σD (%)	MAM De	Cosmic dose (mGy a ⁻¹)	Dose rate (mGy a ⁻¹)	Age (a)	MAM age (a)	Age (AD)
	TKN-1A	125	0.80±0.01	11.3±0.05	1.1±0.02	0.19±0.01	22(24)	3	—	1.02±0.10	2.59±0.27	73±8	—	1927- 1942
	TKN-1B	210	0.76±0.00	13.4±0.03	1.3±0.01	0.17±0.01	21(24)	2	—	0.58±0.06	2.27±0.24	73±8	—	1927- 1942
	TKN-1C	460	0.83±0.01	19.2±0.07	1.5±0.02	3.02±0.60	22(24)	2	—	0.43±0.04	2.56±0.26	1182±132	—	693- 957
Thethakudi	TKN-2 A	60	0.87±0.01	27.9±0.08	2.1±0.02	0.34±0.31	31(48)	77	0.13±0.01	0.88±0.09	3.64±0.37	94±18	37±4	1968- 1975
North	TKN-2 B	125	0.83±0.01	21.3±0.04	1.7±0.01	0.57±0.30	29(48)	51	0.34±0.02	0.64±0.06	2.92±0.30	194±28	117±14	1877- 1905
	TKN-2 C	185	0.76±0.01	25.4±0.09	1.9±0.02	0.13±0.01	21(24)	2	—	0.47±0.05	2.96±0.30	44±5	—	1959- 1969
	TKN-2 D	220	0.75±0.01	29.3±0.06	2.1±0.02	0.18±0.01	24(24)	7	—	0.45±0.05	3.20±0.33	55±6	—	1947- 1958
	TKN-2 E	320	0.68±0.01	27.7±0.08	2.3±0.02	0.90±0.13	22(24)	14	—	0.40±0.04	3.02±0.31	298±32	—	1679- 1742

Table 4.2. (continued...)

Location	Sample ID	Depth (cms)	K (%)	Th (ppm)	U (ppm)	D _e (Gy)	n	σD (%)	MAM D _e	Cosmic dose (mGy a ⁻¹)	Dose rate (mGy a ⁻¹)	Age (a)	MAM age (a)	Age (AD)
Sembodai	SBD-1 A	60	0.86± 0.01	12.6± 0.05	1.2± 0.02	0.17± 0.01	22(24)	5	—	0.45± 0.04	2.16± 0.23	77± 8	—	1923- 1940
	SBD-1 B	300	0.74± 0.01	22.9± 0.05	1.9± 0.01	0.24± 0.03	24(24)	13	0.21± 0.01	0.33± 0.03	2.65± 0.27	89± 10	78± 8	1922- 1939
	SBD-2 A	50	0.72± 0.01	17.9± 0.07	1.3± 0.02	0.11± 0.01	23(24)	8	—	0.56± 0.06	2.48± 0.26	43± 5	—	1961- 1970
	SBD-2 B	145	0.81± 0.01	22.9± 0.06	1.7± 0.02	0.11± 0.01	23(24)	2	—	0.40± 0.04	2.75± 0.28	39± 4	—	1965- 1973
	SBD-2 C	200	0.76± 0.01	16.5± 0.07	1.3± 0.02	0.18± 0.01	19(24)	4	—	0.37± 0.04	2.24± 0.23	79± 8	—	1920- 1937
	SBD-3 A	45	0.74± 0.01	7.1± 0.03	0.7± 0.01	0.09± 0.01	23(24)	7	—	0.71± 0.07	1.92± 0.21	49± 5	—	1953- 1964
	SBD-3 B	230	0.73± 0.01	19.6± 0.08	1.6± 0.02	0.12± 0.01	14(24)	0	—	0.45± 0.04	2.53± 0.26	47± 5	—	1956- 1966
Kodiyakkadu	SBD-3 C	335	0.74± 0.01	19.6± 0.07	1.7± 0.02	0.19± 0.01	21(24)	6	—	0.32± 0.03	2.42± 0.25	80± 8	—	1919- 1936
	KD-1 A	50	1.32± 0.01	5.8± 0.04	0.6± 0.01	1.22± 0.04	23(24)	2	—	0.29± 0.03	1.95± 0.20	624± 65	—	1318- 1449
	Pushpavanam	PV-1 A	40	1.11± 0.01	34.2± 0.09	2.9± 0.02	0.92± 0.40	37(24)	45	0.48± 0.02	0.57± 0.06	4.06± 0.41	227± 28	118± 13
PV-1 B		90	1.11± 0.01	34.2± 0.09	2.9± 0.02	0.13± 0.02	23(24)	0	—	0.54± 0.05	4.03± 0.41	32± 3	—	1972- 1979
Pudupalli	PP-1 A	40	1.09± 0.01	20.8± 0.08	2.0± 0.02	0.18± 0.01	23(24)	0	—	0.30± 0.03	2.84± 0.29	62± 6	—	1939- 1952
	PP-1 B	150	1.01± 0.01	34.2± 0.05	2.5± 0.02	0.34± 0.02	24(24)	2	—	0.21± 0.02	3.55± 0.36	97± 10	—	1902- 1921
	PP-1 C	220	1.1± 0.01	17.4± 0.06	1.6± 0.01	0.24± 0.01	23(24)	1	—	0.19± 0.02	2.48± 0.26	95± 10	—	1903- 1923

4.4.1. Tettagudi dunes

The OSL dating of sample TKN-1C collected from the lowermost part at a depth of 4.6 m gave an age of $\sim 1180 \pm 130$ a. The two samples (TKN-1A, B) collected from the upper bench at depths of 1.25 and 2.1 m yielded identical age of 73 ± 8 a showing a contemporary accumulation of the upper 2.5 m of sand during that period. The sample TKN-2E from the bottom most part of the profile TKN-2 at a depth of 3.2 m showed a deposition age of 298 ± 32 a forming the oldest sand layer deposited in this profile. Two samples TKN-2D and TKN-2C collected at a depth of 2.2 and 1.85 m below surface gave a deposition age of 55 ± 6 a and 44 ± 5 a respectively. The age for the stratigraphically oldest sample and the subsequent younger sample show a gap in deposition most likely associated with the existence of stabilized, less favourable conditions for sand mobility in the region. The uppermost sample collected at a depth of 0.6 m below surface gave a deposition age of 37 ± 4 a, indicating active sand deposition up to this period in the area.

Similar to the TKN-1 profile, the surface layer of the TKN-2 profile was also partly stabilized and slightly indurated with the inclusions of silt and clay into the sand possibly due to water percolation during rain. The dune was covered with creeper grass and small shrubs, which would have arrested the movement of sand in the recent past. The OSL ages calculated using the weighted mean for the upper two samples (TKN-2A, B) were 94 ± 18 a and 194 ± 28 a showing an apparent overestimation of the burial age. These samples were also observed to have high scattering of measured D_e values. The minimum age model (MAM) applied to these samples provided a consistent age of 37 ± 4 a for the upper sample (TKN-2A), whereas the MAM age for TKN-2B was still higher (117 ± 14 a). This is attributed to the effect of pedoturbation, led to post depositional mixing (Bateman et al., 2003) in which the upper sample was less affected by the mixing of older sediments, whereas the second was severely affected by mixing of older grains which overestimated the deposition age of this sample. The over dispersion values (σD) for these samples were the highest among the measured samples by giving values of 77% and 51% respectively compared to the general 0-8% for well bleached samples in this study (Table 1, 2).

4.4.2 Sembodai dunes

Sample SBD-1B collected at the bottom of the profile SBD-1 at a depth of 3 m below surface gave an MAM OSL age of 78 ± 8 a. The sample collected from the upper part of the dune provided a deposition age of 77 ± 8 a, which is similar to the MAM age of the lowermost sample. The section was devoid of any bedding structures or unconformities within the 3.2 m sand unit and having similar depositional age for samples collected from top and bottom indicated a massive stage of sand accumulation (Fig. 4). Profile SBD-2 has a thickness of 2.1 m and one sample (SBD-2C) collected from the bottom part of the profile at 2 m depth, provided an age of 79 ± 8 a. Two samples (SBD-2B, SBD-2A) collected above this bed at depths of 1.45 and 0.5 m below dune surface furnish ages of 39 ± 4 a and 43 ± 5 a, respectively (Fig. 4). In profile SBD-3 the lowermost sample collected at a depth of 3.4 m (SBD-3C) yielded an age of 80 ± 8 a and two samples, SBD-3B and SBD-3A taken at depths of 2.3 m and 0.45 m showed deposition ages between 47 ± 5 a and 49 ± 5 a (Fig. 4).

4.4.3 Eastern coastal dunes

In Puduppalli profile, sample PP-1C collected at a depth of 2.2 m gave an OSL age of 95 ± 10 a and PP-1B and PP-1A collected at depths of 1.5 and 0.4 m provided deposition ages of 97 ± 10 a and 62 ± 6 a, respectively (Fig. 5 a).

In Vedaranniyam profile, the lowermost sample (VDC-1E) collected at a depth of 1.3 m formed the stratigraphically oldest sample in the dune with a deposition age of 17 ± 4 a. Two samples, VDC-1D and VDC-1C collected above this sample from two distinct layers at depths of 1 m and 0.6 m below the surface of the dune yielded identical ages of 9 ± 1 a. Another sample collected above this layer at a depth of 0.4 m provided an age of 6 ± 1 a and the sample collected on top of coarse grained shell bearing sand layer gave an age of 5 ± 1 a (Fig. 5b). The reference sample collected onshore from the intertidal region at a depth of 0.3 m provided an age of 4 ± 1 a indicating an excellent zeroing of the signal

before deposition. The only sample collected from Kodyakkadu profile at a depth of 0.5 m gave a deposition age of 624 ± 65 a.

The OSL ages for the southern part of the delta (this study) and for northern part of the delta (Kunz et al., 2010 a, b) were plotted against the calculated average annual M-index (Fig. 9a, b). The mobility values for Nagapattinam (South dunes, Fig. 9a) were calculated for the inland dunes corresponding to the threshold wind velocity required to initiate the movement of medium grain sand ($\sim 290 \mu\text{m}$). The smaller grain size observed in the coastal dunes ($\sim 180 \mu\text{m}$) was considered as mobile at these wind conditions. An average grain size of $180 \mu\text{m}$ was used for the calculation in Cuddalore region (North dunes, Fig. 9b).

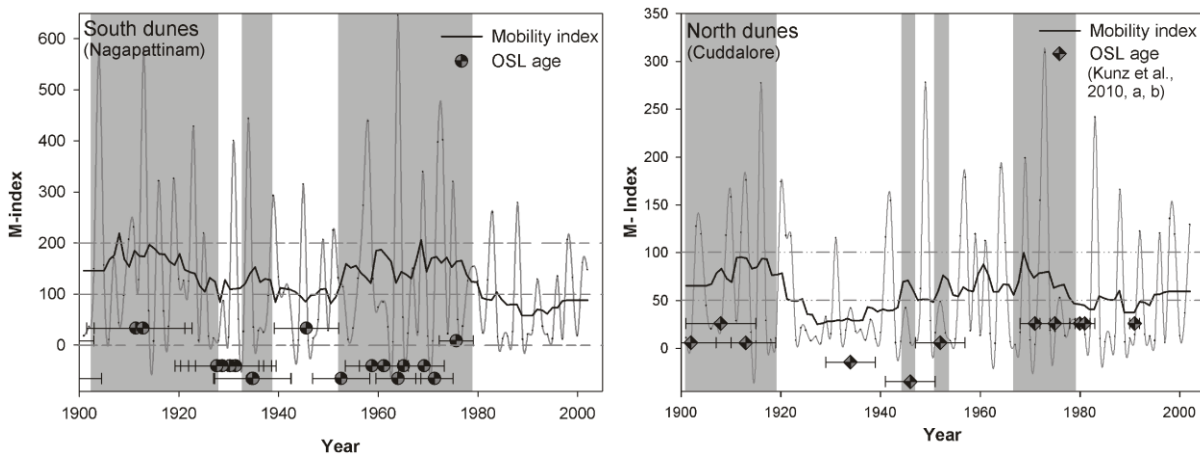


Figure 4.9. Plot showing the Lancaster's sand mobility index (M- index) for the last century. The measured OSL ages are plotted along with the calculated M-index values. Darker line shows the running average of mobility values and the lighter line in the background depicts the annual variation in the mobility index. The observed correlation with enhanced mobility values and OSL ages are highlighted with grey background. a) Sand mobility plot for the southern dunes (Nagapattinam) and b) for Northern dunes (Cuddalore region). The OSL ages for Cuddalore region was obtained from recent studies made by Kunz et al., (2010a, b).

4.5 Results of sedimentological studies

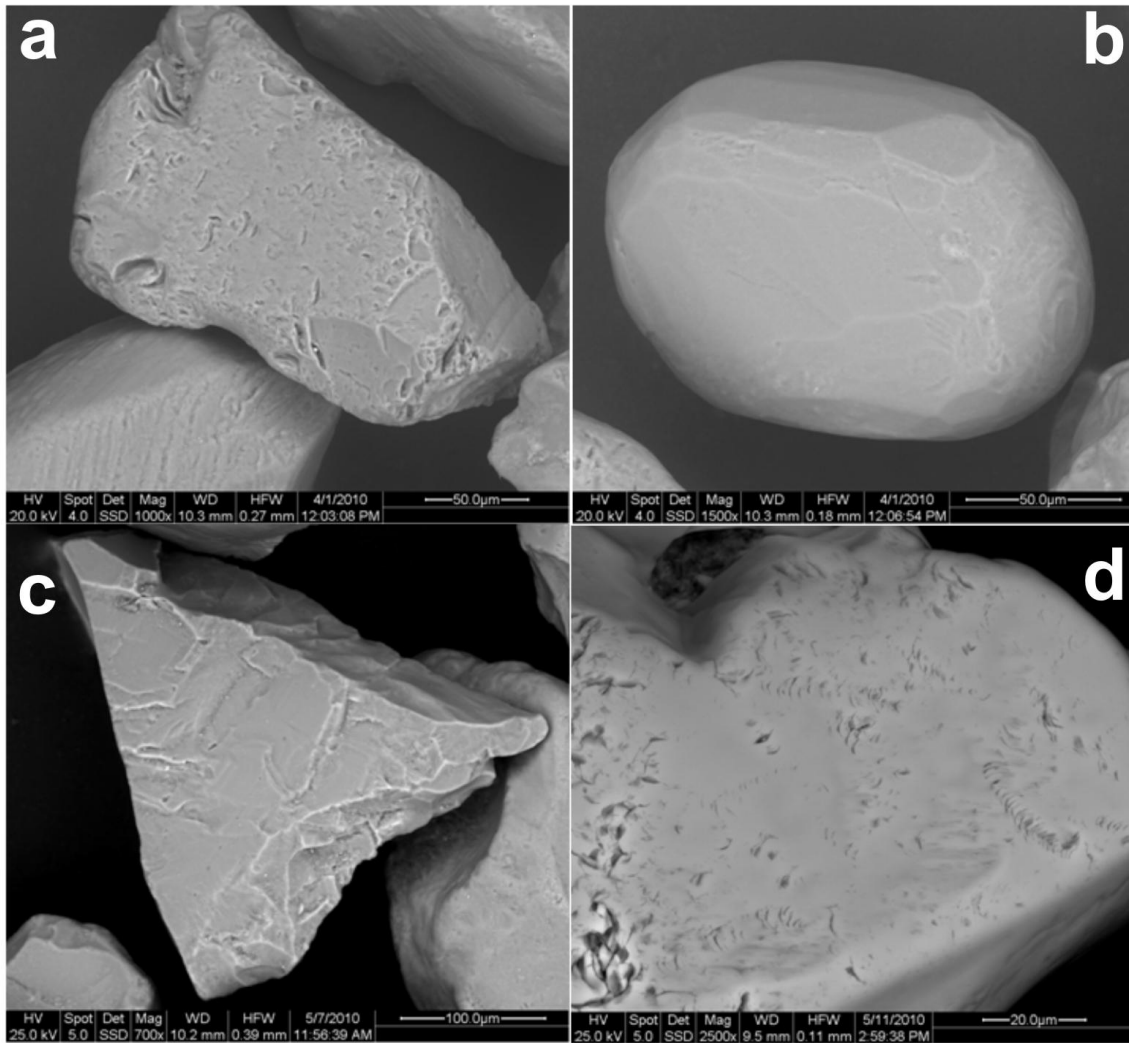
4.5.1 Grain size analysis

In profile TKN-1 the dune was composed of moderately well-sorted medium sand (~275 μm) for the upper and lower layers and a slight increase in grain size (316 μm) in the middle layer (TKN-1B) with well sorted sand. The grain size of profile TKN-2 ranged from 275 to 313 μm (medium sand). The sand was moderately well sorted. In Sembodai region, the dunes were made up of well-sorted to moderately well sorted medium sand (267-318 μm). In the easternmost coastal dunes (PP-1, KD-1, VDC-1 and VDB-1), except two beds in the lowermost part (PP-1B and PP-1C; medium sand) of PP-1 profile, the sands were fine-grained (182-215 μm) and exhibited moderately well-sorting. The grain size variation over the profile in Tettagudi and Sembodai region are illustrated in figures 3 and 4

4.5.2 Quartz grain surface morphology

Two representative samples (TKN-1B, C; TKN-2B, E) from each of the two profiles (TKN-1 and TKN-2) in Tettagudi village, one being the stratigraphically oldest sand deposited and another one from the upper younger bed was identified for SEM analysis. In general, grains in TKN-1C were dominated by angular to sub-angular grains with few (1-2%) being well-rounded, where as more number of well rounded grains were observed in TKN-1B (Fig. 10). TKN-1C from the bottom of the section demonstrated relatively less abrasion. The grains in TKN-1B showed moderate to high level edge abrasion. Grains from both samples revealed conchoidal fractures and stepped breakage plane associated with large flat areas. A few sub-rounded grains with ridge like features and smooth surfaces were also observed. Other features observed in sample TKN-1B were crescentic shaped impact marks (sickle pits) (Fig. 10), straight and curved grooves and irregular surface pits. Few well-rounded grains showed shallow crescentic pits on generally smooth

surfaces. The original mechanical surface had been covered by crystal growth formed



from silica precipitation.

Figure 4.10. Scanning electron microscope image shows the quartz grain surface textures for selected grains. a) Grain showing the crescentic shaped impact marks on the grains due to wind action. b) A moderately well rounded grain with the signatures of previous transportation event is largely masked due to the last event of aeolian transport of grain. c) An angular grain with freshly broken appearance indicating very little transport and source proximal deposition of the sands. d) A polished grain shows drag marks on the surface observed in the easternmost coastal dunes, likely to have been formed due to contact with bed during sub-aqueous transport by coastal currents.

Quartz grains in sample TKN-2B and TKN-2E were largely sub-rounded, angular to sub-angular in nature with few grains showing chemical etching on the surface. Edge abrasion was moderate to severe. Other mechanical features include arcuate step-like breakage plains, conchoidal fractures, small sickle pits on the flat area of the grain. In sample TKN-2E grains showed v-shaped pit marks and polished surfaces.

Sample SBD-1B collected from the bottom of the dune showed few well-rounded grains with a majority of sub-rounded to sub-angular grains. The grains were found to have numerous triangular pits, conchoidal fractures and step-like features. Chemical features include solution etching pits and secondary silica precipitation on few grains. Quartz grains in KD-1 section were largely angular to sub-angular with few sub-rounded grains. Edge abrasion was moderate to less with few grains exhibiting polished surfaces featuring crescentic shaped impact marks and irregular pit marks.

Samples VDC-1A and VDC-1E largely consisted of angular to sub-angular grains with few sub-rounded grains. Many grains were severely stressed exhibiting thin cleavage lines all over the grain prominently on the abraded edges. Most of the sub-rounded grains showed triangular pits and crescentic shaped impact marks on the smooth surface. The grains also showed features like concave depressions, conchoidal fractures, streak /drag marks (Fig. 10) and step like breakage plains. Chemical features like silica precipitation and solution etch marks were also observed on few grains.

4.5.3 Heavy mineral assemblages

Eight representative samples (Table 3) from the sampled profiles were analysed for heavy mineral studies. The heavy-mineral suite of the dune sediments consists of amphiboles (mainly light green to green/ colourless hornblende), opaque minerals (ilmenite and magnetite), clinopyroxenes (augite and diopside /colourless), epidote (clinozoisite and zoisite), garnet (pink and colourless) and accessory amounts of aluminosilicates (sillimanite and kyanite), zircon, rutile, staurolite, monazite, tourmaline and titanite (sphene). The light minerals consist of quartz, feldspar and some mica. Except sample KD-1A and PP-1C all the analysed samples showed high content of opaque

minerals ranging between 23- 38%. KD-1A contains 1% of opaque minerals and PP-1C had only trace amount of them. These samples exhibited high contents of hornblende, e.g., 57% and 58% for samples KD-1A and PP-1C, respectively. The hornblende contents of the remaining sample were between 26-43 %. KD-1A and PP-1C also showed high amounts of clinopyroxene with 18 and 17%, respectively. The remaining samples showed clinopyroxene content of sparse to a maximum of 2%. The results of heavy mineral analysis including the percentage of mineral assemblages are given in Table 3.

Table 4.3. Data showing the details of heavy mineral analyses in the selected samples using optical microscopy. 300 grains from each sample was mounted on a glass slide and grains were counted for various heavy mineral assemblages. Percentage of heavies present in each sample is given.

Heavy minerals	TKN-1 B	TKN-1 C	TKN-2 B	TKN-2 E	SBD-1 B	SBD-3 B	KD-1 A	PP-1 C
Hornblende	36	36	43	26	36	31	57	58
Opagues (Ilmenite, Magnetite)	23	32	25	37	35	38	1	Sp.
Garnet	12	8	12	15	11	11	5	9
Epidote	13	13	10	14	9	10	8	11
CPX (Augite, Diopside)	2	Sp.	Sp.	1	Sp.	Sp.	18	17
Zircon	2	2	Sp.	3	1	5	Sp.	—
Sillimanite	3	7	3	1	2	1	2	1
Kyanite	2	1	2	1	1	1	Sp.	1
Rutile	5	Sp.	1	Sp.	2	2	Sp.	—
Monazite	Sp.	—	—	—	Sp.	Sp.	—	—
Tourmaline	—	Sp.	Sp.	—	—	—	—	Sp.
Titanite (Sphene)	—	—	—	—	Sp.	—	—	Sp.
Staurolite	Sp.	Sp.	Sp.	Sp.	1	1	Sp.	Sp.

4.6 Discussion

4.6.1 Luminescence chronology

The inland dunes along the southeast coast of India are largely considered as remnants of palaeo-strandlines formed during late Holocene sea level high stand (Rao, 1982). ^{14}C dating of samples collected at Tettagudi and Kodiyakkarai region provided ages such as 3570 ± 205 years B.P. and 1020 ± 80 years B.P. indicating a higher sea level stand in this region during this period (Ramasamy et al. 1998). The occurrence of sandy beach ridges with marine shells at Godavari delta in the east coast of Andrapradesh located 1.5 km inland was reported by Banerjee (2000). OSL dating of beach rock in the south eastern coast of Tamil Nadu between Rameswaram and Kanyakumari revealed a sea level high stand around 4.2 to 2.4 ka (Thomas, 2009). This was in accordance with the previous findings of +3m sea level high stand during 4.3 to 2.5 ka from calibrated radiocarbon ages (Banerjee, 2000). The OSL dating results from this study confirmed the results of two recent studies (Kunz et al., 2010 a, b) showing wide spread dune formation/ reactivation across Cauvery delta region during the last two centuries. The oldest records of dune formation were reported from the Northern part of the delta in Cuddalore region (Chilambimangalam village) giving OSL ages of around 3.3 ka (Kunz et al., 2010a). In the south, in Nagapattinam district the westernmost dune profile (TKN-1) yielded a depositional age of about 1.2 ka, corresponding to 8th century AD. The mode of sand accumulation over a period of time varied in different regions. Tettagudi region showed a break in sand accumulation revealed from the gap in OSL ages indicating possible stages of stabilisation of dune surface whereas in Sembodai and Pudupalli region intense sand accretion was found. This resulted in a rapid accumulation of few meters of sand (~3 m) at some places (SBD-1), where as slightly low rate of accumulation with discontinuities were found at other locations (SBD-2, SBD-3 and PP-1) (Fig.4, 5a).

In general, four stages of dune formations were identified from the westernmost and middle dunes concentrated at 693- 957 AD, 1679- 1742 AD, 1923- 1939 AD and 1959- 1971 AD. In PP-1 the dune activity recorded from around 1902- 1921 AD and stabilised since 1950's. The Pudupalli dune occurs as an elongated dune with the inter-dunal depressions used for agriculture. The availability of moisture content in the lower part of

the dune where *Casuarina* plantations exists might have restricted the wind scour only to the crest of the dune.

The foredunes sampled in Vedaranniyam coast (VDC-1) represent the stratigraphically youngest dunes studied. The uppermost part of the dune were incorporated with a thin layer of shell bearing coarse sand (Fig. 5b) most probably deposited during the last heavy inundation in the region during the 2004 December Indian Ocean Tsunami. This forms a good constraint for the OSL sample collected above this layer, which yielded an age of 5 ± 1 a in consideration with the sampling period in 2008 January. The suitability of OSL dating method to find ages as young as few years which were recorded in the Vedaranniyam dunes were verified using a modern sample (VDB-1A; 4 ± 1 a) collected from the intertidal region. This also shows the reliability of the method to derive ages from a well bleached depositional system. This age was comparable with the age (~ 1 a) for a sample collected from the sub-tidal foreshore region of north east India in Orissa from Murray and Mohanti (2006). However, considering the large errors (50-100%) associated with the D_e values of these modern samples, great caution is required while interpreting the ages without sedimentological evidence and stratigraphic control.

4.6.2 Sediment provenance and transportation

The coarser grain size observed in the western most inland dunes and fine grain sand in the coastal dunes reflects the grain size of two different, immediate dune forming sediments and sources (e.g., Lancaster et al., 2002). The sands for the inland dunes are transported mainly from the alluvial plains of Cauvery River and are sorted and gathered by high energy winds. The sands in the coastal dunes are transported from the onshore region and sand in transport from the beach is relatively fine grained. Signatures of weak pedogenesis such as presence of increased clay, silt content due to illuviation and numerous root casts were observed in the upper layer of Tettagudi profile (Fig. 3a). SEM analysis of individual quartz grains showed a predominance of angular to sub-angular grains with few rounded to well-rounded grains. It was observed that in some samples it is possible to distinguish sub-aerial or subaqueous transportation of grains with the presence

of crescentic marks, drag marks and v-shaped pits (possibly due to along shore transport). The abundance of drag marks/ scratches which were formed due to grain to grain collision or contact with bed (Williams and Thomas, 1989) in the sands of near coastal dunes confirms the input of sand directly from the onshore region by landward migration. However, a precise discrimination of the transportation environment would require detailed analyses of samples with quantification of textures and comparison with known environments. The sample from the topmost layer analysed in TKN-1 shows more features of aeolian transport (crescentic marks, moderately abraded edges) compared to lower layers possibly due to exposure to multiple cycles of aeolian reworking and transportation. Less abrasion of edges of grains from the lowermost layers may indicate little exposure to aeolian reworking once it deposited. A source proximal dune formation can be attributed in this region based on the quartz grain surface textures and heavy mineral assemblages in the dune sand. The drop of sea level during late Holocene may have exposed plenty of sand from the shallow continental shelf region, and also sands were available in the beach ridges, levees and river bank deposits. The general lack of mechanically formed microstructures such as percussion pits, scratches and the angularity and fresh appearance of the majority of grains as well as moderate to less edge abrasion of sand in the inland dunes suggest that the sands were derived from a local source. The Cuddalore sandstone of Miocene-Pliocene age occurs as uplands in the western margin of the delta outcropped in the north at Jayamkondam region and in the south at the Vallam- Pattukottai- Mannargudi region (Ramasamy et al., 2006) (Fig. 2). These detached outcrops formerly existed as a continuous unit starting from Pondicherry to Sivaganga in the south west and intense dissection by the present day streams and tributaries of River Cauvery largely removed the formation in this area (Fig. 2) (Vaidyanadhan and Ramakrishnan, 2008). This also might have acted as a source of sediments in the delta region along with the sediments coming from the upper reaches of the River Cauvery. Few grains in the western inland dunes were well rounded to sub-rounded indicating long transport distance implying that the grains may have transported and incorporated from the upper reaches of the Cauvery River.

However, the grains from the eastern most coastal dunes particularly the Vedaranniyam foredunes are very fine grained. These dunes may be formed by the onshore wind accumulating sand on the back shore region and gradually migrating towards inland. Occasionally in near coastal areas these dunes are intercalated by layers of coarse

sand and small shell debris, which were most likely to have been deposited during the event of storms or tsunamis. A similar grain size was observed for the sands in Kodyakkadu area where the progradation of coastline is pronounced indicating the emergence of coast (Fig. 1c). Bounded by salt marshes in the west, the OSL sample collected at this area at a depth of 0.5 m may represent the westernmost part of modern sand ridge complex. OSL dating results of this sample shows a period of sand accumulation in the area around 624 ± 65 a. As the current coastline is situated ~ 5 km towards the east, an emergence of land at a rate of more than 1 km per century is very likely in this area. Based on ^{14}C dating Ramasamy et al. (1998) proposed a shore line progradation of 2.8 km per century between Kodyakkadu and present day coast. Other evidences of rapid accumulation of sediments in the east coast of India reported in previous studies (Vaz and Banerjee, 1997) such as formation of young dunes/ beach ridge complex on Sriharikota Island and depletion of depth of the Pulicat lagoon in southern Andhra Pradesh is attributed to a drop in sea level during Little Ice Age. Such a high rate of sand accretion along the Point Calimere region is attributed to the southward transport of sediments eroded from the north, mainly late Holocene coastal alluvium, palaeobeach ridges and dunes as well as sediments from the tributaries of Cauvery River (Sundararajan et al., 2009).

The occurrence of heavy mineral placer deposits along the east and west coast of India have been correlated with the association of country rock (Roonwal, 1997; Mallik et al., 1987). Two major sedimentary provenances can be distinguished based on the observed heavy mineral assemblages in the inland and coastal dunes. The inland dunes are dominated by opaques (Ilmenite and Magnetite), hornblende, epidote, garnet with sillimanite, kyanite and zircon. The coastal dunes are abundant in hornblende (57-58 %), clino-pyroxene, epidote and garnet with little sillimanite (1-2%), noticeably with very little opaques (1% to sparse) (Table 3). Ilmenite is a common accessory mineral in many rocks of granitic- tonalitic composition as well as amphibolites and high grade metamorphic rocks such as charnockites and sillimanite- kyanite bearing metasediments (Bernstein et al., 2008). Magnetite is found in igneous rocks as accessory minerals and is a constituent mineral in sedimentary and metamorphic banded iron-formation (Klein and Hurlbut, 1985). The terrain exposes intermediate to felsic charnockites with a varied assemblage of orthopyroxene, hornblende, plagioclase feldspar- K-feldspar and quartz with or without

garnet. The pyroxene granulites contain orthopyroxene, clinopyroxene and plagioclase with garnet present in the contact zone (Janardhan, 1999).

From the heavy mineral assemblages found in the dunes it is certain that the minerals were derived from the weathering of basin lithology. Heavy mineral analysis of beach samples collected along the coasts of Point Calimere provided evidences that the sediments were derived mainly from Cuddalore sandstone, low grade metamorphic rocks, granites, granite gneiss, charnockites and alluvium (Sundararajan et al., 2009). The change in heavy mineral content observed in coastal dunes demonstrated by presence of small amounts of Ilmenite, absence of other minerals having high specific gravity (monazite, magnetite and zircon) which are found in inland dunes may suggest a preferential concentration or sorting of sediments by the wind rather than a difference in source. It is also reported that the sediments transported from the north by long shore currents particularly during NE monsoon deposits heavy mineral placers as lag deposits at north of Nagapattinam between Vellar and Karaikkal (Mohan, 1995; Chandrasekar and Rajamanickam, 2001) and transports predominantly light minerals to the Vedaranniyam coast (Sundararajan et al., 2009).

4.6.3 Climate variability and dune reactivation

The OSL ages were compared with precipitation records of the past century recorded in Nagapattinam district and yielded a cluster of ages falling within the periods of reduced precipitation than average (Fig. 11). Both the summer rainfall and annual precipitation was plotted along with measured OSL ages as probability density function in which each peak represent maximum probability of an event of sand movement (Fig. 11). The major rainfall occurring in the region is during NE monsoon which is accounted for in the annual precipitation. Sand mobility in the region is likely to occur in the first half of the year during summer months. During this time the meteorological conditions are favourable for dune reactivation. The atmospheric humidity during this time is lowest in the year (60-65%) and with highest mean temperature between 31-33°C. May and June months show maximum average wind speed with highest percentage of time when wind was blowing

above threshold wind speed (4.1 ms^{-1}) and exhibits highest rate of potential evapotranspiration (PE) (between 181-194 mm) during this time of the year. The dune reactivation in the region can be expected due to failure of summer monsoon (SW) than normal and causes long exposure of sands to high average atmospheric temperature and minimum soil moisture along with high average wind speed. Similar situation of dune mobility is reported in the west coast of Jutland in Denmark where moderate increase in windiness triggers dune mobility during spring and summer months when evapotranspiration is relatively high (Clemmensen and Murray, 2006; Clemmensen et al., 2009). The accretion of sediments are assumed to be instantaneous under normal depositional conditions, but a slow accretion rate (due to less availability of sand) may cause few years of time lag from the real event of burial since deposition. This shows a temporal offset between peak aridity and dune mobility revealed by OSL ages (Singhvi and Porat, 2008). The inter-annual variation in sand mobility (i.e., sand movement during summer months and stable during NE monsoon) and relatively large errors associated with the OSL ages (few years of errors) compared with the nearly alternate years of monsoon variability masks the clear correlation of OSL ages with precipitation records. However, it shows that the enhanced dune-building centred at AD 1930, 1960 and 1995 during the last century may be a response to arid periods which was initiated by failure of monsoon precipitation than normal (Fig. 11).

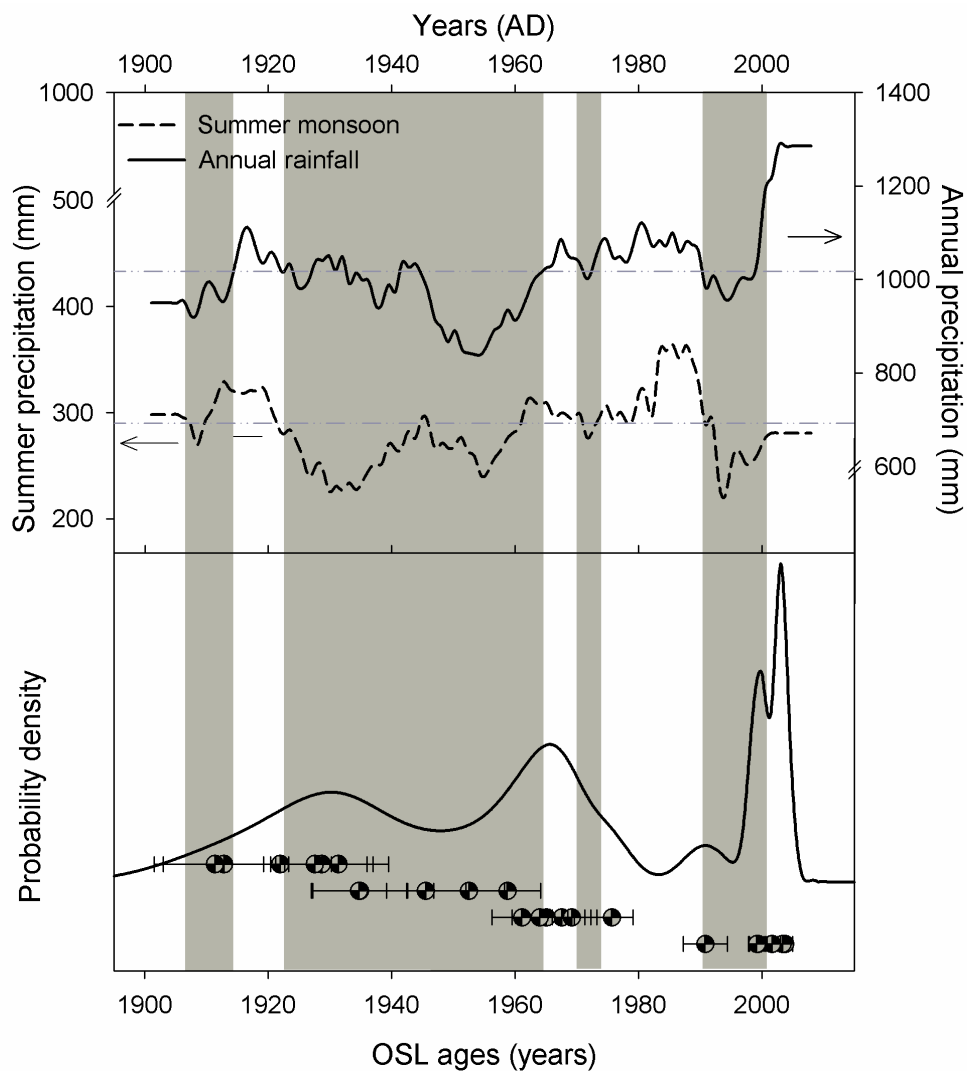


Figure 4.11. Plot showing the correlation between the OSL ages and regional precipitation. The summer rainfall (SW) and annual rainfall (mainly SW and NE) for the Nagapattinam district is plotted (1901-2008) along with measured OSL ages as probability density function in which each peak represent maximum probability of certain event of sand movement. The dark line shows the running average of rainfall and observed correlation with OSL ages are highlighted with grey background.

There are two schools of thoughts are proposed in the field of dune research, in which one advocates the presence of unconformities and soil horizon directly related to the periods of humid climate and sand accretion related to droughts/ arid climate (Lomax et al., 2011; Kunz et al., 2010a; Forman et al., 2006, 2008; Lancaster, 2008). Review by

Chase (2009) suggested a re-evaluation of simple correlation of cold glacial periods associated with aridity and the interpretation of dune accumulation as a proxy of aridity. Studies on coastal dunes in NE Brazil attributed higher wind regime as a governing factor for dune activity rather than lower precipitation (Tsoar et al., 2009). The mobility index accounts for the effect of wind strength and dune surface moisture on sand grain movement. The average monthly precipitation is at its lowest during February and March (13-16 mm) (continues to be below or around 50 mm until end of July) and this gives a low value (0.1) for the P/PE giving highest M-index (>200) for the months of February and March indicating fully active dunes. It is demonstrated that most of the OSL ages fall in the stage of partially (M-value between 100 and 200) or fully active phase (M values >200) in Nagapattinam region (South dunes, Fig. 9a) and mainly dune crests were active during the last century in the Cuddalore region (North dunes, Fig. 9b). The mobility index also shows that short periods of dune stabilisation in Cuddalore region centred at ~AD 1930 and after 1990. The un-smoothed plot in the background (grey thin line) shows the temporal reactivation of dunes (single M value >100) between these periods which may explain the OSL ages falling within this period of stability (Fig. 9b). In Nagapattinam, particularly in the inland region, dunes are active throughout the first three quarters of the century with single intermittent years of stabilisation and the mobility index shows dunes were largely stabilised after ~1980. These results corroborate well with the results of Kunz et al. (2010 a, b) (Fig. 12) which proposed that the cause for dune formation was aridity due to lower precipitation.

When considering the available correlation with luminescence ages and precipitation record, and the dune mobility index, it is possible to argue that a period of reduced rainfall and enhanced windiness facilitate the sand mobility (Thomas and Shaw, 2002) in the region. The beach ridges at Vedaranniyam region formed on a prograding coast having large quantity of sediment supply. This sediment availability supported enhanced sand accretion during the event of high windiness and less than normal precipitation during summer months. Similar observation is reported by Madsen et al. (2007) for Rømø Island, SE coast of Denmark.

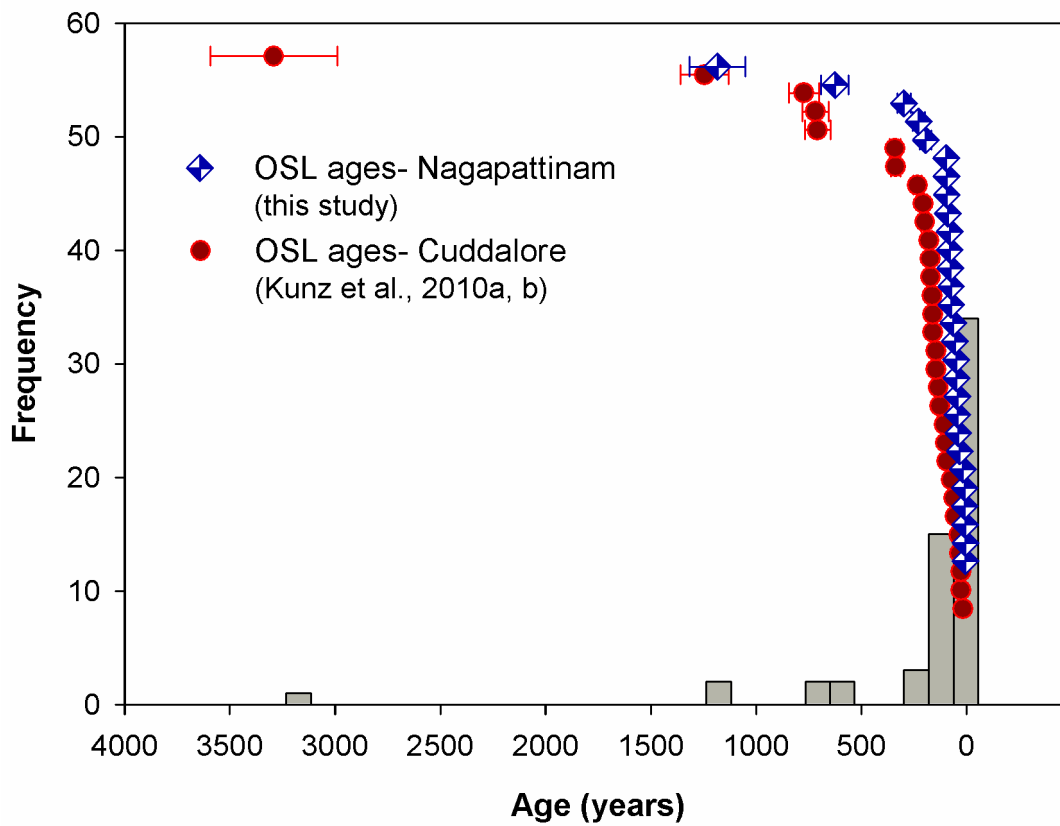


Figure 4. 12. Histogram showing the periods of sand mobility in Cauvery delta region during the last 3.5 ka. The OSL ages along with observed errors are shown for Nagapattinam (this study) and Cuddalore region (Kunz et al., 2010a, b).

Similar to the precipitation record, mobility index also possesses sets of disadvantages considering the inter-annual variability in the climatic conditions and the fact that vegetation cover does not reflect the instant deficit of precipitation but depends on moisture availability over subsequent years (Bullard et al., 1997; Lancaster and Helm, 2000; Yizhaq et al., 2009). Model studies by Yizhaq et al. (2009) shows dune reactivation and stabilization as an irreversible process in such a way that once a sand dune is active due to increasing wind power, prolonged drought or intense human activity, it will stay active even under the conditions under in which it was formerly stable. This transition period may bring some time lag for the real onset of certain climate period. However, in a region like Cauvery delta where the short term stabilisation of dunes occurs mainly during monsoon where the majority of the vegetation covers on the coastal dunes are creeper

plants and shrubs which are prone to seasonal variation in moisture while the deep rooted trees are not affected by the temporal variation in precipitation. It is also important to note that the agricultural activities in the area which leave swale regions exposed to wind action during summer when there is no water available for cultivation and also grazing of animals on dune surface may contribute to sand mobility. Many dunes are partly or completely removed in the area mainly for the purpose of land fillings and the settlements erected on top of the dunes leave sands exposed in certain areas. The coastal beach ridges and dunes are converted in to plantations such as coconut, cashew and casuarina and the swale region is largely used for cultivation of paddy, groundnut and other vegetables (Rao, 1982).

The dune formation in the Cauvery Delta region is an ongoing phenomena at least since late Holocene (Kunz et al., 2010a) to modern times. The dunes are mainly formed by the reworking of beach ridges all along the east coast in response to varying meteorological parameters. Unconformities were observed in many sequences mostly due to the stabilisation of dune surface by improved climatic conditions. The reactivation of dunes in the recent past is largely due to a coupled reaction of change in weather pattern (shown by mobility index) and anthropogenic activities through change in land use pattern.

4.7 Conclusion

This study demonstrates the successful application of OSL dating to modern samples as young as few years. In the south-east coast of India widespread periodic dune formation/ reactivation have taken place during the Late Holocene to very recent times (Fig. 12). The results of the study shows that,

1. The dunes in the area are periodically active since late Holocene when sea level changes and land emergence occurred in the south east coast. The reactivation of dunes was found to be associated to the changes in climate and landuse pattern.
2. Relatively large errors associated with the luminescence chronology make it difficult to correlate periods of dune formation/ reactivation with short term seasonal variation in precipitation. Shift in the peak of sand mobility observed

through luminescence ages may be a time lag between the period of aridity and sand mobility as its response.

3. The sand mobility index calculated for the past century shows that the dunes in the area have been largely active in the southern part in Nagapattinam region and most of the crests are active in the northern Cauvery delta in Cuddalore region.
4. The dune formation in the region was not restricted to sand supply, but related to the wind speed, vegetation cover and sand moisture content. The large scale reactivation of dunes in the area during the last century points to the anthropogenic influence caused by settlements and agricultural activities.
5. Heavy mineral concentration of the dune sands suggests origin of sand from the weathering of country rock in the drainage basin. The heavy minerals observed in the eastern most coastal dunes may be segregated by wind with heavies (monazite, magnetite zircon, Ilmenite) having higher specific gravity being absent or present in minor quantities indicating a preferential concentration of heavy mineral rather than varied provenance.

4.8 Acknowledgements

This research has been supported by Leibniz DAAD fellowship funded by the German Academic Exchange Service (DAAD) and the Leibniz Institute for Applied Geophysics (LIAG), Hannover, which is greatly acknowledged. The authors are grateful to Mr. D. Klosa and Ms. Irene Bitz, technicians from Landesamt für Bergbau, Energie und Geologie, Hannover for the Scanning Electron Microscope analysis and Heavy mineral analysis. Dr. Bor-ming Jahn and two other anonymous reviewers are thanked for providing valuable suggestions which helped to improve the earlier version of this manuscript significantly. Dr. N. Thangadurai and MSc. students from Dept. of Geology, Anna University are thanked for their assistance during the field work.

4.9 References

- Adamiec, G., Aitken, M., 1998. Dose-rate conversion factors: update. *Ancient TL* 16, 37-50.
- Aitken, M.J., 1998. *An Introduction to Optical Dating*. Oxford University Press, Oxford.
- Ash, J.E., Wasson, R.J., 1983. Vegetation and sand mobility in the Australian desert dune field. *Zeitschrift für Geomorphologie (Supplement)* 45, 7-25.
- Bagnold, R.A., 1941. *The Physics of Blown Sand and Desert Dunes*, Morrow, New York, (republished in 1954 by Methuen, London).
- Ballarini, M., Wallinga, J., Murray, A.S., Heteren van, S., Oost, A.P., Bos, A.J.J., van Eijk, C.W.E., 2003. Optical dating of young coastal dunes on a decadal time scale. *Quaternary Science Reviews* 22, 1011-1017.
- Ballarini, M., Wallinga, J., Wintle, A.G., Bos, A.J.J., 2007. A modified SAR protocol for optical dating of individual grains from young quartz samples. *Radiation Measurement* 42, 360-369.
- Banerjee, P.K., 2000. Holocene and Late Pleistocene relative sea level fluctuations along the east coast of India. *Marine Geology* 167, 243-260.
- Banerjee, D., Hildebrand, A. N., Murray-Wallace, C. V., Bourman, R. P., Brooke, B. P., Blair, M. 2003. SAR-OSL ages from the stranded beach dune sequence in south-east South Australia. *Quaternary Science Reviews* 22, 1019-1026.
- Bateman, M.D., Godby, S.P., 2004. Late-Holocene inland dune activity in the UK: a case study from Breckland, East Anglia, *The Holocene* 14, 579–588.
- Bernstein, S., Frei, D., McLimans, R.K., Knudsen C., Vasudev V.N., 2008. Application of CCSEM to heavy mineral deposits: Source of high-Ti illmenite sand deposits of South Kerala beaches, SW India. *Journal of Geochemical Exploration* 96 (1), 25-42.

- Blott, S.J., Pye, K., 2001. GRADISTAT: A grain size distribution and statistics package for the analysis of unconsolidated sediments. *Earth Surface Processes and Landforms* 26 (11), 1237-1248.
- Bullard, J.E., Thomas, D.S.G., Livingstone, I., Wiggs, G.F.S., 1997. Dune field activity and interactions with climatic variability in the southwest Kalahari Desert. *Earth Surface Processes and Landforms* 22 (2), 165-174.
- Chase, B. M., 2009. Evaluating the use of dune sediments as a proxy for palaeo-aridity: a southern African case study. *Earth-Science Reviews* 93, 31- 45.
- Chandrasekar and Rajamanickam, 2001. Nature of distribution of heavy minerals along the beaches of central Tamil Nadu coast. *Journal of Indian Association of Sedimentologist* 20, 167- 180.
- Chepil, W.S., Siddoway, F.H., Armbrust, D.V., 1963. Climatic Index of Wind Erosion Conditions in the Great Plains. *Soil Science Society of America Proceedings* 27 (4), 449- 452.
- Clemmensen, L.B., Murray, A., 2006. The termination of the last major phase of aeolian sand movement, coastal dunefields, Denmark. *Earth Surface Processes and Landforms* 31, 795- 808.
- Clemmensen, L.B., Murray, A.S., Heinemeier, J., Jong, R D., 2009. The evolution of Holocene coastal dunefields, Jutland, Denmark: A record of climate change over the past 5000 years. *Geomorphology* 105, 303- 313.
- Duller, G.A.T., 2003. Distinguishing quartz and feldspar in single grain luminescence measurements. *Radiation Measurements* 37, 161- 165.
- Folk, R.L., Ward, W.C., 1957. Brazos River bar, a study in the significance of grain-size parameters. *Journal of Sedimentary. Petrology*, **27**, 3- 27.
- Forman, S.L., Spaeth, M., Marin, L., Pierson, J., Gomez, J., Bunch, F., Valdez, A., 2006. Episodic Late Holocene dune movements on the sand-sheet area, Great Sand Dunes National Park and Preserve, San Luis Valley, Colorado, USA. *Quaternary Research* 66, 97- 108.

- Forman, S.L., Mari'n, L., Gomez, J., Pierson, J., 2008. Late Quaternary eolian sand depositional record for southwestern Kansas: landscape sensitivity to droughts. *Palaeogeography, Palaeoclimatology, Palaeoecology* 265, 107- 120.
- Frechen, M., Neber, A., Dermann, B., Tsatskin, A., Boenigk W., Ronen, A., 2004. Chronostratigraphy of Pleistocene sedimentary cycles in the Carmel Coastal Plain of Israel, *Quaternary International* 121 (1), 41- 52.
- Fryberger, S.G., 1979. Dune forms and wind regimes, in: McKee, E.D. (Ed.), *A Study of Global Sand Seas*. Geological Survey Professional Paper, vol. 1052. United States Government Printing Office, Washington, pp. 305- 395.
- Galbraith, R.F., Roberts, R.G., Laslett, G.M., Yoshida, H., Olley, J.M., 1999. Optical dating of single and multiple grains of quartz from Jinmium Rock Shelter, northern Australia: Part 1, experimental design and statistical models. *Archaeometry* 41, 339- 364.
- Hsu, S.A., 1977. Boundary-layer meteorological research in the coastal zone, in: Walker H.J., (Ed.), *Geoscience and Man, V. of XVIII. Research Techniques in Coastal Environments*, pp. 99-111.
- Hsu, S.A., Weggel, J.R., 2002. Wind-blown sediment transport, Chapter III-4, in: *Coastal Engineering Manual*. Vicksburg, Mississippi: U.S. Army Corps of Engineers, Coastal Engineering Research Center, pp III-4-8.
- Janardhan, A.S., 1999. Southern Granulite Terrain, South of the Palghat-Cauvery Shear Zone: Implications for India-Madagascar Connection. *Gondwana Research* 2 (3), 463- 469.
- Kar, A., 1993. Aeolian processes and bedforms in the Thar Desert. *Journal of Arid Environments* 25, 83- 96.
- Klein, C., Hurlbut, C. S., 1985, *Manual of Mineralogy: 20th ed.*, John Wiley & Sons, New York, N.Y., pp 596.
- Kunz, A., Frechen, M., Ramesh, R., Urban, B., 2010 a. Luminescence dating of Late Holocene dunes showing remnants of early settlement in Cuddalore and evidence of

- monsoon activity in south east India. *Quaternary International* 222, 194-298.
doi:10.1016/j. quaint.2009.10.042
- Kunz, A., Frechen, M., Ramesh, R., Urban, B., 2010 b. Periods of recent dune sand mobilisation in Cuddalore, south east India. *Zeitschrift der Deutschen Gesellschaft für Geowissenschaften (ZDGG)* 161/3, 353- 358.
- Lakshmanan, N., Gomathinayagam, S., Harikrishna, P., Abraham, A., Chitra Ganapathi, S., 2009. Basic wind speed map of India with long-term hourly wind data. *Current Science* 96 (7), 911-922.
- Lancaster, N., 1988. Development of linear dunes in the southwestern Kalahari, southern Africa. *Journal of Arid Environments* 14, 233-244.
- Lancaster, N., Helm, P., 2000. A test of a climatic index of dune mobility using measurements from the southwestern United States. *Earth Surface Processes and Landforms* 25, 197- 207.
- Lancaster, N., Nickling, W.G., McKenna Neuman, C., 2002. Particle size and sorting characteristics of sand in transport on the stoss slope of a small reversing dune. *Geomorphology*, 43, 233-242.
- Lancaster, N., 2008. Desert dune dynamics and development: insights from luminescence dating. *Boreas* 37, 559- 573.
- Lomax, J., Hilgers, A., Radtke, U., 2011. Palaeoenvironmental change recorded in the palaeodunefields of the western Murray Basin, South Australia - new data from single grain OSL-dating. *Quaternary Science Reviews* 30, 723- 736.
- Madsen, A.T., Murray, A.S., Anderson, T.J., 2007. Optical dating of dune ridges on Rømø, a barrier island in the Wadden Sea, Denmark. *Journal of Coastal Research* 23, 1259 - 1269.
- Mallik, T.K., Vasudevan, V., Aby Verghese, P., Terry Machado, 1987. The black sand placer deposits of Kerala beach, Southwest India. *Marine Geology* 77, 129- 150.
- Mejdahl V., 1979. Thermoluminescence dating: deta-dose attenuation in quartz grains. *Archaeometry* 21, 61- 72.

- Mohan, P.M., 1995. Distribution of Heavy mineral in Parangipettai, (Portonova) beach, Tamil Nadu, *Journal of Geological Society of India* 46, 401- 408.
- Muhs, D.R., Maat, P.B., 1993. The potential response of Aeolian sands to greenhouse warming and precipitation reduction on the Great Plains of the U.S.A. *Journal of Arid Environments* 25 (4), 351- 361.
- Murray, A.S., Mohanti, M., 2006. Luminescence dating of the barrier spit at Chilika Lake, Orissa, India. *Radiation Protection Dosimetry* 119, 442- 445.
- Murray, A.S., Wintle, A.G., 2000. Luminescence dating of quartz using an improved single-aliquot regenerative-dose protocol. *Radiation Measurements* 32, 57- 73.
- Murray A.S., Wintle A.G., 2003. The single aliquot regenerative dose protocol: potential for improvements in reliability. *Radiation Measurements* 37 (4-5), 377- 381, doi: 10.1016/S1350- 4487(03)00053-2.
- Pant, G.B., Rupa Kumar, K., 1997. *Climates of South Asia*, Journal of Wiley and Sons, pp. 292.
- Pattanaik, J.K., Balakrishnan, S., Bhutani, R., Singh, P., 2007. Chemical and Sr isotopic composition of Kaveri, Palar and Ponnaiyar rivers: significance to weathering of granulites and granitic gneisses of Southern Peninsular India. *Current Science*, 93, 523- 531.
- Porat, N., Botha, G.A., 2008. The luminescence chronology of dune development on the Maputaland coastal plain, southeast Africa. *Quaternary Science Reviews* 27, 1024- 1046.
- Prescott, J.R., Hutton, J.T., 1994. Cosmic ray contributions to dose rates for luminescence and ESR dating: large depths and long-term time variations. *Radiation Measurements* 23, 497- 500.
- Prescott, J.R., Stephan, L.G., 1982. The contribution of cosmic radiation to the environmental dose for thermoluminescent dating - latitude, altitude and depth dependences. *PACT* 6, 17-25.
- Pye, K., Tsoar, H., 1990. *Aeolian Sand and Sand Dunes*. Unwin Hyman, Boston

- Quang-Minh, D., Frechen M., Nghi, T., Jan Harff., 2010. Timing of Holocene sand accumulation along the coast of central and SE Vietnam. *International Journal of Earth Science (Geol Rundsch)* 99, 1731- 1740. doi: 10.1007/s00531-009-0476-7
- Ramanathan A.L., Subramanian V., Das B.K., 1996. Sediment and Heavy metal accumulation in the Cauvery Basin. *Environmental Geology* 27(3), 155- 163.
- Ramasamy, S.M., Saravanavel, J., Selvakumar, R., 2006. Late Holocene geomorphic evolution of Cauvery delta, Tamil Nadu. *Journal of the Geological Society of India* 67, 649- 657.
- Ramasamy, S. M., Ramesh, D., Paul, M. A., Kusumgar, S., Yadava, M. A., Nair, A. R., Sinha, U. K., Joseph, T. B., 1998. Rapid land building activity along Vedaranniyam Coast and its possible implications, *Current Science* 75, 884- 886.
- Rao S.M., 1982. Morphology and evolution of modern Cauvery delta, Tamil Nadu, India. *Transactions of the Institute of Indian Geographers* 4, 67- 78.
- Reimann, T., Naumann, M., Tsukamoto, S., Frechen, M., 2010. Luminescence dating of coastal sediments from the Baltic Sea coastal barrier-spit Darss–Zingst, NE Germany, *Geomorphology* 122, 264- 273. doi:10.1016/j.geomorph. 2010.03.001
- Roonwal, G. S. 1997. Marine mineral potential in India's Exclusive Economic Zone; Some issues before exploitation. *Marine Georesearch Geotechnology* 15, 21- 32.
- Singh P., Rajamani V., 2001. REE Geochemistry of recent clastic sediments from the Kaveri floodplains, southern India: Implications to source area weathering and sedimentary processes. *Geochimica et Cosmochimica Acta* 65, 3093- 3108.
- Singhvi, A. K., Porat, N., 2008. Impact of luminescence dating on geomorphological and palaeoclimate research in drylands. *Boreas* 37, 536- 558.
- Sundararajan, M., Usha-Natesan., Babu, N., Seralathan, P., 2009. Sedimentological and Mineralogical investigation of beach sediments of a fast prograding cusped foreland (Point Calimere), Southeast coast of India. *Research Journal of Environmental Sciences*, 3 (2) , 134-148.

- Talbot, M.R., 1984. Late Pleistocene rainfall and dune building in the Sahel. *Palaeoecology of Africa* 16, 203- 214.
- Thomas, P.J., 2009. Luminescence Dating of Beachrock in the Southeast Coast of India - Potential for Holocene Shoreline Reconstruction. *Journal of Coastal Research* 25 (1), 1- 7.
- Thomas, D.S.G., Shaw, P.A., 2002. Late Quaternary environmental change in central southern Africa: new data, synthesis, issues and prospects. *Quaternary Science Reviews* 21, 783- 797.
- Thomas, D.S.G., Wiggs, G.F.S., 2008. Aeolian system responses to global change: challenges of scale, process and temporal integration. *Earth Surface Processes and Landforms* 33, 1396- 1418
- Tsoar, H., 2001. Types of Aeolian Sand Dunes and Their Formation. In: Balmforth, N.J. and Provenzale, A. (Eds.). Springer-Verlag Berlin Heidelberg 582, 403- 429.
- Tsoar, H., 2002. Climatic Factors Affecting Mobility and Stability of Sand Dunes. In : Lee, Jeffrey A. and Zobeck, Ted M., 2002, Proceedings of ICAR5/GCTE-SEN Joint Conference, International Center for Arid and Semiarid Lands Studies, Texas Tech University, Lubbock, Texas, USA Publication 02- 2, 423- 426
- Tsoar, H., Levin, N., Porat, N., Maia, L.P., Herrmann, H.J., Tatumi, S.H., Claudino-Sales, V., 2009. The effect of climate change on the mobility and stability of coastal sand dunes in Ceará State (NE Brazil). *Quaternary Research* 71, 217- 226.
- Vaidyanathan R., Ramakrishnan M., 2008. *Geology of India*. Geological Society of India, Bangalore 2, 557-994
- Vaz, G.G., Banerjee, P.K., 1997. Middle and late Holocene sea level changes in and around Pulicat Lagoon, Bay of Bengal, India. *Marine Geology* 138 (3-4), 261- 271.
- Wasson, R.J., 1984. Late Quaternary environments in the desert dune fields of Australia. in: Vögel, J.C., (Ed.), *Late Cainozoic Palaeoclimates of the Southern Hemisphere*, A.A. Balkema, Rotterdam pp. 419- 432.

Application of OSL dating on coastal sediments...

Williams, A.T., Thomas, M.C., 1989. Analysis of Barrier Island Surface Sediments by Scanning Electron Microscopy. *Marine Geology* 86, 101- 118.

Wintle, A.G., Murray, A.S., 2006. A review of quartz optically stimulated luminescence characteristics and their relevance in single-aliquot regeneration dating protocols. *Radiation Measurements* 41, 369- 391.

Yizhaq, H., Ashkenazy, Y., Tsoar, H., 2009. Sand dune dynamics and climate change: A modeling approach, *Journal of Geophysical Research* 114, 1- 11. doi:10.1029/2008JF001138

Prepared for submission to Journal 'The Holocene'

Evidences of Late Holocene shoreline progradation in the coasts of Kerala, South India obtained from OSL dating of palaeobeach ridges

L. Alappat^{*a}, M. Frechen^{*}, R. Rajan^{**} S. Tsukamoto^{*}

** Leibniz Institute for Applied Geophysics (LIAG), Section S3: Geochronology and Isotope Hydrology, Stilleweg 2, 30655 Hannover, Germany*

*** Department of Geology and Environmental Science, Christ College, Irinjalakuda, Thrissur, Kerala, India, 600 125*

^aCorresponding author: Linto.Alappat@liag-hannover.de, lintoalappat@yahoo.co.uk

Tel. 0049-5116433487; 0091-4802701311; Fax 0049-5116433665

Abstract

Beach ridges are seen on the west coast of India in the central part of Kerala. These beach ridges were studied to establish their chronology of formation and to obtain some information on the coastline progradation. The study presents the results of 15 optically stimulated luminescence (OSL) ages derived from quartz using single aliquot regenerative dose (SAR) protocol. Samples were subjected to strict analysis for the performance tests (recycling, recuperation, preheat and dose recovery), which provided reliable age estimates. Heavy mineral analysis were carried out to know the contribution of heavies in the dose rate of sediments and also to detect the provenance variation. The luminescence ages from most of the sites were stratigraphically consistent with ages close to 3-4 ka, indicating a possible stage of wide spread beach ridge formation all along the west coast of Kerala. The chronological results outlined in this paper provides the first reported OSL ages for beach ridges in the west coast of south India.

Key words: Beach ridge, shoreline, optically stimulated luminescence, Holocene

5.1 Introduction

Beach ridges are defined as “relict, semiparallel, multiple wave- and wind- built land forms that originated in the inter- and supra-tidal zones” (Otvos, 2000). Beach ridges having well defined wave built origin may be used as indicators of former higher sea level stands than present (Otvos, 2000) and hence can assist in the construction of sea level curve and identification of palaeo-shore line. Evidences of variation in sea level during late Pleistocene to Holocene time have been observed all along the coasts of India, but the chronology of these deposits associated with various sea level stands are largely lacking. Majority of evidences of Holocene high sea level stands can be found as fossil coral reefs, marine terraces, beach rocks, and strand lines during recession of the seawater, and those of sea level low stands are submerged by present day sea level (Banerjee, 2000; Thomas, 2009). Hashimi et al., (1995) reported the evidences of the low sea level stand such as presence of submarine terraces at -92, -82 and -30m depths in the west coast of India. Geophysical investigations on the western continental shelf of India between latitudes of 11°- 20°N also revealed a series of submarine terraces, such as wave-cut terraces, coral/ - algal reef terraces and palaeo- beach/ barrier terraces at depths between 50- and 115m (Wagle et al., 1994). Evidences of a number of transgressive and regressive phases along the shore line of Kerala are marked by a number of beach ridges (Mallik, 1986). Shore parallel multiple beach ridges behind the modern beaches along the coasts of Goa in the west coast of India was reported by Kunte (1994). Chronology of these individual ridges makes it possible to reconstruct the spatial and temporal development of regional coast line (Nielson et al., 2006). Both geological and archaeological features observed in the west coast, particularly along the Saurashtra coast towards north have been studied in the recent past (Gaur et al., 2007; Gaur and Vora, 1999) which revealed evidences of palaeo sea level fluctuations along the coast. Hashimi et al. (1995) proposed a sea level curve for the period from Late Pleistocene (14.5 ka) to present in the west coast of India and postulated that the sea level has remained more or less stable for the last 7 ka.

Beach ridges located 2 to 4 km inland, in which individual ridges vary in length from 2 to 5 km, have been previously recognised as representing ancient strand lines during post Miocene retreat of sea in the central part of Kerala between 9- 11° latitudes (Bhattacharya et al., 1979). The landscape of Kerala in the coastal area is directly related to variations in the late Quaternary climate and tectonics. The knowledge of the chronology of events is therefore a prerequisite to investigate the palaeo-climate and to interpret the processes

which played a role in the modification of the geomorphology of the area that moulded the present day landforms. Given the contrary arguments about sea level stand during the middle Holocene period in the Kerala coast with arguments favouring more or less stable sea level since 7-6 ka BP (Hashimi et al., 1995) and oscillatory sea level (Wagle, 1990; Narayana and Priju, 2006) with high stand reached between 4-6 ka BP, a unanimous and clear conclusion is required in the interpretation of the sea level curve in the west coast of India. The information about the sea level stands during Holocene in the west coast of Kerala is so far fragmentary and palaeo-strand lines in this area offer a unique opportunity to study the coastline variation in the past. The present study investigates the chronology of beach ridges along the west coast of Kerala using optically stimulated luminescence (OSL) dating techniques in order to understand its coastline progradation during middle and late Holocene. This paper also attempts to explain the coastal processes involved in the evolution of coast marginal lands of Kerala in south west India during middle to late Holocene. The study is the primary attempt to apply OSL dating to obtain the timing of beach ridge formation in Kerala.

5.2 Regional geology and Geomorphology

In general Kerala can be divided longitudinally in to four physiographic units (Fig. 5.1), low level coastal strip in the westernmost part of the area (< 10m) bounded by the Arabian Sea, the landforms marked by laterite cappings between altitudes of 30m and 200m, the foot hills of Western Ghats (altitude between 200-600m) and steeply rising Western Ghats with altitude reaching up to 2500m (Rajan and Kumar, 2005; Jayalakshmi et al., 2001; Bhattacharya et al., 1979). Quaternary sediments occupy most of the low lands with maximum thickness observed between 9-11° latitudes (Fig. 5.2) (Jayalakshmi et al., 2001). The area comprises of several geomorphologic land-forms such as coastal plains, beaches, young and old beach ridges, swales, flood plains and valley fills, barrier islands, lagoons and estuaries, wet lands, swamps and marshes, alluvial plains and small lagoonal deltas (Narayana and Priju, 2006; Bhattacharya et al., 1979). Occurrences of coast parallel lagoons with rivers joining these and spits or bars along the central Kerala coast are considered as evidences of coastal progradation (Narayana and Priju, 2006). As many as 44 west flowing streams flow across the coastal belt of Kerala which brings plenty of sediments and join the Arabian Sea through a large number of lagoons and backwaters

(Mallik, et al., 1987). A thick cover of laterite and well developed soil are observed in the midlands adjacent to coastal plains.

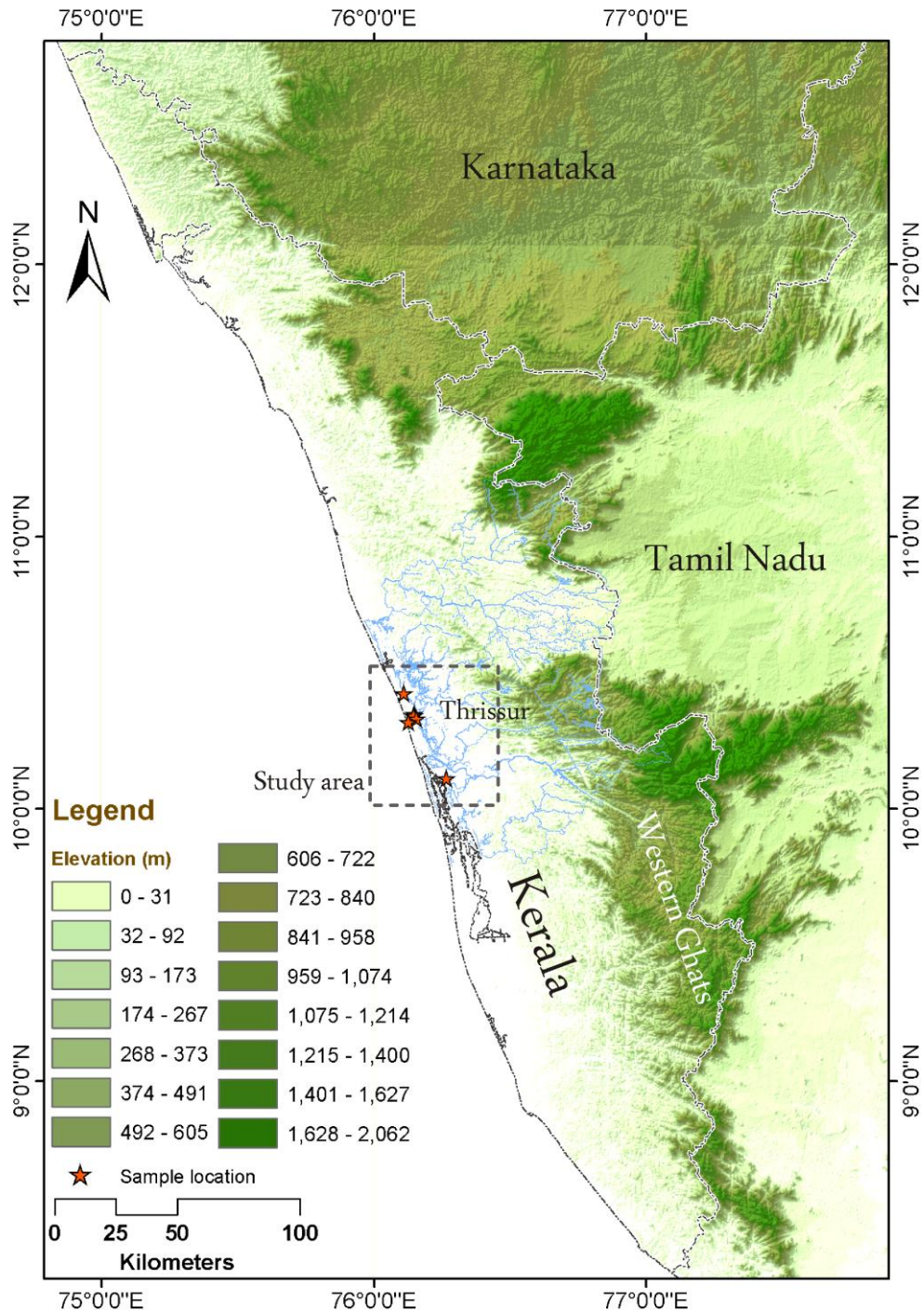


Figure 5.1. Map showing the digital elevation model of Kerala prepared using the DEM images of ASTER-GDEM, a product of METI and NASA. The sampling locations are also marked in the map.

Rocks formed during different magmatic, metamorphic and sedimentary processes since as early as Archean to recent times are exposed in the area. The major geology of the area (Fig. 5.2) is comprised of Precambrian crystalline rocks (khondalites, charnockites, gneiss and meta-sedimentary rocks), acid to ultra basic intrusive of Archaean to Proterozoic age, Tertiary (Mio- Pliocene) sedimentary rocks and Quaternary sediments of fluvial and marine origin (Rajan and Kumar, 2005).

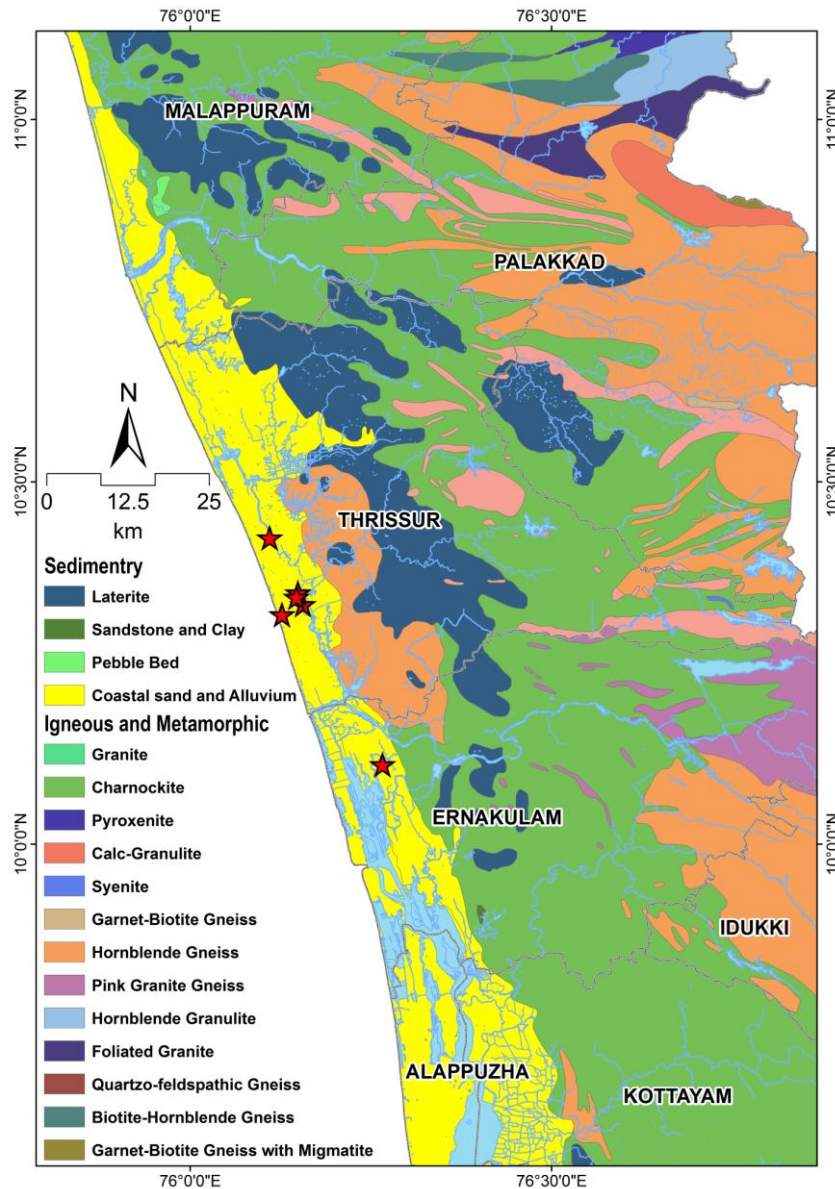


Figure 5.2. General geology map of the study area (Modified from Geological Survey of India map, 1995) showing major rock formations exposed in the area along with drainage net work which contribute to the sediment input to the coastal plain.

The major constituents of coastal tracts are recent to sub-recent laterite and alluvium. Laterites also occur as caps on crystalline rocks and Tertiary sediments, and are products of residual chemical weathering. Charnockite and charnockitic gneiss widely occurs in the area (covering 40-50% of the total area of other crystalline rocks), which are well-exposed in the central and northern parts of Kerala including the hill ranges of the Western Ghats (Rajan and Kumar, 2005). Hornblende and biotite-gneiss, derived by retrograde metamorphism and migmatization of biotite gneiss is also observed in the area. (Mallik et al., 1987).

5.2.1 Study area and Sampling

The study area located in the central part of coastal tract of Kerala between latitudes and longitudes of $N10^{\circ}0' - 10^{\circ}30'$; $E76^{\circ}0' - 76^{\circ}30'$ respectively and is characterised by a low topographical relief. The Kerala coast which is bounded by the Arabian Sea is affected by two monsoons with opposing winds (Kunte, 1994). This seasonal reversal of wind direction causes a strong and humid SW- monsoon in Kerala during summer months (June- September) and a less intense and dry NE monsoon in winter (Thamban et al., 2001). Due to orographic forcing of Western Ghats, south - west India receives 80% of its annual rainfall (Samsuddin, 1986) from summer rainfall with an average annual precipitation of 2500- 3000mm. The main land use in the area is coconut, paddy, plantain, cashew plantations along with many other tropical plants and seasonal crops, and is also densely populated. The land use is highly altered due to the increased pressure of human settlements and agricultural activities. At present beach ridges occur as isolated outcrops in the inland. Major roads in the area have been constructed on top of the beach ridge morphology, running parallel to the coast. Undisturbed sections of beach ridges are rarely preserved in this part and are steadily declining due to increased usage of beach ridges for land reclamation and construction purposes. However, seven locations were identified with areas having less inhabitation and undisturbed in terms of stratigraphy. Samples were generally obtained at 1-2m depths by cutting a vertical section in the ridge and the disturbed upper section was not sampled. Samples were also recovered from suitable road embankments or domestic well cuttings or pits by inserting tubes horizontally in to the section. Altogether fifteen medium-grained homogeneous sands deposited in the beach ridges of west coast of Kerala (Fig. 5.1) were sampled using hand held PVC corer (maximum size 15x6 m).

Four sample locations namely, Kooniparambu (KNP-1, 10°19.871" N; 76° 09.331" E), Cherakal (CHK-1, 10°20.677"N; 76°08.925" E), Edathirithi (EDT-1, 10°20.815"N; 76°08.940"E) and Cherakalpalli North (CKP(N)-1, 10°20.470"N; 76°08.848"E) are located 3-8 km inland in the vicinity of the Chentrappini area south west of Thrissur. Among these, profile KNP-1 was excavated 2.2m from the surface and four samples (KNP-1B,1C and KNP-2B,2C; Fig. 5.3) were collected for OSL dating. In this profile the upper part of bench- I was covered by a ~ 20cm thick moderately well developed brownish grey sandy soil (A). A ~ 30cm thick bed of bioturbated brownish yellow sand (B) was observed below this layer and a bed of brownish yellow sandy soil (C) with signatures of weak pedogenesis on the upper part such as increased content of silt due to illuviation was observed at the bottom.

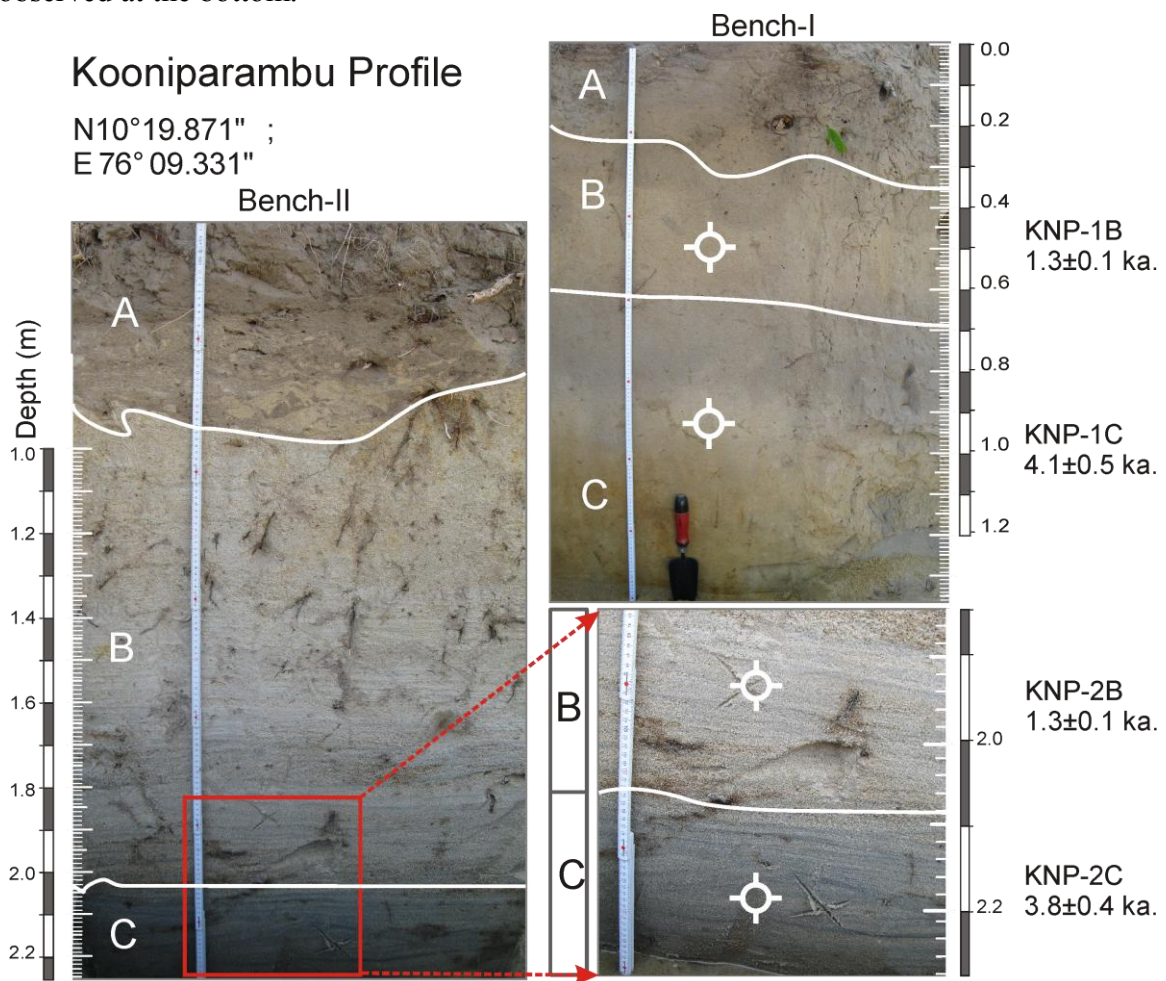


Figure 5.3. Picture showing the vertical profile of Kooniparambu, Chaliyangad (KNP-1) with different sand units and depth marked. Four OSL samples were collected from the profile (KNP-1B, D, E and F. Visible unconformities and measured OSL ages are shown.

In bench- II (KNP-2), the profile consists of ~30 cm thick moderately well developed soil horizon (A horizon in Fig. 5.3) in the upper part. The bottom part of this layer shows worm like structures and sandy lenses shows heavy bioturbation. This bed is followed by a light yellow massive sand unit (B) and a bed with thin layers of dark sand. The lower part of this bed contains brownish yellow sand with dark layers, which covers a bed of fine grained grey sand with dark layers (C). CHK-1A was collected from the bottom part of a massive light yellow sand unit from a 1.8m pit dug in to a sandsheet.

A 1.6 m profile was excavated in Edathirithi area and two samples (EDT-1A, B) were collected for OSL dating. The upper part of the profile consists of a 0.6m thick bioturbated massive grey sandy soil horizon with numerous root casts. EDT- 1A was collected from a grey coloured fine to medium sand unit below this layer at a depth of 1m and EDT- 1B was taken from the bottom most bed of the profile at a depth of 1.4 m. Another profile (Fig. 5.4) with a height of ~2m was excavated in a nearby area and four samples were collected for OSL dating. The upper 15cm of the profile consist of grey sandy soil with signatures of weak pedogenesis. Sample CKP (N) - 1A was collected from this layer. This layer was followed by 1.25m thick massive dark yellow fine to medium sand with occasional bioturbations in the upper part. Two samples (CKP (N)- 1B,C) were taken from this bed at depths of 0.6 and 1.1m respectively. CKP (N) - 1D was collected from a fine grained grey colored sand unit at the bottom part of the profile at a depth of 1.9m (Fig. 5.4).

WNJ-1A was collected from a modern beach ridge at a depth of 1m which is located about 200m away from the coast. The upper part of this profile was composed of light yellow massive sand followed by light yellow colored fine sand. WNJ-1A forms the westernmost (towards coast) sample collected in the study. Two samples (SNC-1A and SNC-2A) were collected in Nattika, which is the northern most part of the area sampled in this study. Each sample was recovered from two adjacent beach ridges occurring at different elevation. SNC-1A was collected from an elevated ridge at a depth of 1.2m. The upper 70cm of the profile excavated for bench-1 was bioturbated, organic rich brownish grey massive sand with numerous roots intercalated. This was followed by a brownish yellow, medium grained homogeneous sand unit. Bench-2 was excavated in a well cutting a few meters away from bench-1. The upper 0.4m of bench-2 contains light grey, massive sand unit with bioturbations. This was followed by a greyish yellow massive sand unit and

medium grained light grey sand up to a depth of 0.9 m. SNC-2A was collected from a medium to coarse grained light yellow sand unit with lenses of coarse grained sand at a depth of 1m below surface.

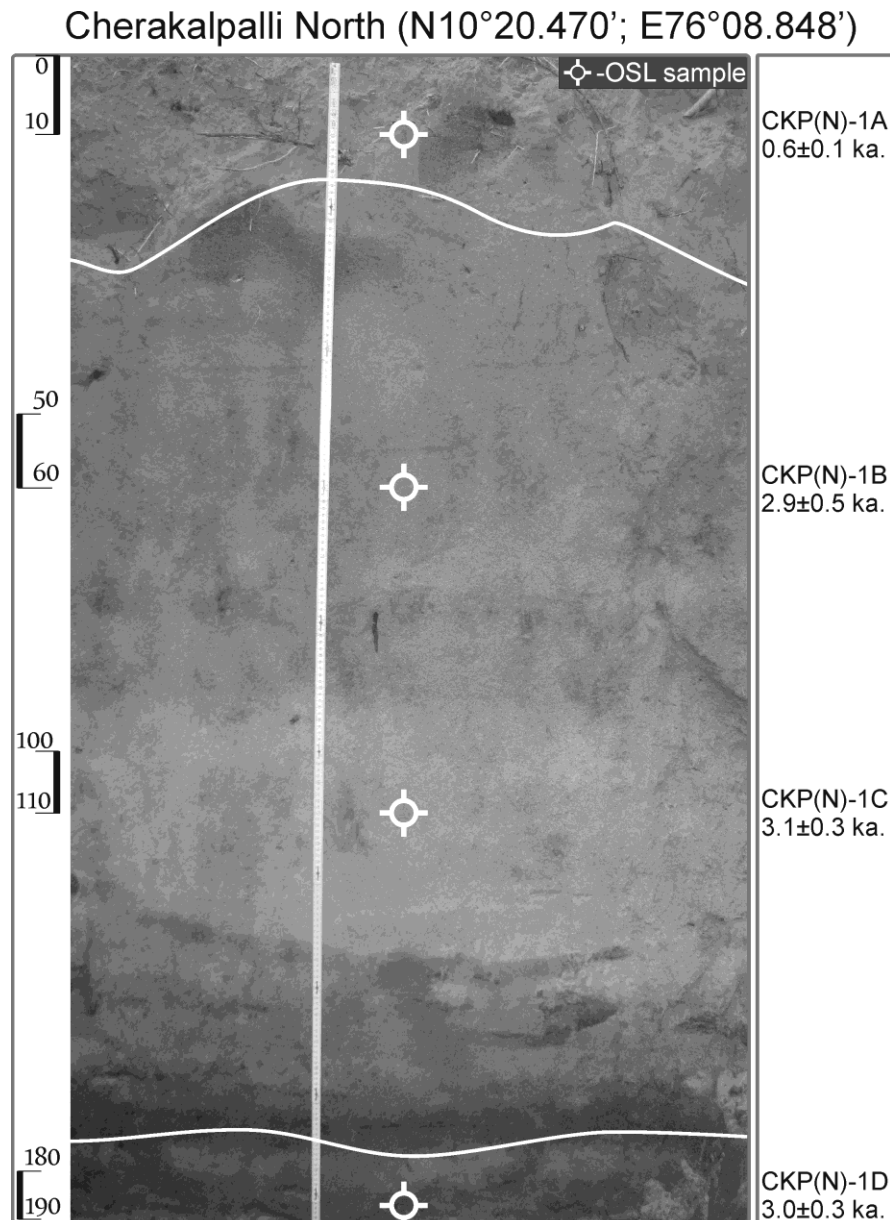


Figure 5.4. Picture showing the sampling profile in Cherakalpalli area (CKP (N)-1). OSL sample points, visible unconformities in the ridge and measured OSL ages are shown.

Profile KHL-1 excavated in an elevated beach ridge found more towards the inland and the area forms the southernmost part of the study area. The profile was dug to a depth of 1.8m below surface. The brownish grey sandy soil present in the upper part of the

profile up to 0.5m depth was found to be disturbed with burrow marks and root casts. This was followed by an organic rich, light grey fine sand unit up to a depth of 0.9m. KHL-1A was collected from a layer of light yellow fine sand bed below this sand unit at a depth of 1.7m. Remains of clay pots were observed from this profile at a depth of 1m.

5.3 Experimental details

In the laboratory, samples were processed under subdued red light. The sample was dry sieved to separate sands of 150-200 μm . The sample was treated with 0.1 N hydrochloric acid (HCl) to dissolve carbonates and to partly remove any iron oxides, 0.01 N sodium oxalate ($\text{C}_2\text{Na}_2\text{O}_4$) to remove the clay coatings, and 30% hydrogen peroxide (H_2O_2) to remove organic matter from the samples. The quartz- rich fraction ($\sim 2.65 \text{ g cm}^{-3}$) was separated by density separation using an aqueous solution of sodium poly-tungstate ($3\text{Na}_2 \text{WO}_4 \cdot 9\text{WO}_3 \cdot \text{H}_2\text{O}$) and subsequently etched using 40% hydrofluoric acid (HF) for 60 minutes to remove feldspar. For most of the samples even after 1 hr of HF etching there was a substantial amount of feldspar signal and these samples were re-etched to nullify the signals from feldspar. Samples were then washed, dried and sieved again through the respective meshes. The etched quartz grains were held as a monolayer on 6mm/2mm diameter stainless steel discs using silicone oil and 24- 48 aliquots per sample were used for each measurement.

The single aliquot regenerative dose (SAR) protocol for quartz (Murray and Wintle, 2000; Wintle and Murray, 2006) was used to determine the equivalent dose of the samples in this study. An automated Riso TL/OSL DA-15 reader attached with a $^{90}\text{Sr}/^{90}\text{Y}$ beta source which delivers a dose rate of 0.16 Gy/s was used for the measurements. Blue light emitting diodes (LED) ($470\pm 30 \text{ nm}$) were used for the optical stimulation of quartz and a Hoya U-340 (7.5 mm) filter was placed between photomultiplier and sample to screen light of stimulating wavelength.

The test for consistency of the measurement in SAR cycle involves repetition of a SAR cycle (usually the initial one) for a second time towards the end of the protocol. This verifies that the sensitivity corrected luminescence signal obtained in the first measurement is identical to the second one, by providing a ratio known as the recycling ratio (Fig. 5.5). To ensure the accuracy of D_e values estimated and the efficiency of the protocol to recover

a given dose, a dose recovery test (Roberts et al., 1999; Murray and Wintle, 2003) was performed.

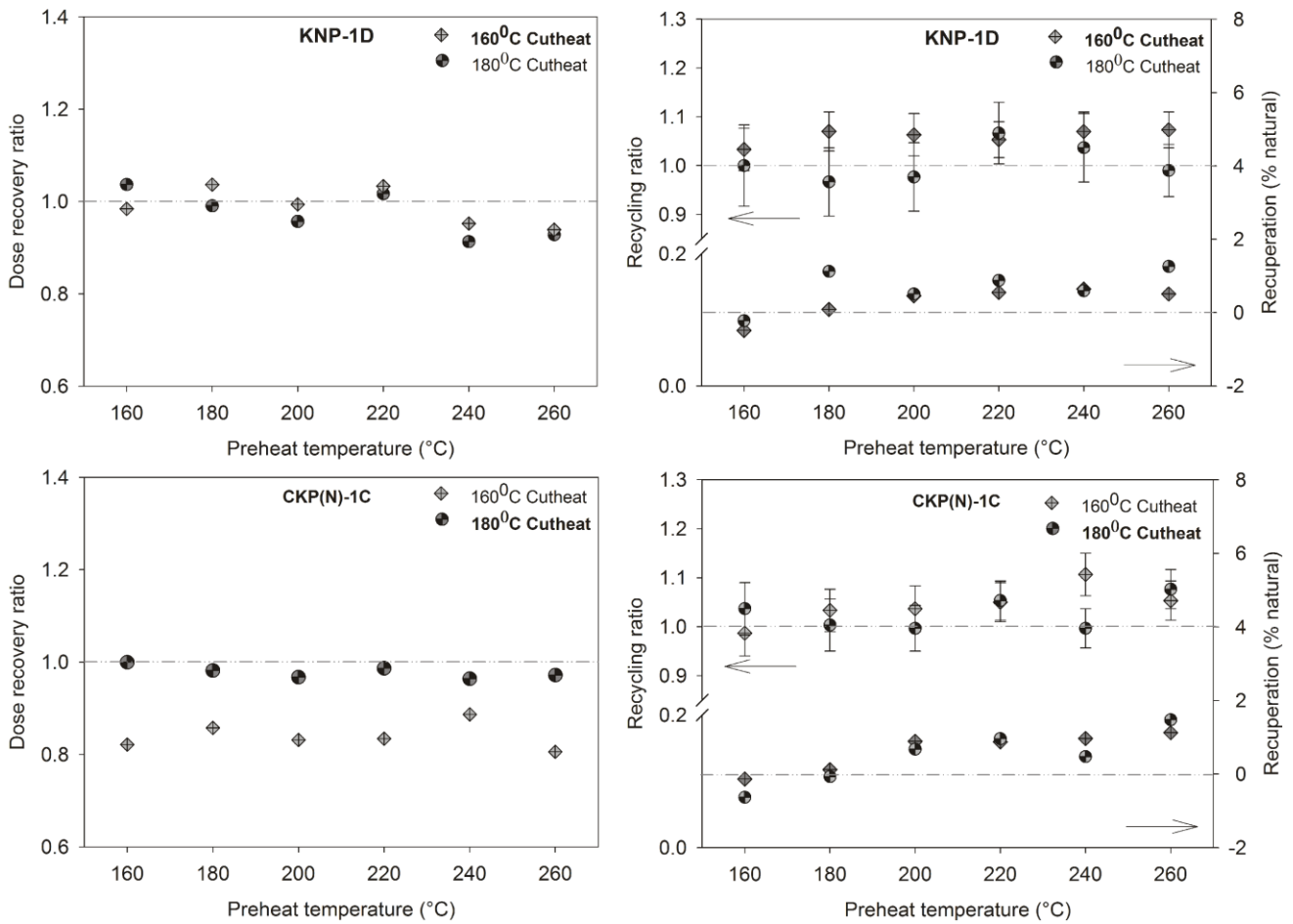


Figure 5.5. Diagram showing the details of quality checking criteria tested for all the samples in the study. Test results of two selected samples from the study (CKP (N)-1C and KNP-1D) are shown. Tests were carried out at two different cut-heat temperatures (160 and 180° C). A final preheat temperature of 160/180° C was selected for measurements and early background subtraction was applied to extract the fast component of the quartz decay curve. The plot shows the dependence of recycling and recuperation ratios on various preheat, cut-heat temperatures for the samples. For each temperature the mean D_e of three aliquots are shown.

The test involves resetting the natural signal level to zero by artificial stimulation and administering a known laboratory dose to the sample. For ideal measurement conditions the SAR protocol recovers the given dose close to unity, which underlines the choice of heat treatment and test dose in the measurement cycle. Tests for dose recovery for all samples were carried out prior to measurement at different pre heat temperatures ranging between 160°C - 260°C with an increment of 20°C in every cycle. The test was carried out at two different cut heat temperatures (160°C or 180°C). The dose recovery at various preheat temperatures (between 160°C - 260°C) was plotted for two different cut heat temperatures used (Fig. 5.5). The dose recovery combined preheats test shows that the given dose was recovered during the subsequent measurement step and the D_e value obtained is independent of the applied pre heat temperature.

The separated quartz extracts may contain some feldspar as inclusions or feldspar with inclusions of ferromagnesian minerals. This was tested by prior exposure of sample to infra red radiation for identifying feldspar contamination (Duller, 2003). This OSL-IR depletion test provides a measure of feldspar contamination in the sample. It is calculated from the ratio of OSL response of a beta dose to that of a subsequent step of measurement with the same beta dose and preheat after exposing the sample for 40s of IR stimulation at 125°C (Duller, 2003). The thermal transfer test showed that the samples did not have any significant influence of charge transfer from light insensitive thermally shallow traps to the light sensitive OSL traps due to the effect of high temperature treatments.

The measured D_e values were accepted if, i) the recycling ratio (Wallinga et al., 2000) was between 0.90 to 1.10, ii) recuperation was <5% of measured D_e value (Murray and Wintle, 2000, Wallinga et al., 2000), iii) dose recovery ratio was between 0.95 to 1.05 (Wintle and Murray, 2006), iv) OSL-IR depletion ratio was between 0.85 - 1.15 (Duller, 2003) and v) thermal transfer was <5% of the natural signal. Measurement uncertainty of 1.5% was incorporated for calculation of D_e values. The total numbers of accepted aliquots out of measured (in brackets) are shown in Table 5.1.

The D_e values were calculated using signals integrated over the first three channels (0- 0.48s) and an early background subtracted (Ballarini et al., 2007) from the subsequent channels corresponding to 1.12s to 2.4s. Exponential or linear (for modern samples) fitting was applied to the natural and regenerated OSL signal for D_e determination. 24 to 48 aliquots of each sample was used for measurements and weighted mean of the D_e values

were used for final D_e estimation. The uncertainties in D_e values are expressed as standard error of D_e estimates. The over dispersion values (Table 5.1) of the distribution was calculated using the central age model (Galbraith et al., 1999).

Sand samples were collected for dose rate measurements and dried at 50°C, 700g of it were packed into Marinelli- beakers and sealed air tight to prevent radon loss. The samples were stored for one month after preparation to gain ^{222}Rn - ^{226}Ra equilibrium and then used for measurements. External dose rate for the samples were calculated from the activity concentrations of decay chains ^{238}U (^{234}Th , ^{214}Bi , ^{214}Pb , and ^{210}Pb), ^{232}Th (^{228}Ac , ^{212}Pb , and ^{208}Tl) and ^{40}K measured using high resolution gamma spectrometry (High Purity Germanium (HPGe) N-type coaxial detector) (Table 5.1). Adequate counts for required radionuclide peaks were obtained by measuring each sample for 24 hrs. The dose rate conversion factors of Adamiec and Aitken (1998) and beta attenuation factors of Mejdahl (1979) were applied for calculation. The cosmic dose rate was calculated based on the method proposed by Prescott and Stephan (1982) and Prescott and Hutton (1994) taking into consideration the sample's geographic location, altitude and depth. The altitude of the area was approximated from hand held GPS readings and local elevation. An assumed water content of $6\pm 3\%$ was applied in dose rate calculations for all samples. This value was used based on recent studies (Ballarini et al., 2003 and Kunz et al., 2010) for well drained coastal and near coastal dune/ ridge deposits. The effect of alpha dose rate in the sample was considered negligible based on the assumption that 45 minutes of etching of quartz grains with HF (40%) removes the alpha irradiated outer rind of the mineral grain.

Distribution of particle size and degree of sorting of sample were determined by carrying out grain size analysis on selected samples from each bed in all the profiles. The analyses were carried out using Retsch Camsizer on 50g of untreated sand for selected samples from the profile to know the vertical variation in grain size. The result was calculated using the method of Folk and Ward (1957) employing Gradistat programme (Blott and Pye, 2001) for the analysis of grain size statistics.

For heavy mineral studies, the samples were analysed using standard optical microscopy to identify the heavy mineral constituents. Heavy minerals were separated from the same fraction using heavy liquid with densities $>2.7\text{g/cm}^3$. Heavy mineral grains of 150- 200 μm were mounted on glass slides with approximately 300 grains on each and were counted in a petrological microscope using a mechanical stage. The total number of identical mineral grains in each sample was counted and the number percentages of the same were calculated.

5.4 Results

The gamma spectrometry results showed similar concentration of U, Th and K for most of the samples in the profile except sample KNP-2B. A considerably high value of K, Th and U content in this sample resulted in high dose rate of $3.05 \pm 0.31 \text{ mGya}^{-1}$. The dose rate for other samples in this profile (KNP-1,2) ranges between 1.26 ± 0.14 and $1.37 \pm 0.15 \text{ mGya}^{-1}$. Sample SNC-1A yielded a dose rate of $2.67 \pm 0.27 \text{ mGya}^{-1}$ primarily due to the comparatively higher content of Th and U. Samples from profile CKP (N)-1 exhibited higher dose rate between 1.71 ± 0.18 and $2.60 \pm 0.27 \text{ mGya}^{-1}$. Results of the high resolution gamma spectroscopy and calculated dose rate for all samples given in table 5.1. The uncertainties in table 5.1 indicate the Standard Error (SE) for all results.

Table 5.1: Summary of quartz measurement details including depth, radionuclide concentration, dose rate, cosmic dose, D_e , number of aliquots accepted/measured (n), and OSL age of beach ridges of Kerala. The ^{40}K , Uranium and Thorium concentrations in the sediment was measured using high-resolution gamma spectrometer. An average water content of $6 \pm 3\%$ (Kunz et al, in press) was applied in the dose rate calculation. The over dispersion, σD represents the relative standard deviation of the measured single aliquot D_e distribution obtained using the 'central age model'. The number of accepted aliquots 'n' using the acceptance criteria are given with the total measured aliquots in the brackets. The inferred final ages are given in bold. Errors are given as $\pm 1\sigma$.

Location	Sample ID	Depth (cms)	K (%)	Th (ppm)	U (ppm)	Cosmic dose (mGy a ⁻¹)	Dose rate (mGy a ⁻¹)	D_e (Gy)	n	σD_e (%)	Age model	Age (ka)
Chaliyangad	KNP-1A	50	0.78± 0.01	6.39± 0.03	0.52± 0.01	0.20± 0.02	1.37± 0.15	1.8± 0.1	21(24)	20	CAM	1.3± 0.1
	KNP-1B	90	0.85± 0.00	3.89± 0.10	0.44± 0.09	0.19± 0.02	1.26± 0.14	5.2± 0.1	20(24)	11	CAM	4.1± 0.5
	KNP-1C	195	1.78± 0.00	11.48± 0.16	3.25± 0.06	0.16± 0.02	3.05± 0.31	3.8± 0.1	45(48)	11	CAM	1.3± 0.1
	KNP-1D	220	1.01± 0.01	3.17± 0.02	0.37± 0.01	0.16± 0.02	1.33± 0.15	5.0± 0.1	22(24)	10	CAM	3.8± 0.4
Chandrapinni	CHK-1A	160	0.81± 0.00	19.74± 0.07	1.36± 0.08	0.17± 0.02	2.28± 0.24	7.2± 0.2	23(30)	13	CAM	3.2± 0.3
Edathirithi panchayath	EDT-1A	100	0.88± 0.00	3.96± 0.70	0.45± 0.13	0.18± 0.02	1.31± 0.15	4.0± 0.1	46(48)	14	FMM	3.1± 0.3
	EDT-1B	140	1.06± 0.01	3.08± 0.02	0.39± 0.01	0.17± 0.02	1.39± 0.15	5.8± 0.1	39(48)	14	CAM	4.2± 0.5

Table 5.1 (continued..)

Location	Sample ID	Depth (cms)	K (%)	Th (ppm)	U (ppm)	Cosmic dose (mGy a ⁻¹)	Dose rate (mGy a ⁻¹)	D _e (Gy)	n	σDe (%)	Age model	Age (ka)
Cherakalpalli North	CKP(N)-1A	10	1.30± 0.01	13.55± 0.04	0.75± 0.01	0.17± 0.02	2.33± 0.24	1.0± 0.1	34(48)	--	CAM	0.6± 0.1
	CKP(N)-1B	60	1.37± 0.01	18.82± 0.03	1.07± 0.01	0.21± 0.02	2.60± 0.27	5.2± 0.1	46(48)	21	FMM	2.0± 0.2
	CKP(N)-1C	110	1.15± 0.00	5.44± 0.14	0.40± 0.19	0.19± 0.02	1.71± 0.18	5.2± 0.1	22(24)	6	CAM	3.1± 0.3
	CKP(N)-1D	190	1.52± 0.01	17.56± 0.07	0.84± 0.01	0.18± 0.02	2.59± 0.27	7.7± 0.1	22(48)	6	CAM	3.0± 0.3
Wanjipura, Kaipamangalam	WNJ-1A	100	1.56± 0.01	1.72± 0.01	0.17± 0.00	0.16± 0.02	2.18± 0.22	0.1± 0.0	20(24)	--	CAM	0.06± 0.01
S.N.College, Nattika	SNC-1A	120	0.61± 0.00	32.87± 0.04	2.62± 0.05	0.18± 0.02	2.67± 0.27	12.3± 0.4	43(48)	17	FMM	4.7± 0.5
	SNC-2A	210	0.95± 0.01	2.63± 0.02	0.34± 0.01	0.16± 0.02	1.24± 0.14	4.1± 0.5	39(48)	14	FMM	3.3± 0.4
Kochalungal	KHL-1A	170	0.87± 0.01	1.68± 0.02	0.26± 0.01	0.17± 0.02	1.10± 0.13	4.4± 0.1	18(24)	8	CAM	4.0± 0.5

The sample yielded bright OSL signals for both natural and regenerated dose and SAR performance tests (Fig. 5.5) such as recycling, recuperation, IR depletion and dose recovery show that the results obtained using SAR procedure are reliable within given uncertainty. The number of aliquots accepted for final D_e calculation out of total number of measured aliquots (in brackets) is given in table 5.1. Among the rejected aliquots most of it was due to poor recycling ($> \pm 10\%$) and IR depletion ($> \pm 15\%$). For modern samples linear fitting was used for D_e calculation and for all remaining samples a saturating exponential function was used for curve fitting. The D_e values obtained in the study ranges from a low of 0.1 ± 0.0 Gy to a maximum of 13.2 ± 1.9 Gy. Such low D_e values ($\sim 0.006 \pm 0.004$ Gy) for modern samples and tight distribution for the older samples have been reported (Armitage et al., 2006; Kunz et al., 2010) for well bleached aeolian sands. Few samples in the present study (EDT-1A, CKP (N)-1B, SNC-1A and 2A) showed large scattering in the D_e values by giving discrete number of distribution in each samples (Fig. 5.6). Considering the deposition of sample in a well bleached depositional setting, partial bleaching was ruled out as a likely cause of scattering. Evidences in the field showed that the post-depositional reworking due to bio-turbation could be the source of scattering. For these samples Finite mixture model (FMM) was used to find the different population in the D_e distribution of a sample (Fig. 5.6).

The OSL dating of sample KNP-1B collected from the upper part of profile KNP-1 (bench I) at a depth of 0.5 m gave an age of 1.3 ± 0.1 ka. The two samples (KNP-1C, 2C) collected from the lower part of Bench-I and II at depths of 0.9m and 2.2m yielded similar ages (4.1 ± 0.5 and 3.8 ± 0.4 ka respectively) within uncertainty showing a contemporaneous accumulation of these sand units. Sample KNP- 2B collected from the upper sand unit (B) of Bench-II showed identical age of 1.3 ± 0.1 ka to that of the upper sample (KNP-1B) of Bench- I (Fig. 5.3). CHK-1 profile is situated towards North West of KNP-1 and sample CHK-1A collected from the lower part of this profile at a depth of 1.6m gave an age of 3.2 ± 0.3 ka. Profile EDT-1 is located few meters North West of CHK-1 profile. Sample EDT-1A and EDT-1B collected from this profile at depths of 1m and 1.4m yielded OSL ages of 3.1 ± 0.3 and 4.2 ± 0.5 ka respectively.

Application of OSL dating on coastal sediments...

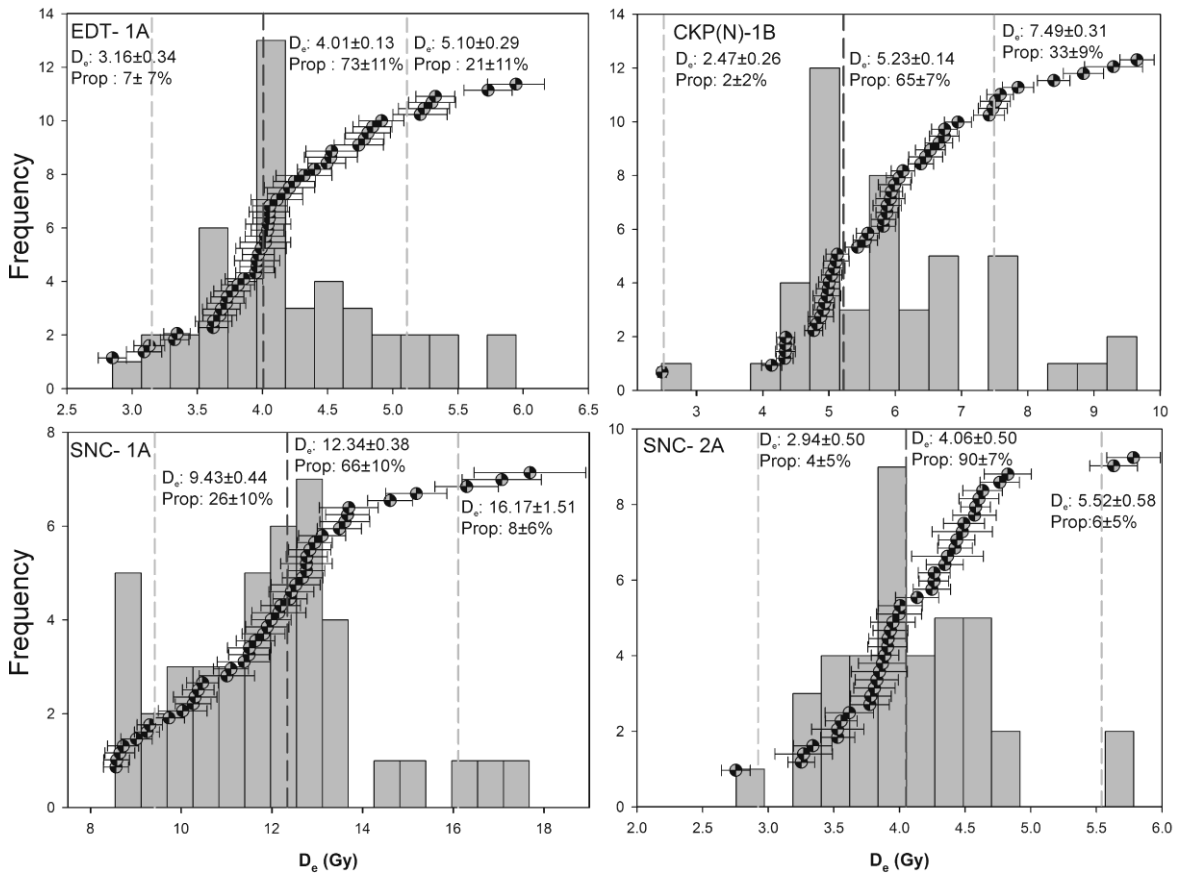


Figure 5.6 Examples of distribution of selected samples having large scatter in the measured D_e values. Finite mixture model was applied for the samples and relative proportion of different distributions and D_e values are marked with hatched line in the background. Bold hatched line in the diagram indicates the selected D_e distribution for the age calculation.

Among the four samples collected from CKP (N)-1 profile (Fig. 5.4), two samples taken from the lower part at depths of 1.10, and 1.90m yielded similar ages such as $3.1±0.5$ and $3.0±0.3$ ka respectively indicating that the sand unit was deposited in the same period. CKP (N)-1A and 2A collected from the upper part of the profile at depths of 0.1m and 0.6m provided OSL ages of $0.6±0.1$ and $2.0±0.2$ ka respectively.

Profile WNJ-1 was excavated in a modern beach ridge and sample WNJ-1A collected from a depth of 1m gave an OSL age of $60±10$ a. The area is located about ~200m away from the modern coastline. Two samples, SNC-1A and SNC-2A collected from section SNC-1, 2 at depths of 1.2m and 2.1m yielded OSL ages of $4.7±0.5$ (SNC-1A)

ka and 3.3 ± 0.4 ka (SNC-2 A) respectively. Sample KHL-1A collected at a depth of 1.7m gave an OSL age of 4.0 ± 0.5 ka.

In profile KNP-1 the dune was composed of moderately well-sorted medium sand ($\sim 380\mu\text{m}$) except for layer KNP-1E which showed an average grain size of $566\mu\text{m}$ with moderately sorted sand. The grain sizes of sand from profile CKP (N)-1 ranged between 402 to $468\mu\text{m}$ (medium sand). The sand was moderately well sorted in the top of the profile and well sorted towards bottom (CKP (N)-1C and D). In profile EDT-1, the ridge was made up of moderately well-sorted to moderately sorted medium sand ($373\mu\text{m}$). In the northernmost ridge sampled in this study (SNC-1 and SNC-2), the sands were medium to coarse grained ($410\text{-}605\mu\text{m}$) and exhibited moderately well-sorted.

Ten samples (Table 5.2) from various profiles were analysed for heavy mineral assemblages. The heavy-mineral suite of the dune sediments consists of light green to green/ colourless hornblende, ilmenite, clinopyroxenes (augite and diopside), garnet (pink and colourless), epidote (clinozoisite and zoisite), aluminosilicates (sillimanite and kyanite), and accessory amounts of zircon, rutile, staurolite, chlorite, muscovite and sphalerite. The light minerals consist of mainly quartz and some feldspar. Except sample SNC-1A all the analysed samples showed high content of hornblende (51-66%), ilmenite (1-10%) and clinopyroxene (5-23%) minerals. SNC-1A contained only 12% of hornblende and 63% ilmenite. The results of heavy mineral analysis including the percentage of mineral assemblages are given in Table 5.2.

5.5 Chronology of beach ridges of Kerala

The area has high rate of sediment supply owing to the large number of rivers flowing west in to the Arabian Sea. The rivers originate from the Western Ghats which lies towards the east of Kerala. Due to the steep gradient and proximity of the Ghats to the coast, sediments experience only short transporting distance and grains are sub-angular in nature. Beach ridges are found in prograding shoreline having large supply of sand sized clastic sediment available in the littoral zone. Availability of fluvial sediments and large quantity of unconsolidated aeolian sands in the littoral zone contribute to the formation of well developed beach ridges in the area. During the stages of sea level low stands, large

extents of coastal areas are directly exposed to sunlight which increases the potential sediment supply available for aeolian processes.

Table 5.2 Data showing the details of heavy mineral analyses in the selected samples using optical microscopy. 300 grains from each sample was mounted on a glass slide and grains were counted for various heavy mineral assemblages. Percentage of heavies present in each sample is given.

	Heavy minerals	KNP -1B	KNP -1D	KNP -1E	KNP -1F	EDT -1B	CKP (N)-1B	CKP (N)-1D	SNC-1A	SNC-2A	KHL-1A
	Hornblende	58	65	66	57	63	50	51	12	70	65
	Ilmenite	10	7	5	4	3	10	18	63	1	6
	CPX (Augite, Diopside)	10	9	13	17	12	23	13	5	12	15
	Garnet	7	3	Sp.	2	2	10	13	7	4	5
Mineral (Wt %)	Sillimanite	5	4	3	4	4	2	1	1	3	5
	Epidote	2	1	1	1	1	2	Sp.	1	2	1
	Kyanite	3	2	sp	3	sp	1	sp	2	Sp	sp
	Rutile	1	sp	1	sp	2	sp	sp	4	Sp	
	Chlorite, Muscovite	sp	—	1	—	1	sp	sp	—	—	sp
	Zircon	sp	sp	—	—	—	—	1	5	—	—
	Staurolite	sp	—	—	—	—	sp	sp	—	Sp	—
	Sphalerite	—	sp	—	—	—	—	—	—	—	—

The OSL ages of profile KNP-1 show good stratigraphic order within the given uncertainty with bottom samples of older ages and younger ages for uppermost samples. Weak soil development with signs of illuviation observed in the profile (C- unit) between KNP-1B and KNP-1C indicate a stage of surface stabilization. The sand unit KNP-1B in the profile may indicate a period of sand mobility in the region after the coastline had prograded further west and the ridge surface was exposed to aeolian activity.

Profile SNC-1 forms an older ridge located ~15m towards west of SNC-2 profile. The older age for sample SNC-1A may be due to the fact that SNC-1 and SNC-2 represent two different ridges running parallel to each other. However, from the present morphology it is difficult to identify the two ridges as SNC-2 has been largely removed for settlements.

Heavy mineral analysis of these two profiles revealed varying heavy mineral assemblages indicating two different sediment sources with SNC-1A having high concentration of ilmenite and lesser hornblende (Table 5.2). The sample also showed high dose rate ($2.67 \pm 0.27 \text{ mGya}^{-1}$) due to high concentration of U and Th in the surrounding sediments. The sample showed a U content of $2.62 \pm 0.05 \text{ ppm}$ and Th content of $32.9 \pm 0.04 \text{ ppm}$ (Table 5.2). Thorium is a trace element commonly associated with clays and heavy minerals (Frias et al., 2004). Sample KNP- 2B also showed a higher dose rate of $3.05 \pm 0.31 \text{ mGy/a}$ due to higher concentration of U, Th and K in the sample (Table 5.1). However, heavy mineral analysis of this sample did not show much variation in its relative abundance (Table 5.2). Occurrence of heavy mineral placers that contain monazite is reported in the southern parts of coastal Kerala (Mallik et al., 1987).

The investigation on heavy minerals present in the beach ridges yielded high concentration of ilmenite and hornblende in the heavy mineral suite, which is comparable with the previous findings of Maillik et al., (1987) for the same region. The heavy mineral placers of Kerala beach are derived from Khondalites, granite gneisses, charnokites, pegmatities and syenites of the Western Ghats, and have been transported to the coast by the west flowing rivers (Mallik, 1986). Heavy minerals are reworked by long shore currents and are concentrated during south west monsoon (Mallik, 1986). Major source of hornblende in the sediments are from retrograde charnokites and hornblende gneisses. Zircon is known to be liberated from the charnokites and also occurs as a minor constituent in all the rocks. Tertiary and recent alluvial sediments occur along the coastal plains with the tertiary units capped by laterites (Mallik et al., 1988). Except the upper sample layer in the profile CKP (N), a contemporaneous sand accumulation was observed from OSL dating of samples collected from this profile.

5.5.1 Late Pleistocene to Holocene scenario on Indian west coast

Bhattacharya et al. (1979) postulated that the coast parallel alignment of beach ridges, absence of soil development in the younger beach ridges and thin layer of soil in the older beach ridges indicates younger age of regression whereas, the differences in the morphology and elevation of ridges indicates a hiatus in the coastline progradation. In our present study, apart from the two modern samples collected from the upper part of the profile, majority of the samples collected from depths of ~1.5 to 2m yielded a depositional age of 3 to 4ka (Fig. 5.7). The sample WNJ-1A was collected from a modern beach ridge close to the present day coast shows that OSL dating used in the present study is reliable within the given uncertainty. The OSL ages obtained in the study can thus be used with confidence which indicates a late Holocene coast line progradation in the west coast of south India and may furnish some evidences of sea level high stand during this period. Similar ages (2-4 ka) were obtained from the OSL dating of beach rock formation (Thomas, 2009) and radiocarbon dating of emerged coral colonies (Banerjee, 2000) in the east coast of India which suggested a higher sea level during this period. A maximum aridity around 18 ka (LGM) and period of mangrove extension along the west coast of South India has been reported. This started around 16.5 ka and reached its maximum during 11 ka from the pollen records (Campo, 1985). Greatest abundance of monsoon rain during 11 ka was inferred by the enhanced content of mangrove pollen in offshore core sediments of the west coast of India and is synchronous with European Younger Dryas (Campo, 1985; Kumaran et al., 2005). Decreasing relative frequencies of mangrove pollen was observed between 11 ka to 6 ka. The variation in abundance of mangrove forests in the area may be attributed to climate change. A large shift in $\delta^{18}\text{O}$ records with higher values in early Holocene (~9-8 ka) culminating at 5.6ka was attributed to major variation in surface hydrography (Thamban et al., 2001). The inundation of sea water during Early Holocene transgression occurring between 8 - 6 ka and submergence of mangrove swamps resulted in the formation of carbonic wood/peat deposits (Kumaran et al., 2005) along the present day onshore regions in Kerala. Ideal conditions for peat formation prevailed during mid Holocene times and mangrove swamps appeared in sheltered environments. Occurrences of peat deposits have been reported in many onshore and offshore locations along the west coast of Kerala.

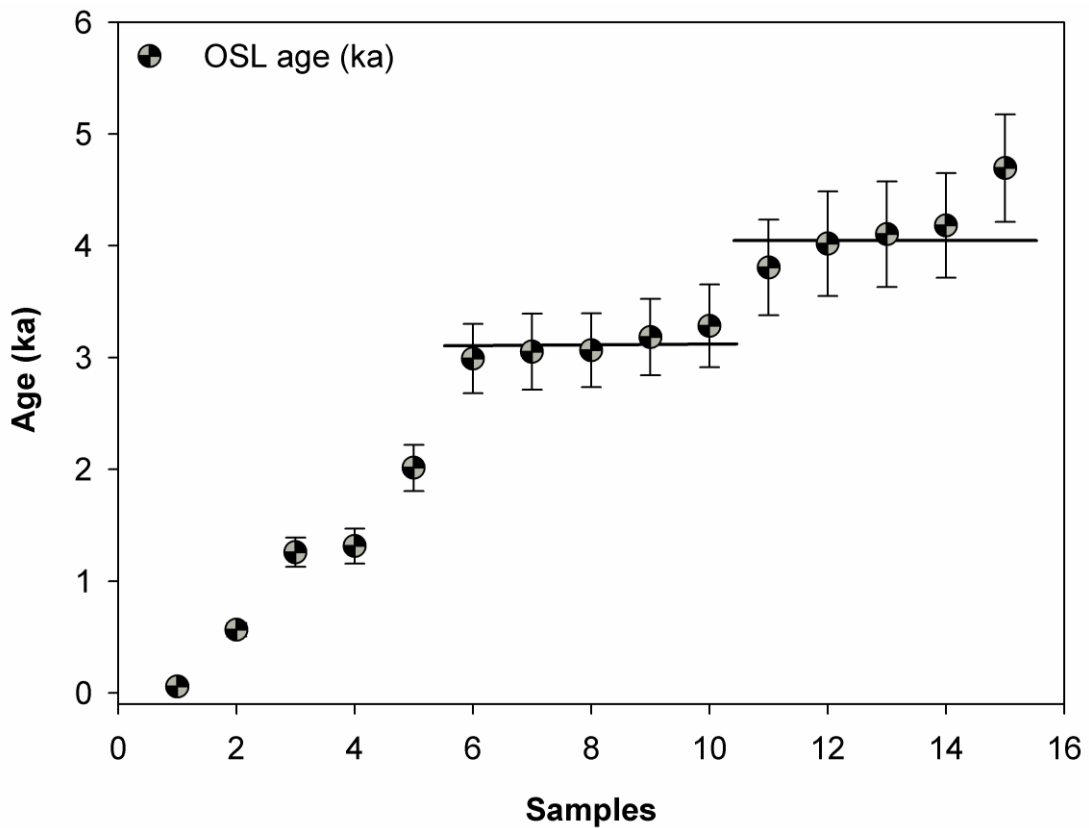


Figure 5.7. OSL ages plotted against total number of samples measured in this study showing the periods of deposition of beach ridges centred at 3 and 4 ka.

During our field study in parts of central Kerala 1m thick peat deposits were observed at 1.5 - 2m below the surface ~10km inland. A 1.5m thick plastic clay layer was observed overlying the peat layer and this was deposited on top of a grey sandy clay layer. Campo (1986) reported high sedimentation rate in the western continental shelf of South India between 11-10 ka, due to high accumulation of terrigenous clays. The radiocarbon dating of peat deposits reported (Rajendran et al., 1989) from Tellicherry (North Kerala) and Tannisseri (Central Kerala, close to the study area) yielded ages of 7230 ± 120 and 6420 ± 120 years BP respectively. All these observations have been suggested to be related to a rising sea level during early to middle Holocene. Dating (uranium series) of fossil coral reefs considered as the remnants of sea level high stand located 2km inland at an elevation of 2-4 m in the Saurashtra coast of west India suggests that sea level was 2-6m higher than present level during middle Holocene (~6 ka) (Gupta and Amin, 1974).

Based on the archaeological findings at Bet Dwarka in western India, it was suggested that sea level was higher than the present at around 6000 yrs and remained more or less stable until 3500 years (Gaur et al., 2007). It was pointed out that a large number of Harappan port towns (3000 – 1500 BC) in Gujarat and Pakistan are located inland at higher positions (Gaur and Vora, 1999). Indication from archaeological sites such as Lothal and Padri demonstrate that maritime practices during the last 4000 years point to shore line migration to off shore (Gaur and Vora, 1999) and suggested 2 - 6m higher sea level during this period. These observations from various studies and results from the OSL dating of sands from the beach ridges of central Kerala in the west coast in the present study indicates a higher sea level until after 6ka which gradually receded during 5-3 ka. This is in agreement with the observations of Mathur et al. (2004) who have suggested that the onset of regression in the west coast of India occurred since 4.5ka demonstrated from the presence of old tidal flats inland to the newer tidal flats.

The OSL ages are in agreement with the findings of Mathur et al. (2004) who have reported 4-1m higher mid to late Holocene (4-1 ka) sea level stand all along the west coast of India. As the study area is located further inland (3-8 km) to the present day coast and a sea level high stand between 4-1m above present day level would bring the shoreline close to the inland beach ridges. However the occurrence of such events has been inferred only from evidences of morphological and chronological results of random samples collected from the beach ridges. Thus in order to establish the exact position of shore line further detailed studies need to be carried out on local elevation with respect MSL and high resolution dating as well as morphological studies.

The OSL ages from the present study shows two major periods of sand accumulation centred at ~3 and 4 ka (Fig. 5.7). It was reported that the absence of mangrove pollen in the late Holocene (after 4ka) sediments indicates a gradual reduction of monsoon intensity from 5ka to 3ka BP (¹⁴C ages, Kumaran et al., 2005). The probable reason for an enhanced sand mobility during this period may be due to the fact that the prograding coast might have exposed plenty of sand in the onshore region which was reworked and deposited on top of the ridge morphology during the dry span of late Holocene.

5.6 Conclusions

The beach ridges along the west coast of Kerala are composed of moderately well sorted to well sorted medium to coarse sand (mean grain size $442\mu\text{m}$; sorting 1.4 to 2.0ϕ), consisting of light (mainly quartz and little feldspar) and heavy minerals (mainly hornblende, illmenite and clino-pyroxene). As there is no independent age control available in the area, a direct comparison of the measured OSL ages could not be made in the present study. The reliability of the measured OSL age estimates however, in this study is based on the following reasons. 1.) Firstly, tests performed as a part of SAR procedure shows that it is possible to measure a dose given in the laboratory prior to any thermal transfer or without any significant change in sensitivity. Secondly, the OSL age of a sample collected from the modern beach ridge gave an age resolution of few decades which is in agreement with field evidences. The luminescence ages from most of the sites are stratigraphically consistent and with ages close to 3-4 ka, indicating a possible stage of wide spread sand accumulation all along the west coast of Kerala. This is another evidence for a regressing sea during middle to late Holocene period in the west coast of India particularly in the coasts of Kerala.

5.7 Acknowledgements

This research has been supported by Leibniz DAAD fellowship funded by the German Academic Exchange Service (DAAD) and the Leibniz Institute for Applied Geophysics, Hannover (LIAG), which is greatly acknowledged. The authors are grateful to Mr. D. Klosa and Ms. Irene Bitz, technicians from Landesamt für Bergbau, Energie und Geologie, Hannover for the Scanning Electron Microscope analysis and Heavy mineral analysis. L. A is grateful to Mr. Abhishekh P.V. for his help and suggestions in the preparation of maps using GIS.

5.8 References

- Adamiec, G., Aitken, M.J., 1998. Dose-rate conversion factors: update. *Ancient TL* 16, 37-49.
- Armitage, S.J., Botha, G.A., Duller, G.A.T., Wintle, A.G., Rebêlo, L.P., Momade, F.J., 2006. The formation and evolution of the barrier islands of Inhaca and Bazaruto, Mozambique. *Geomorphology* 82, 295-308.
- Ballarini, M., Wallinga, J., Murray, A.S., Heteren, S.v., Oost, A.P., Bos, A.J.J., Eijk, C.W.E.v., 2003. Optical dating of young coastal dunes on a decadal time scale. *Quaternary Science Reviews* 22, 1011-1017.
- Ballarini, M., Wallinga, J., Wintle, A.G., Bos, A.J.J., 2007. A modified SAR protocol for optical dating of individual grains from young quartz samples. *Radiation Measurements* 42, 360-369.
- Banerjee, P.K., 2000. Holocene and Late Pleistocene relative sea level fluctuations along the east coast of India. *Marine Geology* 167, 243-260.
- Bhattacharya, A.K., Kurien, T.K., Krishnanunni K., Senti, D.N., 1979. Geomorphic mapping in parts of Kerala state. *Journal of the Indian Society of Photo-Interpretation and Remote Sensing*, VII (I), 1-9.
- Blott, S.J., Pye, K., 2001. GRADISTAT: A grain size distribution and statistics package for the analysis of unconsolidated sediments. *Earth Surface Processes and Landforms* 26 (11), 1237-1248.
- Campo, E.V., 1986. Monsoon fluctuations in two 20,000-Yr. B.P. oxygen- isotope/ pollen records off Southwest India. *Quaternary Research* 26, 376-388.
- Duller, G.A.T., 2003, Distinguishing quartz and feldspar in single grain luminescence measurements. *Radiation Measurements* 37, 161-165.
- Folk, R.L. Ward, W.C., 1957. Brazos River bar, a study in the significance of grain-size parameters. *Journal of Sedimentary. Petrology*, 27, 3-27.
- Frias, J.M., Lunar, R., Benito, R., 2004. Th- and U-bearing minerals in the SE Mediterranean margin of Spain. *Episodes* 27(1), 33-37.
- Galbraith, R.F., Roberts, R.G., Laslett, G.M., Yoshida, H., Olley, J.M., 1999. Optical dating of single and multiple grains of quartz from Jinmium Rock Shelter, northern Australia: Part 1, experimental design and statistical models. *Archaeometry* 41, 339-364.

- Gaur, A.S. Vora, K.H., 1999. Ancient shorelines of Gujarat, India, during the Indus Civilization (Late Mid-Holocene): A study based on archaeological evidences. *Current Science* 77, 180-185.
- Gaur, A.S., Vora, K.H., Sundaresh, 2007. Shoreline changes during the last 2000 years on the Saurashtra coast of India: Study based on archaeological evidences. *Current Science* 92(1), 103-109.
- Geological Survey of India, 1995. Geological and mineral map of Kerala. Scale 1:50,000 with explanatory brochure, Geological Survey of India, Calcutta, 8pp
- Gupta S.K., Amin, B.S., 1974. Io/U ages of corals from Saurashtra coast. *Marine Geology* 16 M79-M83.
- Hashimi, N.H., Nigam, R., Nair, R.R., Rajagopalan, G., 1995. Holocene sea level fluctuations on western Indian continental margin: An update. *Journal of geological Society of India* 46, 157-162.
- Jayalakshmi, K., Nair, K.M., Kumai, H., 2001. Quaternary Geology of Kerala Coast: An Overview. *Gondwana Research* 4 (4) 644-645.
- Kumaran, K.P.N., Nair, K.M., Shindikar, M., Limaye, R.B., Padmalal, D., 2005. Stratigraphical and palynological appraisal of the Late Quaternary mangrove deposits of the west coast of India. *Quaternary Research* 64, 418-431.
- Kunte, P.D., 1994. Sediment transport along the Goa-north Karnataka coast, western India. *Marine Geology* 118, 207-216.
- Kunz, A., Frechen, M., Ramesh, R., Urban, B., 2010a. Luminescence dating of Late Holocene dunes showing remnants of early settlement in Cuddalore and evidence of monsoon activity in south east India. *Quaternary International* doi:10.1016/j.quaint.2009.10.042.
- Kunz, A., Frechen, M., Ramesh, R., Urban, B., in press b. Periods of recent dune sand mobilisation in Cuddalore, south east India. *Zeitschrift der Deutschen Gesellschaft für Geowissenschaften (ZDGG)*.
- Mallik, T.K. Vasudevan, V., Verghese, P.A., Machado, T., 1987. The black sand placer deposits of Kerala beach, southwest India. *Marine Geology* 77, 129-150.
- Mallik, T.K., 1986. Micromorphology of some placer minerals from Kerala beach, India. *Marine Geology* 71, 371-381.

- Mallik, T.K., Mukherji, K.K. Ramachandran, K.K., 1988. Sedimentology of the Kerala mud banks (fluid muds?). *Marine Geology* 80, 99-118.
- Mathur, U.B., Pandey, D.K., Bahadur, T., 2004. Falling Late Holocene sea-level along the Indian coast. *Current Science* 87(4), 439-440.
- Mejdahl, V., 1979. Thermoluminescence dating: beta-dose attenuation in quartz grains. *Archaeometry* 21, 61-72.
- Murray, A.S., Wintle, A.G., 2000. Luminescence dating of quartz using an improved single-aliquot regenerative-dose protocol. *Radiation Measurements* 32, 57-73.
- Murray, A.S., Wintle, A.G., 2003. The single aliquot regenerative dose protocol: potential for improvements in reliability. *Radiation Measurements* 37, 377-381.
- Narayana, A.C., Priju, C.P., 2006. Evolution of Coastal Landforms and Sedimentary Environments of the Late Quaternary Period along Central Kerala, Southwest Coast of India. *Journal of Coastal Research*, Special Issue 39, 1898-1902.
- Nielsen, A., Murray, A.S., Pejrupa, M., Elberling, B., 2006. Optically stimulated luminescence dating of a Holocene beach ridge plain in Northern Jutland, Denmark. *Quaternary Geochronology* 1, 305-312.
- Otvos, E.G., 2000. Beach ridges - definitions and significance. *Geomorphology* 32, 83-108.
- Prescott, J.R., Hutton, J.T., 1994. Cosmic ray contributions to dose rates for luminescence and ESR dating: large depths and long-term time variations. *Radiation Measurements* 23, 497-500.
- Prescott, J.R., Stephan, L.G. (1982): The contribution of cosmic radiation to the environmental dose for thermoluminescence dating - latitude, altitude and depth dependences. *PACT* 6: 17-25.
- Rajan, T.N., Kumar, A.P.S., 2005. Geology and mineral resources of Kerala. In: Geological Survey of India- Miscellaneous publication no. 30. *Geology and mineral resources of the states of India*, Part IX - Kerala. 93pp.
- Rajendran, C.P., Rajagopalan, G., Narayanaswamy, 1989. Quaternary geology of Kerala: Evidence from radiocarbon dates. *Journal Geological Society of India* 33, 218-222.
- Roberts, R.G., Galbraith, R.F., Olley, J.M., Yoshida, H., Laslett, G.M., 1999. Optical dating of single and multiple grains of quartz from Jinmium rock shelter, northern Australia: Part II, results and implications. *Archaeometry* 41, 365-395.

- Samsuddin, M., 1986. Textural differentiation of the foreshore and breaker zone sediments on the northern Kerala coast, India. *Sedimentary Geology* 46, 135-145.
- Thamban, M., Rao, V.P., Schneider, R.R., Grootes, P.M., 2001. Glacial to Holocene fluctuations in hydrography and productivity along the southwestern continental margin of India. *Palaeogeography, Palaeoclimatology, Palaeoecology* 165, 113-127.
- Thomas, P.J., 2009. Luminescence Dating of Beachrock in the Southeast Coast of India- Potential for Holocene Shoreline Reconstruction. *Journal of Coastal Research* 25 (1), 1-7.
- Wagle, B.G., 1990. Beach Rocks of the Central West Coast of India. *Geo-Marine Letters* 10, 111-115.
- Wagle, B.G., Vora, K.H., Karisiddaiah, S.M., Veerayya, M. and Almeida, F., 1994. Holocene submarine terraces on the western continental shelf of India: Implications for sea-level changes. *Marine Geology* 117, 207-225.
- Wallinga, J., Murray, A., Wintle, A., 2000. The single-aliquot regenerative-dose (SAR) protocol applied to coarse-grain feldspar. *Radiation Measurements* 32, 529-533.
- Wintle, A.G., Murray, A.S., 2006. A review of quartz optically stimulated luminescence characteristics and their relevance in single aliquot regeneration dating protocols. *Radiation Measurements* 41, 369-391.

CONCLUSIONS AND FUTURE DIRECTIONS

The major scope of the study is to apply contemporary techniques in OSL dating to unravel chronology in a dynamic environment for palaeoclimatic research. The key focus was given to depositional environments in the coastal regions such as continental shelf sediments, deltaic environment, beach ridges and coastal dunes from two different geographical locations having varied sediment provenance and depositional history. The results from the study provides vital information on the sediment accumulation periods in Pleistocene to Holocene in the coastal environment from a variety of geographical locations synthesised from a large set of data. The OSL based study outlined in this thesis provides the following new information on the Pleistocene to Holocene climate forcing.

The study demonstrates the effective application of OSL dating in determining ages of sediments as young as less than ten years (VDB-1A from coastal fore dunes of the east coast of India; 4 ± 1 a) up to as old as ~ 350 ka (core sediments of Cauvery delta) from different depositional settings like fluvial and aeolian. It was observed that the OSL signal from quartz in the Cauvery delta region has a low near-saturation dose with an average D_0 of 52 ± 5 Gy ($n = 8$). So the application of elevated temperature post-IR IRSL protocol was found to be useful in the age determination of these older sediments. Quartz grains from south India exhibited bright OSL signal from quartz, which was of advantage in the dating of extremely young sediments. The preheat and cut-heat combination for each sample was determined by carrying out tests on an individual sample basis and a thorough analysis of recycling, recuperation and IR depletion ratios helped to obtain consistent D_e values. In general lower temperature thermal treatments without any hot bleach were preferred for young samples and higher temperature preheats with hot bleach incorporated at the end of the cycle was necessary for older samples to produce meaningful D_e . The study considered the intricate details involved in the bleaching phenomena of samples. The resultant D_e values were attained by considering the complexities involved in the deposition of sediments in the geological past. This provides a certain degree of consistency to the data set and reliability in the age estimates.

Chronology of coastal deposits of south India are largely lacking and this study is among the first to apply OSL dating method to reveal the late Holocene climate changes

and morpho-dynamics in the east (Tamil Nadu) and west coasts (Kerala) of India. OSL and radiocarbon dating of coastal sediments revealed some interesting features common in world coastline during Pleistocene to Holocene. During LGM large areas of continental shelf in North Atlantic (Southern North Sea area), Bay of Bengal and Arabian Sea have been exposed sub aerially allowing large influx of terrestrial sediments into the shelf. Chronology of terrestrial sand overlain by marine, tidal flat deposits and peats in the southern North Sea provided primary information on sedimentation boundary between late Pleistocene and Holocene sediments. The Pleistocene boundary apparently varies in depth as a function of distance from the shore, accommodation space and palaeo-elevation. The combined OSL and radiocarbon ages of the terrestrial sand deposited between 2 m and 0.5 m below this marine sequence in Southern North Sea shows that sedimentation in a predominantly peri-glacial, fluvial environment continued to occur throughout the latest Weichselian and Early Holocene, right up to the elevation-dependent time of transgression. Followed by the Weichselian glacial maximum, the onset of Flandrian transgression recorded by wide spread formation of peat which was observed in the present day continental shelf region of southern North Sea. A similar phenomenon was observed in the west coast of India with occurrence of ~1 m thick peat at about 10 km inland to present day coast. Radiocarbon dating of peat formations associated with the early Holocene transgression shows that formation of peat in the southern North Sea area took place between ~10 ka and 8 ka which gradually moved onshore.

Series of coast parallel beach ridges located 3-6 km inland of west coast of India were dated using OSL dating of Quartz and provided chronology of their formation between 5 and 3 ka indicating sea level high stand during this period. The quartz grain surface texture analysis and heavy mineral analysis of inland and coastal dunes present in the east coast of India provided convincing evidences of reworking and preferential sorting of sediments in response to recent to modern climate change. The major factors which contributed to the formation of coast parallel dunes in the east coast of India are wind vector and aridity. The sand mobility index calculated for the study area demonstrated good correlation for the dune mobility with reduced precipitation, vegetation cover and wind strength.

There have been no chronological studies available for the subsurface sediments of Cauvery delta and the present study provided primary chronological frame for the upper ~50m sediments. The ages obtained in the study of two cores from the Cauvery deltaic

region reveal that except for a small upper layer of Holocene sediments (~5m depth), the majority of the upper ~50 m of subsurface sediments of Cauvery Delta were deposited during the period of upper Middle Pleistocene to Upper Pleistocene (MIS-5 to10). A relatively large hiatus demonstrated in the sedimentation with in the period of middle Holocene to Upper Pleistocene (MIS-5) was probably due to the lateral migration of streams which hindered the sediment supply in to the region or due to continuous removal of upper sediments due to erosion.

This research work represents only a part of what can be achieved in the field of geochronology using the OSL technique. The study revealed the occurrence of a number of climatic events that took place during late Pleistocene to Holocene in different regions. However a number of events are still poorly understood in the sites studied. In the study on the Southern North Sea for example, the inferences were made from results of seven core samples collected along a transect towards the coast which were spread wide apart. A high resolution sampling with closed core spacing would therefore bring a clearer picture of Pleistocene- Holocene depositional boundary which is vital in terms of understanding the post glacial evolution of this part of the North Atlantic coast.

In a few cases, this study revealed that the evidence of the occurrence of a few events that were believed to have taken place, were indeed not so. For example, the results of the study on sub surface sediments of Cauvery delta showed that the first 50m of the core were deposited during upper middle Pleistocene to middle Holocene, which were earlier considered to be of much younger age. Also the dunes on south east coast of India were considered as strand lines representing Middle Holocene sea level high stand, however the OSL ages obtained in the present study revealed that these are in reality reworked coastal dunes of modern age.

The studies on the different sites were brief and in order to establish more accurate chronology, further detailed research in the area is required. For instance, the outcome of the work on the west coast of South India was based on the ages of a few beach ridges. These findings could be strengthened by carrying out close grid sampling taking into consideration the local elevation with respect to MSL, further towards the north and south of the study area. A multi proxy study could be applied in the area if one chooses to include dating of peat deposits along with studies on other geomorphologic features like coast parallel lagoons and wet lands occurring in this region. Such an approach would bring a clear picture of the coastal response to the climatic forcing during Holocene.

Linto Alappat
Citizenship : Indian

Contact

E-mail:lintoalappat@yahoo.co.uk ;
Linto.Alappat@liag-hannover.de

Address for Communication

For reasons of data protection, the curriculum vitae is not included in the online version.

Education

Ph.D Topic

Application of OSL dating on coastal sediments – Case studies from shallow marine sediments of Southern North Sea, Germany, and coastal sub-surface and surface sediments from south India

List of Publications

- **Alappat, L., Vink A., Tsukamoto S., Frechen M., 2010a.** Establishing the Late Pleistocene - Holocene sedimentation boundary in the southern North Sea using OSL dating of shallow continental shelf sediments. *Proceedings of the Geologists' Association* 121, 43-54. doi:10.1016/j.pgeola.2009.12.006.

- **Alappat, L.**, Tsukamoto, S., Singh, P., Srikanth, D., Ramesh, R., Frechen, M., 2010b. Chronology of Cauvery delta sediments from shallow subsurface cores using high-temperature post-IR IRSL dating of feldspar. *Geochronometria* 37, 37-47. DOI 10.2478/v10003-010-0025-1.
- **Alappat, L.**, Frechen, M., Ramesh, R., Tsukamoto, S. and Srinivasalu, S., 2011(in press). Evolution of late Holocene coastal dunes in the Cauvery delta region of Tamil Nadu, India. *Journal of Asian Earth Sciences* (2011), doi:10.1016/j.jseaes.2011.05.019
- **Alappat, L.**, Frechen, M., Rajan, R. and. Tsukamoto, S. Evidences of Late Holocene shoreline progradation in the coasts of Kerala, South India obtained from OSL dating of palaeobeach ridges (to be submitted in journal, *The Holocene*).

Oral Presentations

- ✓ **Alappat, L.** Srinivasalu, S. and Frechen, M. Chronology of sand dune formation in the southern part of Cauvery Delta, India. AGE 2010- National symposium of Geologist's Association, Department of Geology, Anna University, Chennai, India. January 28-29, 2010.
- ✓ Kunz, A. **Alappat, L.** Frechen, M. Ramesh, R. Srinivasalu, S. and Urban, B. Luminescence Dating of Coastal Dunes at the Cauvery Delta Showing Rapid Environmental Changes. International Workshop on Deltas: Coastal Vulnerability and Management, Anna University, Chennai, India, December 6-12, 2009.
- ✓ **Alappat, L.** Tsukamoto, S. Singh, P. Ramachandran, R. Frechen, M. Chronology of Cauvery delta sediments from shallow subsurface core using elevated post-IR IRSL dating. German Meeting on Luminescence and Electron Spin Resonance Dating, Leibniz Institute for Applied Geophysics, Hannover, Germany, October 9-11, 2009.

Posters

- ✓ **Alappat, L.** Tsukamoto, S. Singh, P. Ramachandran, R. Frechen, M. Chronology of Cauvery delta sediments from shallow subsurface core using elevated post-IR IRSL dating Second Asia Pacific Conference on Luminescence and Electron Spin Resonance Dating, Physical Research Laboratory, Ahmedabad, India, November 12-14, 2009.
- ✓ **Alappat, L.** Frechen, M. Vink, A. Techmer, A. and Tsukamoto, S. OSL dating of shallow continental shelf sediments of Southern North Sea. German Meeting on Luminescence and Electron Spin Resonance Dating, Max Plank Institute for Evolutionary Anthropology, Department of Human Evolution, Leipzig, Germany, October 31- November 2, 2008.

- ✓ **Alappat, L.** Frechen, M. Vink, A. and Techmer, A. Chronology of sediments from Southern North Sea using OSL and radiocarbon dating 12th International Conference on Luminescence and Electron Spin Resonance Dating, Peking University, Beijing, China, September 18-22, 2008.
- ✓ **Alappat, L.** Frechen, M. Vink, A. and Techmer, A. Chronology of Sediments from Southern North Sea using OSL and Radiocarbon Dating. Workshop of Geological Society of Lower Saxony at Leibniz Institute for Applied Geophysics, Hannover, Germany, March 10-11, 2008.

Scholarships and Awards

- ✓ **Leibniz DAAD Fellowship** 2007 for carrying out doctoral research in Germany (2007-2010).
- ✓ **Samburvarayar Endowment scholarship** for academic excellence from University of Madras (2005-2006).
- ✓ **First Rank and Gold medal** in M.Sc. Applied Geology degree programme and Late. T.N. Muthuswamy Iyer endowment award from Anna University (2003-2005).

Selbständigkeitserklärung

Ich versichere, dass ich die eingereichte Dissertation “Application of OSL dating on coastal sediments – Case studies from shallow marine sediments of Southern North Sea, Germany, and coastal sub-surface and surface sediments from south India” selbständig und ohne unerlaubte Hilfsmittel verfasst habe. Alle Stellen, die dem Wortlaut oder dem Sinn nach anderen Werken entnommen sind, wurden durch Angabe der Quellen als solche kenntlich gemacht.

Linto Alappat

Hannover,

15. October 2010